MULTIFUNCTIONAL NANOMATERIALS ON VARIOUS SURFACES

A dissertation submitted to
Indian Institute of Technology Guwahati
for the degree of
Doctorate of Philosophy in Chemistry

Ms Gitanjali Majumdar
Department of Chemistry
Indian Institute of Technology Guwahati
Guwahati 781039, India
April 2007

INDIAN INSTITUTE OF TECHNOLOGY, GUWAHATI

Department of Chemistry

STATEMENT

I hereby declare that the matter embodied in this thesis is the result of investigations carried out by me in the Department of Chemistry, Indian Institute of Technology Guwahati, India under the supervision of Prof. Arun Chattopadhyay, Professor in Department of Chemistry.

In keeping with the general practice of reporting observations, due acknowledgements have been made wherever the work described is based on the findings of other investigations.

I.I.T Guwahati

April 2007

Ms Gitanjali Majumdar

Department of Chemistry
IIT Guwahati

INDIAN INSTITUTE OF TECHNOLOGY, GUWAHATI

Department of Chemistry

CERTIFICATE

It is certified that the work contained in the thesis entitled "MULTIFUNCTIONAL NANOMATERIALS ON VARIOUS SURFACES" by Ms Gitanjali Majumdar, a student of the Department of Chemistry, Indian Institute of Technology Guwahati, for the award of the degree of Doctor of Philosophy, has been carried out under my supervision and that this work has not been submitted elsewhere for a degree.

I.I.T Guwahati
April 2007

Prof. Arun Chattopadhyay
Professor
Department of Chemistry
IIT Guwahati

INDIAN INSTITUTE OF TECHNOLOGY, GUWAHATI

Department of Chemistry

Course Certificate

This is to certify that Ms.Gitanjali Majumdar has satisfactorily completed all the courses required for the Ph.D degree programme. These courses include:

CH 603	Supramolecules: Concepts & Applications
CH 627	New Reagents in Organic Synthesis
CH 630	A Molecular Approach to Physical Chemistry
CH 632	Advanced Group Theory

Ms. Gitanjali Majumdar has successfully completed her Ph.D qualifying examination in December 2002.

Prof. A.T.Khan
Head,
Department Of Chemistry
I.I.T.Guwahati

Dr. A.Saikia
Secretary
Departmental Post Graduate Program
Department of Chemistry
I.I.T.Guwahati

INDIAN INSTITUTE OF TECHNOLOGY, GUWAHATI

Department of Chemistry

Ph.D Grade Card

Name: Gitanjali Majumdar Department: Chemisry
Roll No: 02612203 Semester: July-November 2002

Course	Course name	Credit	Grade
CH 603	Supramolecules: Concepts & Applications	6	BC
CH 627	New Reagents in Organic Synthesis	6	BC
CH 630	A Molecular Approach to Physical Chemistry	6	AA
CH 632	Advanced Group Theory	6	AB

Semester Performance Index (S.P.I) 8.25

Cumulative performance Index (C.P.I) 8.25

Assistant Registrar

I.I.T Guwahati

Academic Section

March 2007

Acknowledgement

First of all I am extremely thankful to my supervisor Prof. Arun Chattopadhyay, for his constant help and inspiration during the entire period of my research. I feel myself very fortunate to pursue my PhD dissertation work in the area of my interest. Sir always inspired me to work on new ideas, and helped to find out “anything new” in my every project. I am also thankful to Dr. Anumita Paul, who gives valuable guidance to every project that I carried out. I am thankful to Indian Institute of Technology Guwahati for providing me infrastructure and facilities for research. I express my sincere gratitude to faculty members of Department of Chemistry, especially Dr. .Manabendra Ray and Prof. Jubaraj B. Baruah for critical evaluations of my work in different stages. I am also thankful to Prof. M. K. Choudhuri, Prof. A. T. Khan, Prof. B. K. Patel, Dr. Anil K. Saikia and Dr. P. K. Iyer for their help and advice. I am also thankful to all the Scientific Officers and Technical Assistants of the Department of Chemistry, Department of Physics, Centre for Nanotechnology as well as Central Instrumentals Facility for providing me with instrumental expertise. I thank my lab senior Tridib da who taught me how to operate various instruments and also helped me learn the first few steps of research. I am very fortunate to have such helping lab juniors, Biswa, Sonit, Krishna, Jashmini, Murugan, who always made the atmosphere of lab so friendly and always put forward their helping hands. I also thank all the research scholar of our department both present and those who have submitted their thesis, for their support and help. Thanks to all my friends always encouraging make me feel confident, helping me whenever I needed, with whom I

have been sharing my moments of happiness and sorrow. I am thankful to my husband Joy for being with me, as a good friend, inspiring me at every stage of work and without his support it would really have not been possible. Thanks are due to CSIR, New Delhi for fellowship, RSIC Shillong and NCL Pune for providing instrumental facilities. I also thank all my teachers right from the beginning of my school K. R. B Girls School, in Handique Girls College and later in Gauhati University, who actually generated in me the interest for science, helping me choosing the course of my career. I also deeply acknowledge the support of my colleagues of Assam Engineering College (AEC). Last but most importantly, I am thankful to all my family members, my parents, my dearest sisters ashima, bubu, and my brother Jitu for helping me, supporting me in my difficult moments, making me laugh, and encouraging me throughout my life.

Abstract

The focus of the thesis is to systematically develop methods to incorporate multifunctional nanoscale materials on various substrate surfaces. The multiple functions that the model systems are expected to perform involve combining the performance of individual nanoscale materials working either in parallel or in sequence so that overall the device could execute multiple tasks. In addition, the nanoscale materials have been combined with conducting polymer to improve their functionalities. The model systems that have been developed are primarily metal or semiconductor nanoparticles (NPs) embedded in polymer substrates. The materials were generated by using chemical or physical methods. These materials have potential applications in chemical and biochemical sensing, displays, opto-electronic devices and in chemical catalysis. Thus, the underlying theme of the experimental investigations, carried out in the present thesis, has been to find newer chemical methods to immobilization of nanomaterials on various surfaces.

First of all, a new method of storage of nanoparticles on the anion exchange resin beads is reported. This method of reversible storage and recovery of silver nanoparticles (NPs) in anion exchange resin beads based on the principle of ion exchange. The Ag NPs were stored by exchange of anions of the resins, which were previously activated with a mixture of OH^- and NO_3^- ions. The so-stored NPs could be regenerated by addition of $NaBH_4$ solution to the resins.

A natural extension of the work is the chemical deposition of bulk as well as nanoscale metal particles on the surfaces of polymer. The method is based on ion exchange of salt of metal with commercially available resin beads followed by reduction of the metal ions using $NaBH_4$ as the reducing agent. The sizes of the metal particles deposited could be controlled by controlling the concentration of the reducing agent as well as the deposited ions. In this way we could deposit bulk metal particles of Au, Ag and Ni as well as nanoparticles of Au and Ag on the surfaces of the resin beads. In addition, we were also able to deposit multiple kinds of particles such as Ag and Au, Au and CdS and Au, Ag and CdS on the surfaces.

Further, the above method was extended to generate Au nanoparticles (NPs) and polyaniline (PANI) on the same cation-exchange resin beads and demonstrate their use as multifunctional devices. The Au nanoparticles immobilized in the resin catalyzed the oxidation of glucose to gluconic acid and PANI deposited on the beads can subsequently detect the formation of the acid by the color change.

The work done so far on various polymeric surfaces were further extended to generate lithographic pattern with quantum dots in a polymeric film. The principle is based on a combination of top-down and bottom-up approaches in which a metallic (transmission electron microscopic) grid is placed on a polyvinyl pyrrolidone film containing Cd^{2+} ions, which is subsequently exposed to H_2S gas. This leads to the generation of a fluorescent yellow colored pattern due to the formation of CdS nanoparticles on exposed parts of the film. Also, we have used the same method to generate patterns in two colors by starting with a green fluorescent dye incorporated in the film and following the same procedure in which a patterned yellow / orange colored CdS nanoparticles are distributed over the background fluorescence of the dye. We have also extended this method to generate pattern of PbS nanoparticles.

Finally, a new method of imprinting predefined patterns of composite of Au and Ag NPs on a glass substrate based on the generation of NPs in polymer matrix and then using the composite to imprint pattern on glass substrate using the principle of soft lithography. The heating of the substrate at elevated temperature helped remove the polymer with the retention of the NPs organized in specific patterns. The patterns could be in the form of parallel lines, of NPs separated by a distance on the order of 1 μm; they could be crossed lines, made of arrays of Au NPs, separated from each other by about a micron. Additionally, these Ag-Au lines could be used as templates to deposit conducting polymer such as polyaniline by a simple chemical method.

CONTENTS

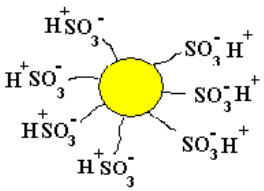

$HAuCl_4$

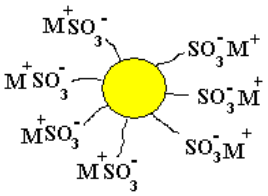

$NaBH_4$

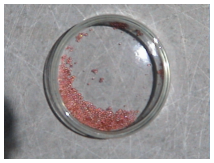

K Chapter 4: Au nanoparticles and polyaniline coating of resin beads for use as colorimetric Glucose sensor.

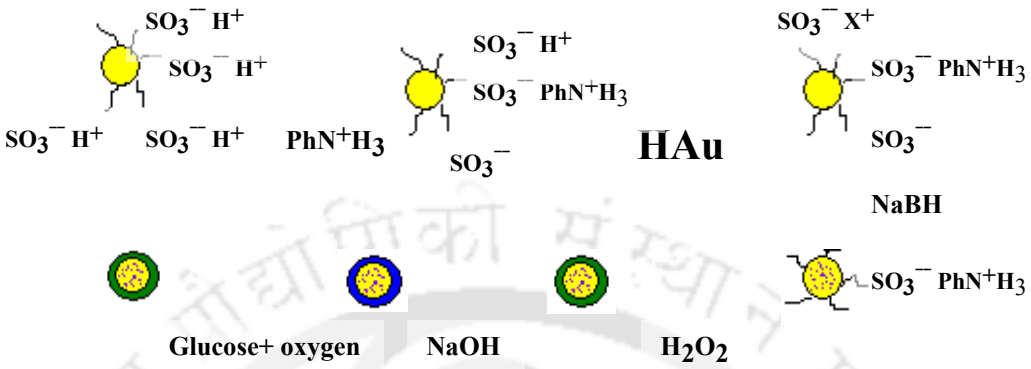

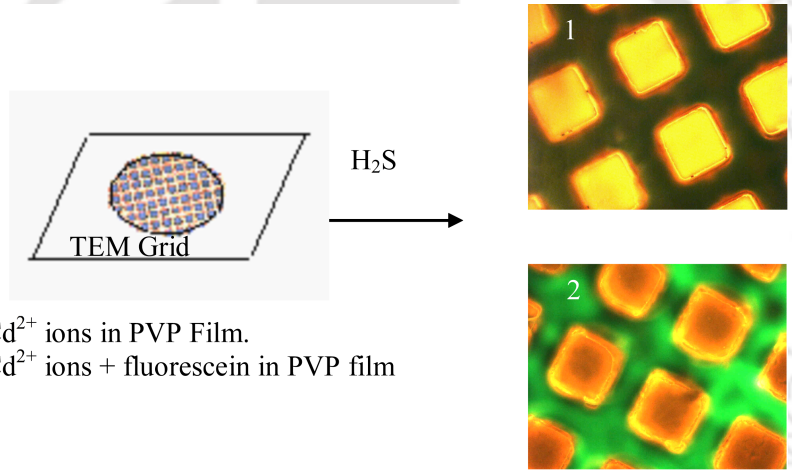

1. Cd^{2+} ions in PVP Film.
2. Cd^{2+} ions + fluorescein in PVP film

Contents

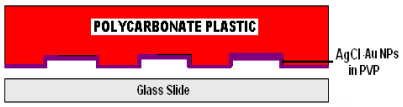

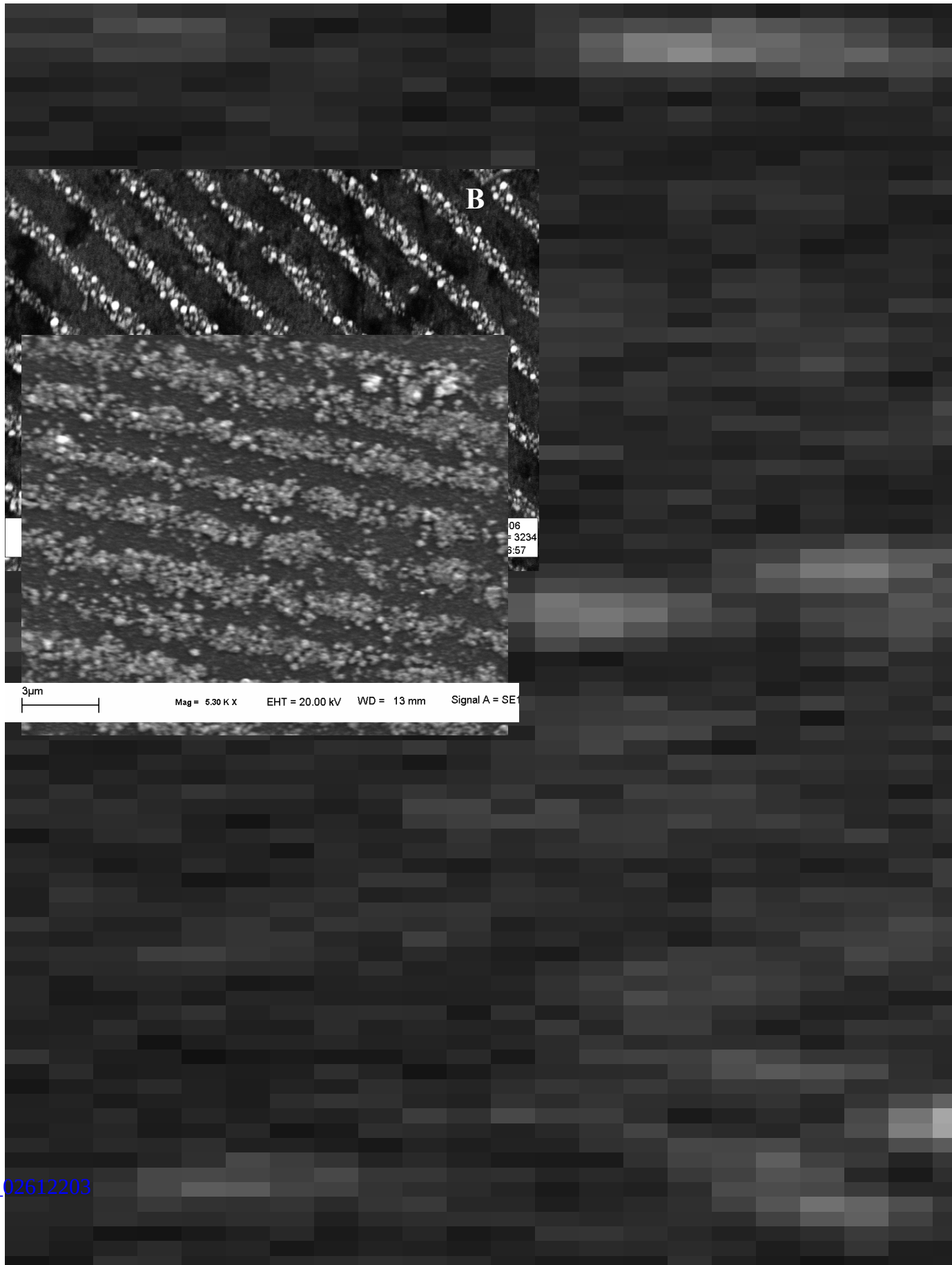

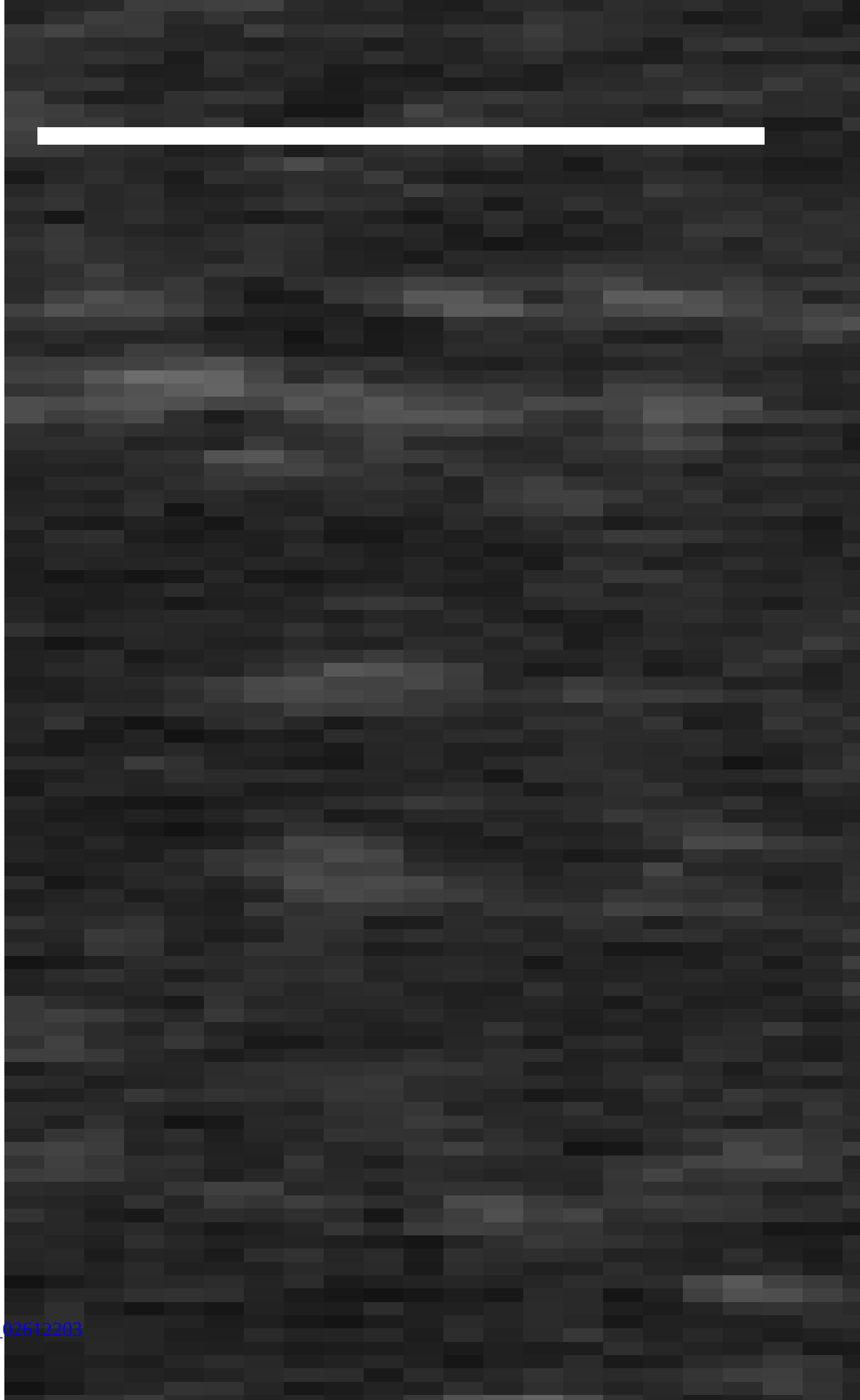

1.1 Introduction

As we pass through the first century of the new millennium, we are destined to witness the immediate impact of developments in science on technology and at the same time technology and other market forces driving the development of science faster than ever. This can be expected to be more evident where the properties of materials would be required to be tuned with extraordinary precision, in order to fabricate integrated devices with molecular scale materials. A natural choice in this regard would be to use materials with molecular or nanoscale functional components. The advantages lie in their stability and tunable properties as amenable to molecular and nanoscale materials in comparison to bulk materials. While in the syntheses of molecular scale materials principles of chemistry are primarily used, the nanoscale materials, however, can be generated by a host of techniques based on principles of chemistry, physics, biology and engineering.

That the physical, chemical and biological properties of materials can be tuned by their sizes and shapes, once their dimensions are reduced to nanoscale, has created research interests, in generating newer materials and methods with potential application in industry, not witnessed since the beginning of silicon industry. Historically, use of nanoscale materials goes back to Egyptian use of hair dyes[1], gold paints on glasses in European churches[2] and Wootz steel[3] used by the crusaders in Europe. However, these developments were based more on empirical studies than sound scientific understanding of the phenomenon. Officially, it was the creation of gold sol in 1857 by Michael Faraday[4] and explanation of properties based on clusters of gold atoms present in the sol that started the modern version of nanoscale

science. The surface plasmon resonance behavior of metal clusters was subsequently explained by Mie scattering[5]. Feynman, in his famous lecture, on 29 December 1959, at the California Institute Technology, laid the foundation for control of properties of materials at the nanoscale and subsequent use for technology [6]. However, it was not until the 1980s the implication of properties of materials with nanoscale dimensions on industrial application was realized. It was then the word "Nanotechnology" was coined[7] by Prof. Norio Taniguchi stating that "Nano-technology" mainly consists of the processing, separation, consolidation, and deformation of materials by one atom or one molecule''which was further developed, in more detail by Dr. Eric Derxler.[8]

Enormous growth has taken place in terms of synthesis, structure formation and demonstration of properties of materials at the nanoscale for the last two decades[9]. One could possibly say that a basic foundation of nanoscience and nanotechnology is already laid by the cumulative works of a large number of scientists throughout the world. Now, it is incumbent on the scientists of the present generation to develop principles and demonstrable models for the use of nanoscale sciences in various applications including chemistry, material science, healthcare and medicine[10], energy[11], the environment[12], space technology[13], information technology[14] and similar applications.

Technological applications of nanoscale science would require generation of newer materials, their systematic assemblies and nanoscale functional structures patterned on two and three-dimensional substrate surfaces. Fortunately, a large number of synthetic schemes

are available for the generation of nanoscale materials[15]. Also, there have been significant developments over the last two decades on newer lithographic techniques that could either create patterned surfaces or deposit nanomaterials in the form of well-defined structures such as arrays on a substrate surface[16]. Among the nanomaterials, solution synthesis of coinage metal nanoparticles (NPs) such as those of Ag and Au and semiconductor NPs (popularly known as quantum dots) of oxides and sulfides of heavy metal such as ZnS, CdS, ZnO and TiO_2 have received extraordinary research attentions because of their special chemical (catalytic), optical and electronic properties[17]. For example, surface plasmon resonance absorptions of Au and Ag NPs have high oscillator strengths and occur in the visible and near infrared region and the absorption maxima are easily tuned by size and or shape changes. Au NPs have been demonstrated to be useful as quick and easy optical probes for genomics and proteomics applications[18]. Examples of attachment of biotin to streptavidin functionalized colloidal gold are aplenty in terms of solution detection as wells as in the form of array sensors[19]. Small Ag and Au NPs are also good chemical catalysts and are therefore of great significance in synthetic chemistry applications[20]. Further, Au nanorods have been potential cancer therapeutic applications through the hyperthermia treatment using their near infrared absorption properties[21]. On the other hand, photo-luminescent and electroluminescent properties of quantum dots can easily be tuned by their size and shape selections and also by heavy metal doping of the NPs[22]. Incorporation of these unusual properties of the metal and semiconductor NPs into functional devices used in the field such as photonics,

optoelectronics, bioassays, fuel cells and chemical catalysis are now subjects of great research activities[23].

Although great strides have been made with respect to generation of nanomaterials and nanoscale structures and subsequent demonstration of their functions, there is much scope for development in the organization of NPs into functional structures. This is especially true with respect to immobilization of materials on supports that would act as multifunctional devices. Lithographic methods such as scanning probe microscopy (SPM) [24] based methods of transferring colloidal materials are limited with respect to the nature of materials to be transferred, surface profiles and also are very slow in terms of rate of deposition of materials on the substrate. On the other hand, electron beam lithography (EBL)[25] ion-beam lithography (IBL)[26] and other similar lithographic methods are limited to the generation of patterns on substrate surface. In this respect, soft-lithography[27] based methods of lithography offer significant advantages over others in terms of nature of materials to be deposited, ease and cost-effectiveness. Soft-lithography based methods also offer subsequent processing of materials for incorporation of materials at several stages where lithographic imprinting can be complimented with chemical reactions for enhancement of performance or chemical deposition of other materials on patterned surface as defined by the lithographic imprints. Overall, chemical methods and soft lithography based methods offer a lot of alternative ways, which might otherwise be difficult if not impossible using other form of lithography, in imprinting organized NP structures on versatile substrate surfaces.

As much as the methods of generation and subsequent imprinting of nanoscale structures are important the substrate too plays a pivotal role in making devices that are convenient and relatively easy to make and also provide flexible alternatives to other substrates like silicon and germanium. Glass is generally the material of choice as support for its rigidity, cost-effectiveness and also for ease of functionalization using common chemical methods. In addition, NPs can be attached to chemically functionalized glass surfaces by covalent bonds, or through electrostatic interactions. On the other hand, organization of NPs on metal surfaces has been an attractive option for organized deposition of NPs. Among the metal surfaces, Au has been the surface of choice due to its ease of preparation, stability and ability for functionalization with thiol, amine and carboxylic groups thereby allowing depositions of organic monolayers[28]. It is also possible to imprint structured organic layers on Au surfaces using thiol as the linker group. In this regard, apart from Au other metal surfaces such as that of silver and aluminum have also been widely used[29]. Similarly graphite surface has also been a suitable choice for deposition of quantum dots and other NPs[30].

The mechanical and chemical flexibilities offered by polymer substrates make them an ideal choice for systematic deposition of nanoscale materials. Since a large number protocols are already available for making conducting polymer surfaces in polymer electronics[31] they can be incorporated in the generation of hybrid functional structures consisting of polymer and NPs.

The availability of a large number of synthetic methods for the generation of metal and semiconductor NPs, the opportunity offered by several lithographic methods that are currently

in use and possibility applications of multifunctional devices with nanoscale functional components have inspired me to pursue, in my PhD thesis, newer methods of immobilization or synthesis of metal and semiconductor NPs on various substrate surfaces. The NPs could be immobilized on a polymer substrate, on glass surface or they could be synthesized in a polymer film supported by glass slide. Also, of interest was to pursue the possibility of such structures for functional use as catalyst, sensor and for information storage and other polymer electronic applications. In pursuing these works I have developed newer ways of synthesizing metal and semiconductor NPs under various conditions keeping in view application potential and also developed newer lithographic principles that could pave ways for futuristic devices with nanoscale functional components.

The primary objectives of the investigations reported in this thesis are described below.

1. To find a new method for the reversible storage of metal NPs in ion-exchange resin beads and subsequent recovery for appropriate use. This also provided a new way of bead-immobilized NPs for use as chemical catalysis, in any solvent, eliminating the need for the use of phase transfer catalyst.

2. To find a general method for the synthesis of various bulk as well as nanoscale single and bimetallic particles on resin surfaces. The general method developed herein could be used for deposition of semiconductor NPs as well as composite metallic NPs, using chemical pathways.

3. To generate Au NPs on the surfaces of resin beads along with co-synthesis of conducting polymer polyaniline (PANI). The Au NPs were to act as chemical catalysts and the polymer was to sense the formation of the product colorimetrically.

4. To generate patterns with quantum dots on polymer films, using a new gas - solid reaction in the presence of a metallic grid as the mask. The generality of this method for patterned growth of quantum dots was also to be demonstrated.

5. To deposit Au NPs with sub-micron scale patterned arrays on glass surfaces, using commercially available compact disc as the mold and metal-polymer composite as the ink. Further the patterned Au NPs deposits could be used as the template for further deposition of PANI, on non-functionalized glass substrates.

Our initial idea started with the possibility of reversible storage and recovery of metal NPs with ion exchange resin beads. The idea is that when NPs are charge stabilized in their colloidal forms by stabilizing agents such as sodium dodecyl sulfate, polyethylene glycol and a host of other reagents which have strong hydrophilic groups, they should also be stabilized by solid resins which have ion exchange groups in addition to the hydrophobic parts just like the common stabilizers of NPs. When we pursued the experiments we observed that commercially available anion exchange resin beads, when suitably modified, could trap Ag NPs by exchange of the replaceable negative groups of the resins. For the purpose, we had used amberlite IR-400, a polystyrene divinylbenzene copolymer with terminal trimethyl ammonium group. We also observed that chloride ions of the resins needed to be replaced

(activated) with nitrate ions and OH^-. When Ag NPs were synthesized in water by $NaBH_4$ and then passed through a column of the activated resin beads then the NPs were trapped in the beads with no detectable presence of them in the elutant. The NPs could again be recovered into the solution (from the resin beads) in the presence of $NaBH_4$. Further, the NP loaded resin beads have been used as a catalyst for the reduction of a dye. We discovered that the Ag NPs were stored in the beads in the form of oxides of silver.

A natural consequence was to find out whether NPs could be generated in the beads so that the possibility of size, shape and oxidation state changes during the transfer could be avoided. In addition, since the amount of ions exchanged with the bead could be controlled the particle sizes could possibly be controlled. Also, would be it possible to deposit one or more kinds of NPs and bulk deposits of metals and semiconductors. In order to achieve these we started with cation exchange resin beads amberlite IR-120. Prior to deposition, the resin beads were activated with hydrochloric acid, to introduce hydrogen ion in the place of sodium ions that are present in commercially available resin beads. The beads were then kept in solution containing the salt of appropriate metal ions. The beads when taken out and treated with $NaBH_4$ produced metal NPs or bulk deposits, depending on the concentration and nature of the metal cation present in the original solution, as was evident from change in color of the beads. The particles – both NPs and bulk deposits – were very stable even for months. The general method developed in this way was used to deposits NPs of Au and Ag, bulk deposits of Au, Ag and Ni and also composites of metal and semiconductor NPs.

Once the method of deposition of metal NPs (especially Au NPs) on resin beads was developed, we were further interested in depositing PANI along with Au NPs in the same bead, in order to develop a multifunctional device. One component of such beads, such as the NPs, could be used as catalyst while the polymer would act as the sensor for the detection of the product formation. In order to achieve this, first Au NPs were generated on the beads followed by PANI generation from anilinium ions, deposited on the same bead, using H_2O_2 as the oxidizing agent. The polymer-Au- NP composite so prepared was used for catalysis of the oxidation of glucose and detection of the product gluconic acid by observing the change in color of PANI. Overall the catalytic properties of Au NPs and the acid - base colorimetric properties of PANI were used for glucose sensing.

One of the requirements of device fabrication is the organized and predefined deposition of the functional elements on the substrate surface. As described above, we were working on polymer based devices where the functional components would be NPs. In our laboratory, one of the important research activities is the development of lithographic principles using NPs as the components. Also, important to mention here is that our laboratory is interested in lithography in color at the micron and sub-micron scale resolutions. My previous works on depositions of NPs and polymer on resin beads provided me an opportunity to extend the work in the realm of lithography. We became interested in generating patterned quantum dots in polymer films. We have developed a new method in this regard using a combination of top-down and bottom-up approaches. Polyvinylpyrolidone (PVP) was chosen as the polymer which was deposited on glass surface as thin film. When the film contained Cd^{2+} ions

(starting with the original solution) and then exposed to H_2S gas formation of fluorescent CdS quantum dots could be observed. Once the film was covered by a metallic grid mask (typically a transmission electron microscope grid) and then exposed to H_2S then formation of CdS NPs could be observed as per the patterns of the grid. In other words, the open parts of the grid allowed the generation of CdS NPs and thus patterned formation. We have generated complex patterns using a two-grid combination. The highest resolution of the fluorescent lines we achieved was 1μm.We have been able to develop two-color generation with a different background color. Further, the principle developed here for the generation of quantum dots in selected part of a film could be extended to other more versatile surfaces as well as with different NPs.

The experience of generation of NPs on polymer surfaces and development of a lithographic principle inspired us to carry our further research in systematic depositions of metal (Ag and Au) NPs on glass. This was followed by deposition of conducting polymer PANI guided by the patterned deposits of Au and Ag NP composite. In order to achieve this, we started with an "ink" made of AgCl and Ag-Au NPs in PVP polymer. A soft lithography principle was used to imprint the ink on a glass slide using a CD component as the mold. The deposits would be in the form of parallel lines of width of about 1μm separated by a distance of 1.5 μm. They could also be deposited in the form of arrays. The glass slide was then heated to remove the polymer and thus arrays of Au-Ag NP composite were deposited on the slide in the form of lines or cross arrays. These NPs (in the slide) were then treated with a solution containing the precursors of Au-PANI NPs composite synthesis. We observed the

formation of well ordered patterned deposits of PANI as per the pattern of the metal NPs. Thus we have a conducting polymer-metal NPs composite deposited in a patterned fashion on glass slide. This is expected to be a boost for modern polymer electronics where NPs also can take functional role in the device along with the polymer and glass being the substrate of choice.

Finally, in my PhD thesis works I have put efforts in trying to solve a few challenges related to nanoscale science and technology. Fundamentally, the idea has been to find newer and easier ways of transforming nanoscale science into technology so that the promise of nanotechnology can be realized through newer developments in nanoscience. In so doing, we have tried to demonstrate that the methods of integrating nanomaterials into effective devices are equally significant as those of properties of the same. In other words, the job of a scientist might not end in finding the methods of generating materials and discovering their properties; the modern times demand that we find ways of integrating them into useful devices. In this regard, I have tried to go beyond syntheses of nanoscale materials through either incorporating them into suitable substrates for testing functionality or have invented newer lithographic principles so that in the end we have a device in making, if not a device. Here is the hope that the endeavors we have made herein, in pursuing the dreams of advanced science may be useful; no matter how little they may be for humanity at large.

1.2 References:

1. Walter, P.; Welcomme, E.; Hallegot, P.; Zaluzec, N.J.; Deeb, C.; Castaing, J.; Veyssiere, P.; Breniaux, R.; Leveque, Jean-Luc; Tsoucaris, G. *Nano Lett.* **2006**, 6, 2215.
2. Rao, C. N. R.; Kulkarni, G. U.; Thomas P. J. Edwards, P.P**.** *Chem. Soc. Rev.* **2000**, 29, 27.
3. Reibold, M.; Paufler, P.; Levin, A. A.; Kochmann, W.; Pätzke, N.; Meyer D. C. *Nature* **2006,** 444, 286.
4. Faraday, M. *Philos. Trans. R. Soc. London*. **1857**, 147, 145.
5. (a). Hutter, E.; Fendler, J. H. *Adv. Mater.* **2004,** 16, 1685. (b). Kreibig, U.; Vollmer, M. *Optical Properties of Metal Clusters*, Springer, Berlin. **1995**, 25. (c). Mie, G. *Ann. Phys.* **1908,** 25, 377.
6. Feynmann, R. P. *Eng. Sci*. **1960,** 23, 22.
7. N.Taniguchi, *"On the Basic Concept of 'Nano-Technology'," Proc. Intl. Conf. Prod. Eng Tokyo, Part II,* Japan Society of Precision Engineering. **1974**.
8. (a). Eric Drexel "*Engines of Creation: The Coming Era of Nanotechnology"*, Anchor Books, New York **1986**. (b). Eric Drexel *Nanosystems: Molecular Machinery, Manufacturing, and Computation,* Wiley and Sons, **1992.**
9. (a). Euliss, L. E.; DuPont, J. A.; Gratton, S.; DeSimone, J. *Chem. Soc. Rev.* **2006**, 35, 1095. (b). Kaasgaard, T.; Drummond, C. *Phys. Chem. Chem. Phys.* **2006**, 8, 4957. (c). Wilcoxon, J. P.; Abrams, B. L. *Chem. Soc. Rev*. **2006**, 35, 1162. (d). Veinot, J. G. C. *Chem.Commun*. **2006**, 4160.

10. Michalet, X.; Pinaud, F. F.; Bentolila, L. A.; Tsay, J. M.; Doose, S.; Li, J. J.; Sundaresan, G.; Wu, A. M.; Gambhir, S. S.; Weiss, S. *Science* **2005**, 307, 538. (b) Radt, B.; Smith, T. A.; Caruso, Frank. *Adv. Mater*. **2004**,16, 2184.

11. (a). Anderson, M. L.; Stroud, R. M.; Rolison, D. R. *Nano Lett.* **2002**, 2, 235. (b). Kamat, P. V. *J. Phys. Chem. C* **2007**, 111, 2834.

12. Kamat, P. V. *J. Phys. Chem. C* **2007**, 111, 2834.

13. (a). Tenne, R. *Nature Nanotechnology.* **2006**, 1, 103. (b). Bastani, B.; Fernandez, D. *Thin. Solid Films*. **2002**, 420, 472.

14. (a). Gates, B. D.; Xu, Q.; Stewart, M.; Ryan, D.; Willson, C. G.; Whitesides, G. M. *Chem. Rev*. **2005**, 105, 1171. (b). Schmid, G.; Simon, U. *Chem.Commun*.**2005,** 697. (c). Cao, G. *Adv. Mater*. **2004**, 16, 1864.

15. (a). Sastry, M.; Swami, A.; Mandal, S.; Selvakannan, P. R. *J. Mater. Chem*. **2005**, 15, 3161.(b). Javey, A.; Dai, H. *J. Am. Chem. Soc.* **2005**,127, 11942. (c). Yan, X.-M.; Kwon, S.; Contreras,A. M.; Bokor, J.; Somorjai, G. A. *Nano Lett.* **2005**, 5, 745. (d). Iskandar, M.; Okuyama, F.; Kikuo. *Adv. Mater*. **2002**, 14, 930. (e). Quake, S. R.; Scherer, A. *Science* **2000**, 290, 1536.

16. (a). Reches, M.; Gazit, E. *Nature Nanotechnology* **2006**, 1, 195. (b). Na, N.; Zhang, S.; Wang, S.; Zhang, X. *J. Am. Chem. Soc.* **2006**,128, 14420.(c). Zhang, X.; Ju, W.; Gu, M.; Meng, X.; Shi, W.; Zhang, X.; Lee, S. *Chem. Commun*. **2005**, 4202. (d). Shu, D.; Moll, W.-D.; Deng, Z.; Mao, C.; Guo, P. *Nano Lett.* **2004**, 4, 1717. (e). Zhou, J.; Xu, N.-S.; Deng, S.-Z.; Chen, J.; She, J.-C.; Wang, Z.-L. *Adv. Mater.* **2003**, 15, 1835.

17. (a). Kamat, P.V. *J. Phys. Chem. B* **2002**,106, 7729. (b). Van Dijk, M. A.; Tchebotareva, A. L.; Orrit, M.; Lippitz, M.; Berciaud, S.; Lasne, D.; Cognet, L.; Lounis, B. *Phys. Chem. Chem. Phys*. **2006**, 8, 3486. (c). Hartland, G.V. *Phys. Chem. Chem. Phys*. **2004**, 6, 5263. (d). Subramanian, V.; Wolf, E.; Kamat, P.V. *J. Phys .Chem. B* **2001**, 105, 11439. (e). Pileni, M. P. *J. Phys. Chem. B* **2001**, 105, 3358. (f). El-Sayed, M. A. *Acc. Chem. Res*. **2001**, 34, 257. (g). Eychmueller, A. *J. Phys. Chem. B* **2000,** 104, 6514.(h). Chen, W.; Zhang, J. Z.; Joly, A. G *J. Nanoscience and Nanotechnology* **2004**, 4, 919. (i). Kumar, S.; Nann, T. *Small* **2006**, 2, 316. (j). Eychmueller, A. *Angew. Chem. Int. Ed*. **2005**, 44, 4839.

18. (a). Li, H.; Rothberg, L. J. *J. Am. Chem. Soc*. **2004**,126, 10958. (b). Kong, X. L.; Huang, L. C. L.; Hsu, C.-M.; Chen, W.-H.; Han, C.-C.; Chang, H.-C. *Anal. Chem*. **2005**, 77, 259. (c). Loo, L.; Guenther, R. H.; Basnayake, V. R.; Lommel, S. A.; Franzen, S. *J. Am. Chem. Soc*. **2006**, 128, 4502. (d). Kerman, K.; Saito, M.; Morita, Y.; Takamura, Y.; Ozsoz, M.; Tamiya, E. *Anal. Chem*. **2004,** 76, 1877.

19. (a). Niemeyer, C. M.; Ceyhan, B. *Angew. Chem. Int. Ed.* **2001**, 40, 3685. (b). Li, M.; Mann, S. *J. Mater. Chem.* **2004**, 14, 2260.(c). Smorodin, T.; Beierlein, U.; Kotthaus, J. P. *Nanotechnology* **2005**,16,1123.

20. (a). Chen, M. S.; Goodman, D. W. *Catalysis Today* **2006**,111, 22.(b). Haruta, M. *Gold Bull.* **2004**, 37, 27. (c). Chen, M.; Goodman, D. W. *Acc. Chem. Res.* **2006**, 39, 739.

21 Huff, T.B.; Tong, L.; Zhao, Y.; Hansen, M. N.; Cheng, J.-X.; Wei, A.

Nanomedicine **2007**, 2, 125.

22. (a). Alivistos, A.P. *Science* **1996,** 271, 933. (b). El-Sayed, M.A. *Acc. Chem. Res*. **2004**, 37, 326. (c). Trindade, T.; O'Brien, P.; Pickett, N. L. *Chem. Mater.* **2001**, 13, 3843. (d). Azad Malik, M.; O'Brien, P.; Revaprasadu, N. *J. Mater. Chem*. **2001**, 11, 2382.

23. (a). Maier, S. A.; Brongersma, M. L.; Kik, P. G.; Meltzer, S.; Requicha, A. A. G.; Koel, B. E.; Atwater, H. A. *Adv. Mater*. **2003,**15, 562. (b). Benaissa, M. *Appl. Phy. Lett*. **1997**, 71, 3685. (c).Imahori, H.; Mitamura, K.; Shibano, Y.; Umeyama, T.; Matano, Y.; Yoshida, K.; Isoda, S.; Araki, Y.; Ito, O. *J. Phys. Chem. B* **2006**, 110, 11399. (d) Raimondi, F. ; Scherer, G. G. ; KÖtz, R. ; Wokaun, A. *Angew. Chem. Int. Ed*. **2005**, 44, 2190. (e). Goluch, E. D.; Nam, J.-M.; Georganopoulou, D. G.; Chiesl, T. N.; Shaikh, K. A.; Ryu, K. S.; Barron, A. E.; Mirkin, C. A.; Liu, C. *Lab Chip* **2006**, 6,1293. (f). Thaxton, C. S.; Hill, H. D.; Georganopoulou, D. G.; Stoeva, S. I.; Mirkin, C. A. *Anal. Chem*. **2005**, 77, 8174.(g). Narayanan, R.; El-Sayed, M.A. *J. Phys. Chem. B* **2005**, 109, 12663.

24. (a). Rolandi, M.; Quate, C. F.; Dai, H. *Adv. Mater*. **2002**, 14, 191.(b). Liu, G.-Y.; Xu, S.; Qian, Y. *Acc. Chem. Res*. **2000**,33,457.(c). Piner, R. D.; Zhu, J.; Xu, F.; Hong, S; Mirkin, C. A. *Science* **1999**, 283, 661. (d). Lee, K.B.; Park, S.J.; Mirkin, C.A.; Smith, J.C.; Mrksich, M. *Science*, **2002**, 295, 1702.(e). Maoz, R.; Cohen, S. R.; Sagiv, J. *Adv. Mater*. **1999**, 11, 55.(f). Zamborini, F. P.; Crooks, R. M. *J. Am. Chem. Soc.* **1998**, 120, 9700. (g). Chow, E.M.; Yaralioglu, G.G.; Quate, C.F.; Kenny, T.W.

Appl. Phys. Lett. **2002**, 80, 664. (h). Sulchek, T.; Grow, R.J.; Yaraloiglu, G.G.; Minne, S.C.; Quate, C.F.; Manalis, S.R.; Kiraz, A.; Aydine, A.; Atalar, A. *Appl. Phys. Lett*. **2001**, 78, 1787.

25. (a). Su, Y.-W.; Wu, C.-S.; Chen, C.-C.; Chen, C.-D. *Adv. Mater.***2003,** 15, 49. (b). Mendes, P. M.; Jacke, S.; Critchley, K.; Plaza, J.; Chen, Y.; Nikitin, K.; Palmer, R. E.; Preece, J. A.; Evans, S. D.; Fitzmaurice, D. *Langmuir* **2004**, 20, 3766.

26. (a). Wallraff, G. M.; Hinsberg, W. D. *Chem. Rev*.**1999**, 99,1801.(b). Watt, F.; Bettiol, A. A.; Van Kan, J. A.; Teo, E. J.; Breese, M. B. H. International .J. *Nanoscience* **2005**, 4, 269.

27. (a). Xia, Y.; Whitesides, G. M. *Angew. Chem., Int. Ed*. **1998**, 37, 550. (b) . Zhao, X. M.; Xia,Y.; Whitesides, G.M. *J. Mater.Chem.* **1997**, 7, 1069.(c). Xia, Y.; Whitesides, G. M. *Annual Review of Materials Science* **1998**, 28,153.

28. (a). Xu, J.; Li, H.-L. *J. Collid. Interface. Sci.* **1995**, 176, 138.(b). Templeton, A.C.; Cliffel, D. E.; Murray, R.W.*J.Am.Chem.Soc.***1999**,121, 7081. (c). Zhu,T.; Zhang, X.; Wang, X.; Fu,X.; Liu, Z.; *Thin solid films* **1998**, 327, 5221.

29. (a). Bandyopadhyay, K.; Patil,V.; Vijayamohnan, K.; Sastry, M**.** *Langmuir* **1997**, 13, 5244. (b). Colvin, V.L.; Goldstein, A.N.; Alivisatos, A. P. *J. Am. Chem. Soc.* **1992**, 114, 5221.

30. (a). Gorer, S.; Ganske, J. C.; Hemminger, J. C.; Penner, R. M. *J. Am. Chem. Soc.* **1998**, 120, 9584.(b). Hsiao, G. S.; Anderson, M.G.; Gerer, S.; Harris, D.; Penner, R.M.; *J. Am. Chem. Soc*. **1997**, 119, 1439. (c). Nyffenegger, R. M.; Craft, B.; Shaaban, M.;

Gorer, S.; Penner, R. M.; *Chem. Mater*. **1998**, 10, 1120.

31. (a). Chen, Y.; Au, J.; Kazlas, P.; Ritenour, A.; Gates, H.; McCreary, M. *Nature* **2003**, 423, 136. (b). Andersson, P.; Nilsson, D.; Svensson, P.-O.; Chen, M.; Malmstrom, A.; Remonen, T.; Kugler, T.; Berggren, M. *Adv.Mater*.**2002,** 14, 1460.

1.1 Introduction

High surface to volume ratio, exhibition of quantum mechanical behavior, chemical reactivity and other physical properties have propelled a "Gold Rush" for generation and utilization of materials with nanometer dimensions. Metal [1-4] and semiconductor nanoparticles (NPs) [5–9] especially have occupied the center-stage in this activity owing to their unique chemical and physical properties associated with particle size and shape at the nanoscale and as a consequence their application potential in various fields such as opto-electronic devices [10] sensors [11-12] magnetic materials [13] and storage systems [14]. In addition to the preferred methods of preparation in colloidal solution, a large number of methods have been developed for synthesis of NPs inside various porous materials [15], depositions of NPs on surfaces [16,17] and their incorporation into polymer matrices [18,19]. Metal NPs have also been utilized in the synthesis of conducting polymer–NP composites [20]. The recent surge in the syntheses and functionalization of NPs offer excellent scope for many a application such as in catalysis[21-22], surface enhanced Raman scattering (SERS)[23], enhanced fluorescence[24], chemical and biochemical sensing[25], non-linear optical devices[26], plasmonics[27], and photonics[28]. Moreover, compatibility of many of the NPs with the bio molecules has created considerable interest in nanobiotechnology[29] with application in DNA sequencing[30], controlled drug delivery[31], anticancer drug[32], bio-chemical sensing and detection[33-35], contrast agents in cellular and biological imaging[36-37].

In parallel with the development of various easy and eco-friendly methods for the generation of the NPs, there are efforts to synthesize nanoparticles in or within various solid matrixes. This would help in multiple usage as well as use of the NPs in different heterogeneous environmental conditions. For example, C. R. Martin[38] and coworkers have synthesized NPs inside the pores of Zeolites to get monodispersed NPs. This template based method has been used to synthesize nanoscopic particles of metal, polymers, semiconductors and other materials. On the other hand Willner co workers[39] have developed several ways for attachment of NPs on the various substrate surfaces like glass, metal, and polymer by either modifying the surface or by functionalizing the NPs. On the other hand, several methods[40-41] have been introduced to trap NPs inside polymers and sol-gel materials. In addition, Kumacheva[42] and coworkers have synthesized metal and semiconductor NPs in dispersed ion exchanged resins. Furthermore, Qun Huo[43-44] *et al*., have reported an interesting method for solid state synthesis of Au NPs, functionalized with single carboxylic acid, using polystyrene resin and they found that this solid phase synthesis is more effective compared to solution based synthesis in controlling the surface functionalities.

Despite a large number of methods that are currently available for the syntheses of NPs, there are few reports about the reversible storage of NPs in solid-state resin beads. Finding ways for solid-state storage of colloidal NPs is important as it would make applications more versatile and transportation easier than if stored in the form of colloidal solution. For example, colloidal NPs stored in solid state can be used for chemical reaction

under different solvent systems eliminating the need of their phase transfer for utilization in different solvents.

Herein we introduce the idea and report a method of storage of Ag NPs in anion exchange resins and also a procedure for their recovery. The method is based on the principle of exchange of ions between the resins and the colloidal solution containing Ag NPs which have overall negative charge on their surfaces. The advantage of the present method is that these NPs could be stored in resins and then the same resins could be taken out of the solvent and dried for further use as such or by extracting the NPs into a solvent. Our observation

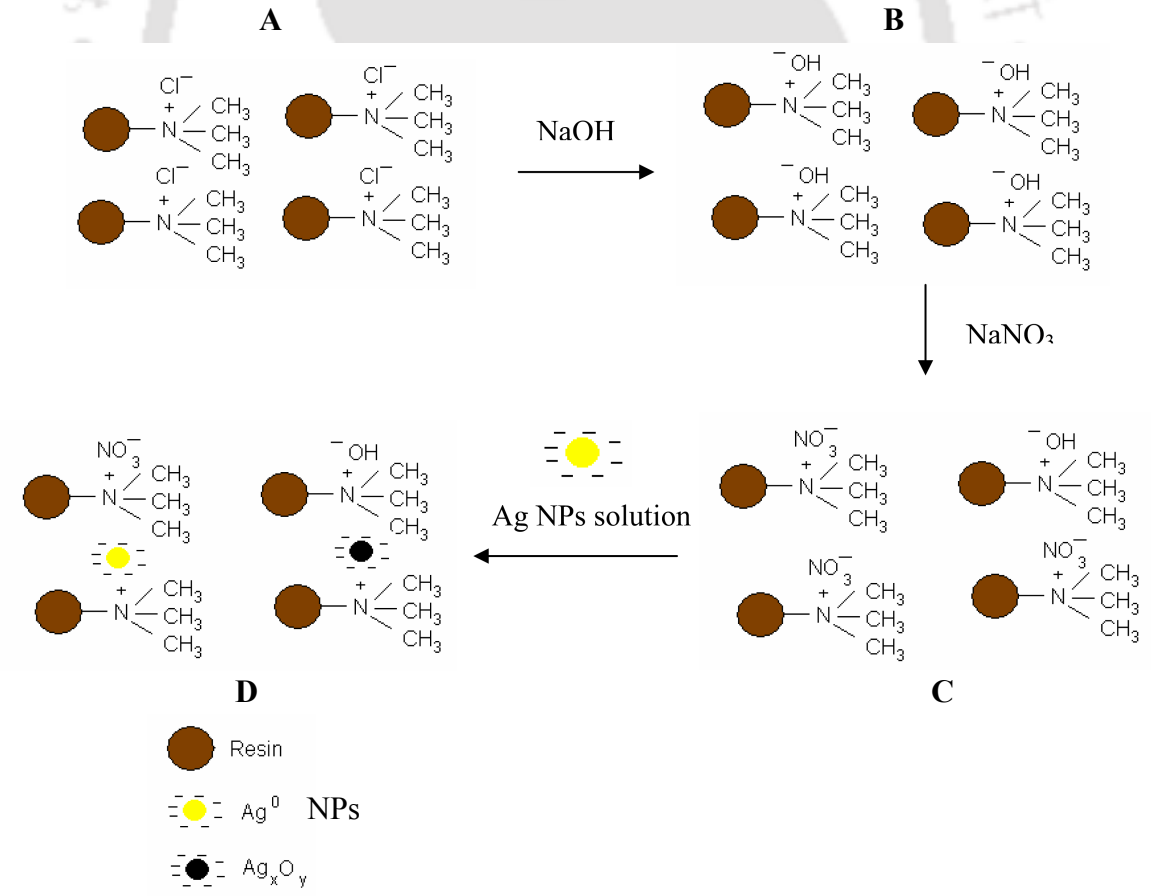

Figure 2.1 An anion exchange resin Amberlite IR-400 is polystyrene divinylbenzene co-polymer with terminal trimethyl ammonium group having chloride as a counter ion is the chosen solid substrate. Treatment with sodium hydroxide (NaOH) results in exchange of the chloride counter ion in the resin with OH^- (B). Further treatment with suitable amount of sodium nitrate replaces some of the exchangeable groups with nitrate ions (C). The silver nanoparticles prepared with and without a stabilizer can be trapped in such resin beads by replacing the counter ions.

Further suggests that Ag NPs we synthesized could however not be stored in cation exchange resins. We also demonstrate that these particles could be recovered and subsequently used for catalytic reduction of a dye in presence of $NaBH_4$. Finally, we report that the Ag NPs while being exchanged with the anions of the resins are converted into silver oxide particles under the present reaction condition and hence are actually stored in the form of silver oxide particles.

These particles are stable for more than a year in their adsorbed state in terms of the size as no significant agglomeration could be observed in scanning electron micrographs (SEM). Also, their characteristic X-ray diffraction (XRD) patterns show no significant change with time. A schematic representation of the present method of storing Ag NPs in anion exchange resin beads and also their recovery is shown in Fig. 2.1. The method takes advantage of the negative surface charge on nanoparticles to exchange itself on to an ion exchange resin.

2.2 Experimental Section

2.2.1 Preparation of Ag nanoparticles (NPs): 40 µL of 0.105 M $AgNO_3$, 30 µL of 0.01 M $NaBH_4$ were mixed in 4.9 mL of H_2O. The mixture immediately resulted in a yellow color solution, which is characteristic of Ag NP formation. It was further confirmed by recording of UV-visible spectrum with a maximum occurring at 405 nm. In separate runs, Ag NPs were also prepared in the presence of 32.4 mM sodium dodecyl sulfate (SDS). In that case 200 µL of SDS solution was added to the solution containing $AgNO_3$ and $NaBH_4$ as of the above concentration.

2.2.2 Activation of Anion Exchange Resins: 3.0 g of Amberlite IR400 resin was first treated with 20 mL of 1N NaOH solution for 1hr. They were then washed with plenty of water to remove excess NaOH. To the resins 40 ml of 2 M $NaNO_3$ was added and kept for 1 hr before washing again with copious amount of water.

2.2.3 Storage of Ag NPs into the activated anionic resins: All of the resins activated as above were loaded into a column. The total volume of Ag NP solution prepared above was added slowly to the column. The solution with the resin was kept in the column for 15 min. Then the eluent was collected in a beaker for further analysis. On the other hand the resins in the column were further washed with plenty of water to remove precipitate, if any, of Ag NPs in between the beads.

2.2.4 Extraction of Ag NPs from the resins

(a) With SDS and $NaBH_4$ in water. 20 µl of 32.4 mM SDS and 60 µl of 0.005 M $NaBH_4$ were added to 5 ml of H_2O. This solution was added to a beaker containing the above Ag NP exchanged resins and kept for 1 min. The characteristic yellow color solution with absorption maximum at 410 nm was obtained.

(b) With Polyethylene Glycol (PEG) and $NaBH_4$ in water: 200 µL of 0.33 M PEG 6000 (mol. Wt.5000-7000) and 60 µL of 0.005 M $NaBH_4$ were added to 5 ml of H_2O. The resultant solution was added to a beaker containing the above amount of Ag NP exchanged resins prepared separately. The solution was kept for 1 min. The characteristic yellow color solution with absorption maximum at 407 nm was obtained.

2.2.5 TEM measurements: Transmission electron microscopic (of Phillips) measurements were performed after evaporating a drop of solution containing SDS stabilized Ag NPs (both before exchange and after recovery from the resins) on a carbon-coated grid.

2.2.6 Catalytic Reduction of Eosin: 0.2 g of Ag NP exchanged resins was kept in a 3 ml quartz cuvette into which 2.9 ml of H_2O, 5 µL of 3.9 mM eosin and 80 µL of 0.005 M $NaBH_4$ were added. The solution was mixed by shaking and then was kept inside the sample compartment of a Hitachi U2001 UV-visible spectrophotometer for measurements of time dependent absorption. Similar set up and concentrations were used for measurements in presence of activated resin, eosin and $NaBH_4$ and in a separate experiment with eosin and $NaBH_4$ solution.

2.2.7 Powder XRD measurements: From the measurement of powder XRD it was observed that use of larger size commercially available resins (which were used for the present studies) did not provide any detectable signal. We found that the resins needed to be finely ground for better signal. Thus resins were activated with NaOH and then treated with 2 M $NaNO_3$ by the method described above. The treated resins were finely ground using a pestle and a mortar, which were then dispersed into an aqueous solution of Ag NPs prepared by $NaBH_4$. After 15 min the solution was centrifuged at a speed of 3000 rpm for 30 min to obtain the powder, which was washed several times before drying for further use. A Seifert powder X – Ray diffractometer (XRD 3003 TT) with Cu - α source with wavelength 1.54 Å was used for recording data at room temperature.

2.2.8 Diffuse Reflectance FTIR: Diffused reflectance FTIR spectroscopic studies were performed on resin samples using a Perkin Elmer Spectrum One spectrophotometer. The sample preparation procedures were the same as in the case for XRD measurements. For each sample 12.5 mg anion exchange resin (activated as well as Ag NP exchanged) was used for recording diffuse reflectance spectra.

2.2.9 SEM measurements and EDX measurements: Scanning electron microscope measurement of the silver NPs stored resin beads was performed using LEO VP 1430, with accelerating voltage 20 KV, and elemental analysis was performed by energy dispersive X-analysis (EDX) measurements using an Oxford INCA X-Sight instrument**.**

2.2.10 Ag NP exchanges with cation exchange resins: 3.0 g of cation exchange resin was activated with 3 M HCl and were then washed with water. They were then loaded into a column. Ag NP solution as prepared above was poured into the column slowly and then kept for 15 min. The eluant was then collected and analyzed using UV-vis spectroscopy.

2.2.11 Instruments: Hitachi U2001 UV-visible spectrophotometer or Perkin Elmer Spectrum25, Perkin Elmer one spectrophotometer was used for spectroscopic absorption measurements; a Seifert powder X – Ray diffractometer (XRD 3003 TT) with Cu - α source with wavelength 1.54 Å was used for XRD measurements; a scanning electron microscope (model no. LEO model no VP 1430) with energy dispersive X-analysis (EDX) measurement facility manufactured by Oxford INCA X-Sight was also used.

2.3 Results and Discussion

2.3.1 Anion exchange resin

We were successful in storing the Ag nanoparticles in anion exchange resin, Figure 2.2 shows the steps involved in this process. As shown in the figure Ag nanoparticles prepared separately when loaded into the column filled with anion exchange resin beads get trapped in the resin. Trapped nanoparticles can be released simply by treating the loaded resin with sodium borohydride solution.

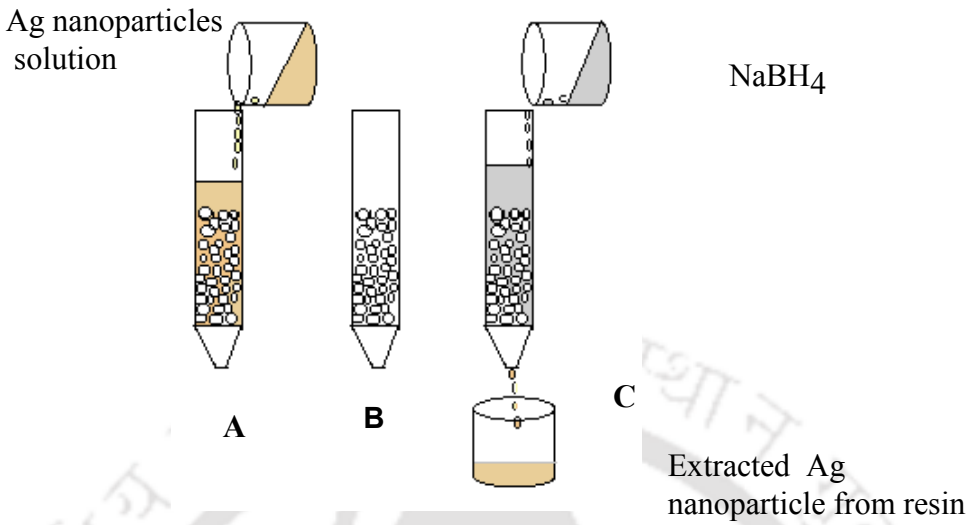

Figure 2.2 Schematic diagram of the present method of storage and recovery of Ag NPs in anion exchange resin beads. (A) Ag NP solution being loading into the resins in a column. (B) Ag NPs containing resins after washing with water. (C) Ag NPs being extracted from resins using $NaBH_4$ solution.

We have observed that simultaneous presence of both OH^- ions and NO_3^- ions in the activated resins were needed for efficient exchange of Ag NPs. On the other hand, if the resins were activated with either of OH^- and NO_3^- ions no exchange of Ag NPs took place. It was observed that the suitable ratio of NO_3^- ions to OH^- ions was found to be 77:23 for achieving the best exchange. In addition, it is important to note here that we have not been able exchange Ag NPs with cation exchange resins (see later). This could be due to overall

negative charges on the surface of Ag NPs that help in storing them in anion exchange resins[45]. Further, we would like to mention here that the Ag NPs were prepared both in presence and absence of SDS stabilizer. We used the stabilizer when the time required for a particular set of experiments was long. On the other hand when the experiment could be completed in a shorter time we did not use any stabilizer. The ion exchange of NPs took place equally efficiently in both the cases.

In Figure 2.3A we show the UV-vis absorption spectrum of colloidal Ag NPs solution prepared using the present method. The peak at 430 nm is characteristic of Ag NPs present in the solution. In Figure 2.3B, we show the UV-vis spectrum of the remaining solution after Ag NPs were exchanged with the resins. Shown in Figure 2.3C is the UV-vis absorption spectrum of the Ag NPs solution extracted from the resins using $NaBH_4$. As clear from the UV-vis spectra, the characteristic absorption of Ag NPs at 405 nm is absent in 2.3B that was present in both 2.3A and 2.3C. In addition, we observed that the color of the solution of Ag NPs vanished upon treatment with resins, which reappeared upon treatment with $NaBH_4$. These observations support the idea that Ag NPs could be exchanged with anion exchange resins and they could also be recovered using the present method (by treatment with $NaBH_4$). Further, that the silver NPs were exchanged in resin beads and did not precipitate on the column was confirmed by the observation that even after washing with water the Ag NPs did not come out of the resins and also by the requirement of $NaBH_4$ to extract the NPs back from the resins. FTIR spectroscopic measurements also indicate exchange of NPs in the resin by replacement of NO_3^- ions (see later). The above experiments demonstrate the ability of the

present method to store Ag NPs in anion exchange resins by exchanging with the anions of the resins.

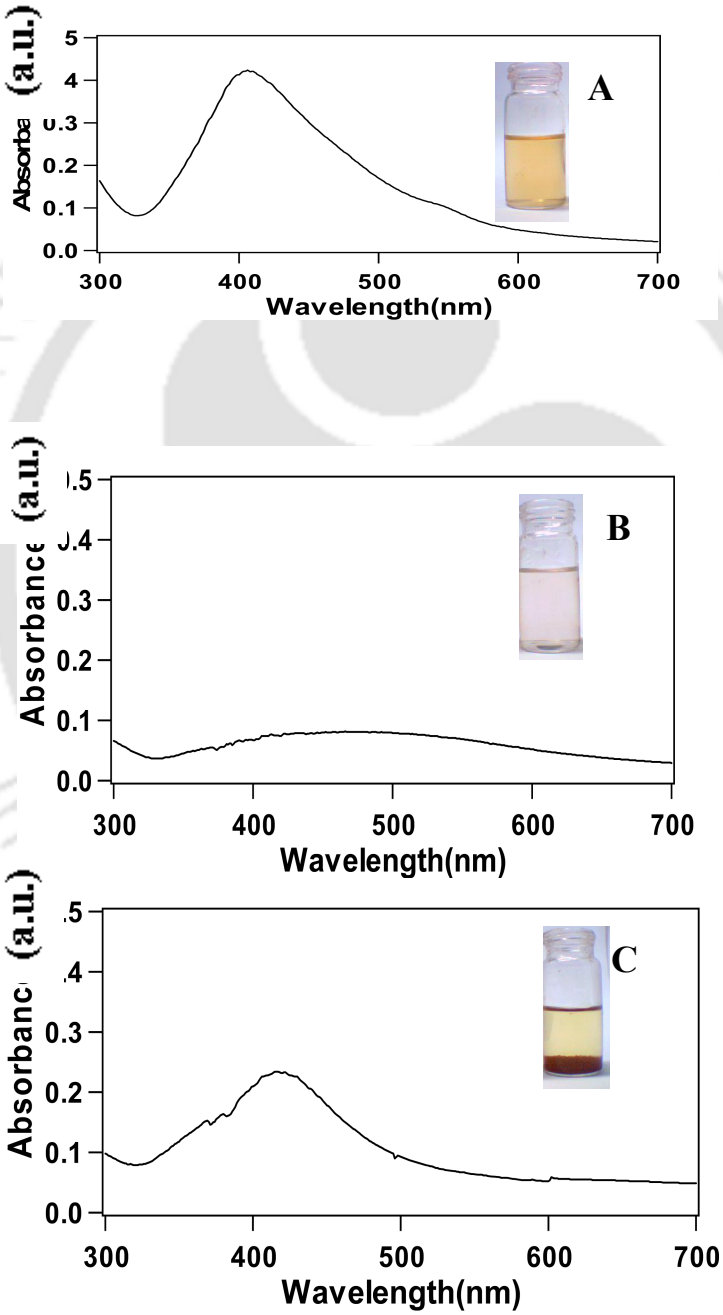

Figure 2.3 UV-vis absorption spectra of (A) Ag NPs solution in presence of SDS stabilizer (B) Ag NPs solution after passing through resin and (C) Ag NPs extracted from resin.

2.3.2 Cation exchange resin

Here we report our observation that while anion exchange resins could store Ag NPs, cation exchange resins however were not able to store the Ag NPs synthesized using the present method. This is evident from Figure 2.4 where the UV-vis absorption spectra of Ag NPs before and after passing through cation exchange resin column did not differ significantly. This could be due to overall negative charges on the surface of Ag NPs that help in storing them in anion exchange resins while they cannot be exchanged with cation exchange resins.

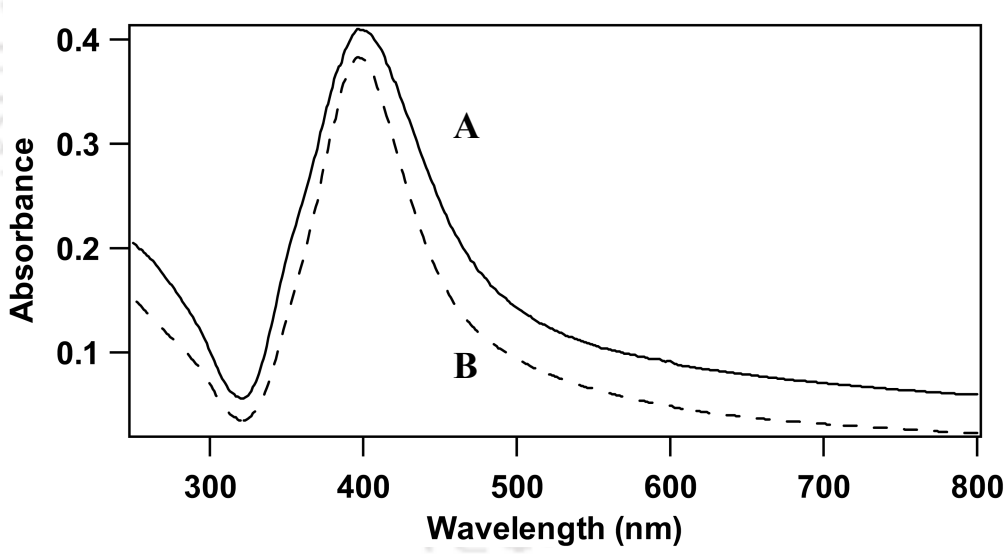

Figure 2.4 UV-vis absorption spectra of (A) Ag NPs solution before and (B) after passing through cation exchange resin column.

2.3.3 FTIR Studies on exchange of Ag NPs with anion exchange resins

The idea behind the study was to determine the nature of ions the Ag NPs were exchanging in the process of their storage in the resins. For this we performed diffuse reflectance FTIR measurements of OH^- activated resins, resins activated by OH^- and NO_3^- ions and that of resins after Ag NPs solution was passed through them (starting with resins activated by OH^- and NO_3^- ions).

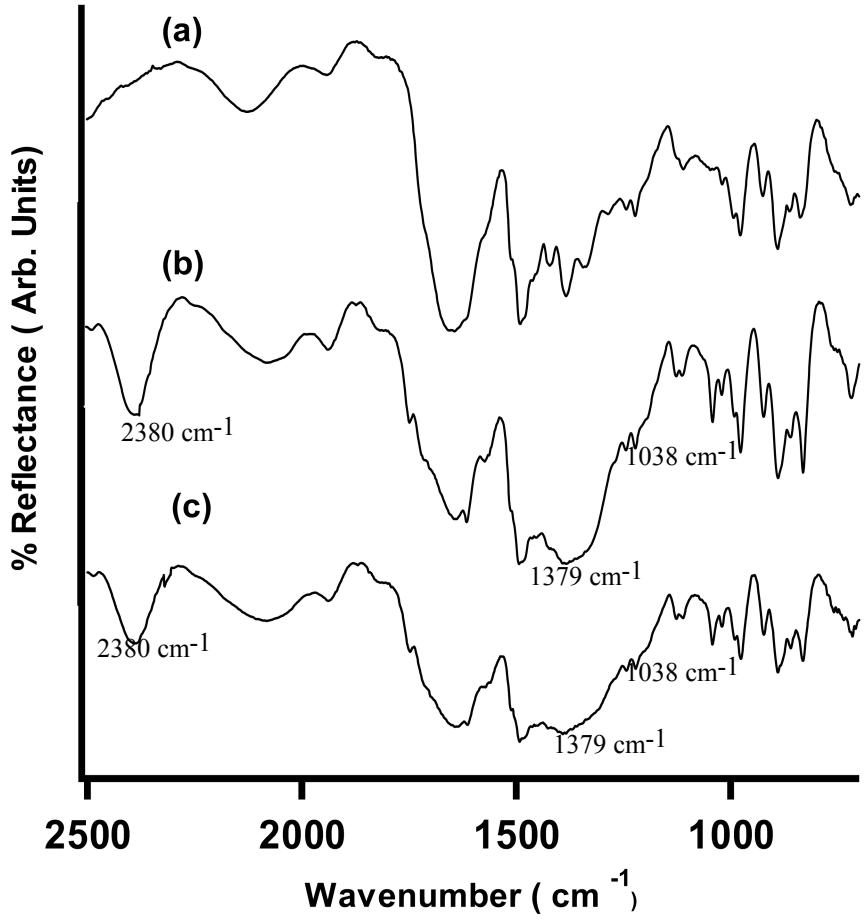

Figure 2.5 Diffuse Reflectance FTIR of ground anion exchange resin showing the exchange of NO_3 . The resin activated with (a) NaOH (b) NaOH and $NaNO_3$, and (c) that of resins after Ag nanoparticle solution was passed through them.

As shown in Figure 2.5, three characteristic peaks due to NO_3^- occurred, at 2380, 1379 and 1038 cm^{-1}, in resins activated by OH^- and NO_3^- ions. These peaks were absent in OH^- activated resins. Intensities of them were considerably stronger in NO_3^- plus OH^- activated resins compared to those in Ag NPs exchanged resins. The reduction in peak intensity shows that Ag NPs were replacing NO_3^- present in the resins even though the solution of Ag NPs contained additional NO_3^- ions carried over from the parent $AgNO_3$ solution. Thus the storage of Ag NPs in the resins accompanied exchange of NO_3^- ions.

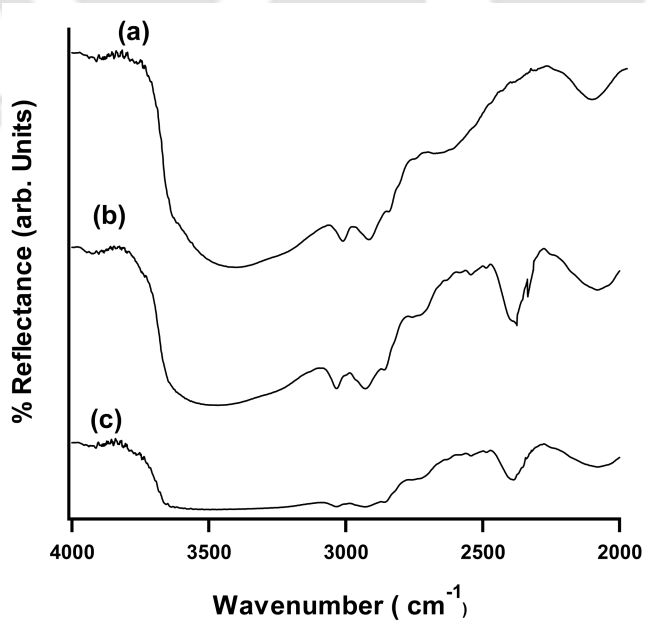

Figure 2.6 Diffuse Reflectance FTIR of ground anion exchange resin showing the exchange of OH. The resin activated with (a) NaOH (b) NaOH and $NaNO_3$, and (c) that of resins after Ag nanoparticle solution was passed through them.

In addition, the OH peak intensity at 3400 cm^{-1} shown clearly in Figure 2.6, gradually diminished from OH^- activated resins to OH^- and NO_3^- activated resins to Ag NPs exchanged resins (Figures 2.6a, 2.6b and 2.6c respectively) indicating possible loss of OH^- ions during exchange. This may possibly indicate the involvement of OH^- ions in oxidation of Ag NPs during storage as Ag oxides (see later). Further, we found the pH of the solution after exchange was reduced from 5.8 to 4.2 indicating loss of OH^- ions in the resulting solution that was passed through the resin column.

2.3.4 Transmission electron microscopic study

We further confirmed the formation and extraction of Ag NPs using the present method by performing transmission electron microscopic (TEM) measurements on the samples. Figure 2.7(A) shows the TEM picture of Ag NPs prepared by usual borohydride method. Figure 2.7(B) shows the TEM picture of the Ag NPs extracted from the resin beads. Ag NPs in this case were prepared as well as extracted from the resins in the presence of SDS. The Ag NPs

have majority particle sizes distributed between 5 nm and 55 nm in the parent solution (Figure 2.7A') and between 3 nm and 33 nm (Figure 2.7B') in the extracted solution. Similar results were obtained with Ag NPs synthesized and extracted by using $NaBH_4$ in presence of polyethylene glycol.

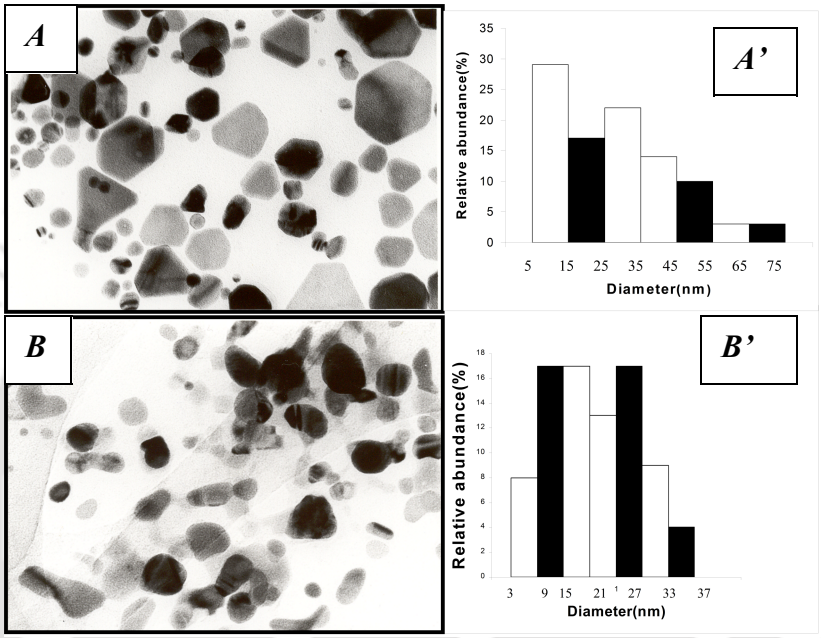

Figure 2.7 (A) Transmission electron microscopic pictures of silver nanoparticles prepared by borohydride methods and (B) that of silver nanoparticles extracted from the resin beads. The particle size distributions are shown in A' and B' respectively.(The scale bar in the picture is 66 nm)

2.3.5 Time dependent reduction of eosin by Ag NPs extracted from resins

We further demonstrate that the stored Ag NPs could be extracted from the resins by using $NaBH_4$ and subsequently utilized for catalytic reduction of an organic dye (eosin). $NaBH_4$, needed to extract NPs from the resins, is also known to reduce eosin in aqueous solution.

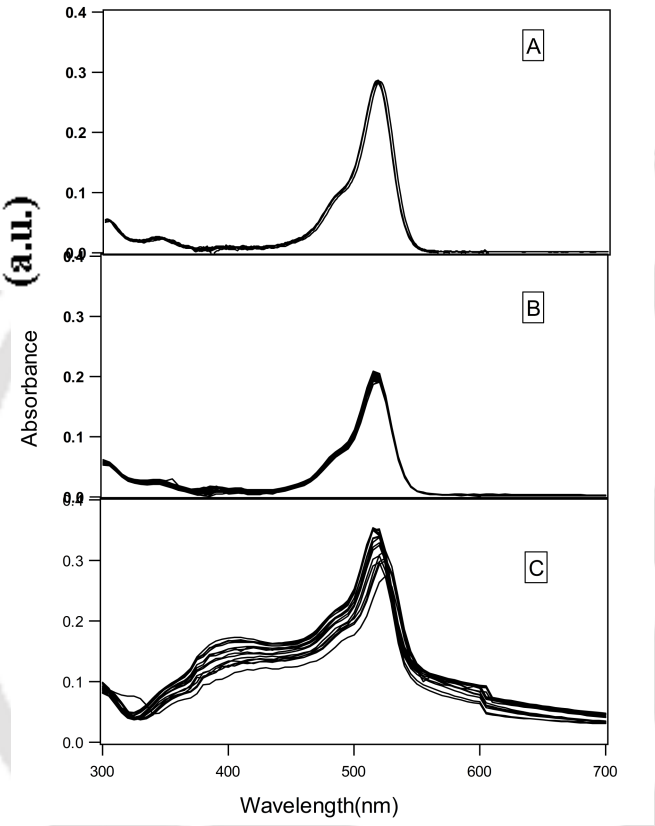

Figure 2.8 Time depended UV-vis absorption spectra (10 min interval between two consecutive spectra) of reduction of eosin in presence of (A) $NaBH_4$ (10 spectra shown), (B) $NaBH_4$ and activated resin (15 spectra) and (C) $NaBH_4$ and Ag NP exchanged resins (15 spectra).

Further, Ag NPs are known to catalyze the reduction of eosin. We have taken advantage of this and have followed the reaction by time dependent UV-vis absorption of the dye with a

peak at 510 nm. The extraction of Ag NPs was also simultaneously monitored with a peak at 400 nm. The results are shown in Figure 2.8. Figure 2.8A is the UV-vis time evolution of absorption spectrum of the dye in presence of only $NaBH_4$, while shown in Figure 2.8B is the rate of reduction of eosin in presence of $NaBH_4$ and OH^- plus NO_3^- activated resins. On the other hand, Figure 2.8C, representing the reduction of dye in presence of Ag NP exchanged resins and $NaBH_4$, clearly demonstrates that the rate of reduction was the fastest in the present case. It is also noteworthy that reduction of intensity of the dye peak occurred concurrently with appearance of the peak due to Ag NPs. This means that the NPs were regenerated into the solution, which further catalyzed the reduction of the dye.

2.3.6 XRD patterns of NPs in the resin

We also wanted to learn whether the Ag NPs were stored in the resins in the form of Ag NPs or not. We observed no XRD peaks in the ordinary Ag NP exchanged resins. To improve the intensity of the signal the resins were activated and then ground into finely divided powder, which were then dispersed into an aqueous solution of Ag NPs prepared by $NaBH_4$. They were washed and then dried for recording powder XRD. As shown in Figure 2.9, the X-Ray diffraction pattern of the Ag NPs exchanged resins had peaks at $2\theta = 27.7^o$ (PDF 84-1261), 32.1^o (PDF 76-1489) and 46.0^o (PDF 42-874), which correspond to (110) Ag_3O_4, (111) AgO and (003) Ag_2O respectively. Thus the characteristic XRD peaks were those of Ag oxides and the peaks characteristic of Ag were not observed. This observation indicates that while exchanging with the anions of the resins the Ag NPs were converted into

oxides of silver. It is well known that in presence of $NaBH_4$ and dissolved oxygen in water Ag NPs form oxides[24]. Here it may be further facilitated by adsorption of NPs into the anion exchange resins, which may be the reason for the present observation.

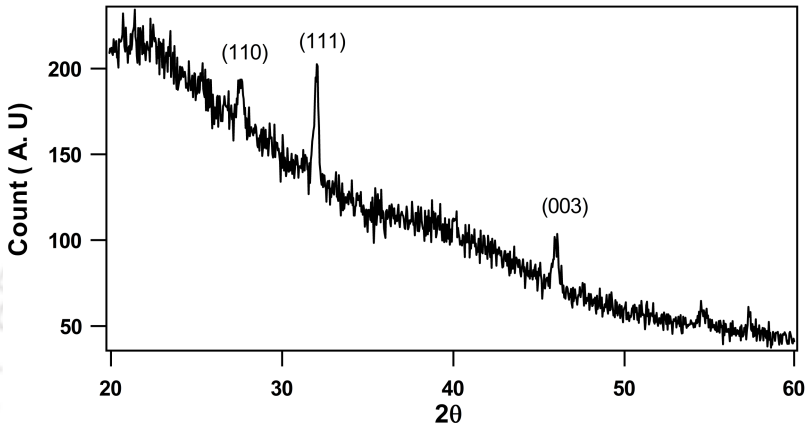

Figure 2.9 Powder X-Ray diffraction pattern of Ag NP exchanged resins.

2.3.7 Time dependent XRD of the stored NPs on the resin surface

We further pursued studies regarding the stability of the stored NPs on the resin surface. In case these particles (i.e. the oxides of Ag) get transformed to other Ag compounds with time then a corresponding shift in the peak positions of XRD can be expected.

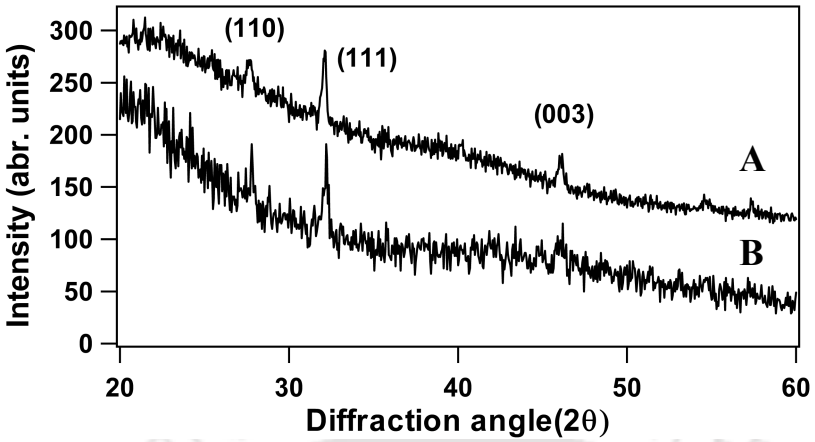

Figure 2.10 XRD patterns of one-day old resin beads where NPs were stored (A) and also the beads recorded after more than one-year (B).

For this XRD study also we have used ground resin as already mentioned in the previous experiment. The results are shown for a one-day old sample versus more than one-year old sample in Figure 2.10. The figure clearly shows that the three peaks due to oxides of Ag were intact even after one year as there is no shift in values of 2θ in the diffraction pattern. In addition, the intensities of the peaks did not change with time. This means the stored NPs were stable on the surface of the resins for more than a year.

2.3.8 State of aggregation of the stored NPs on the resin as shown by SEM

Finally we wanted to find out the state of aggregation of the stored NPs on the resin surface as a function of time. For this purpose we prepared samples in the same way as for recording XRD. We then recorded the SEM of such samples one day after the storage the NPs and kept the same sample for one month and once again recorded the SEM. The results are shown in Figure 2.11A (one-day old sample) and Figure 2.11B (one-month old sample). As

clear from the figure, there are NPs which are presented as isolated particles and there are some which are agglomerated.

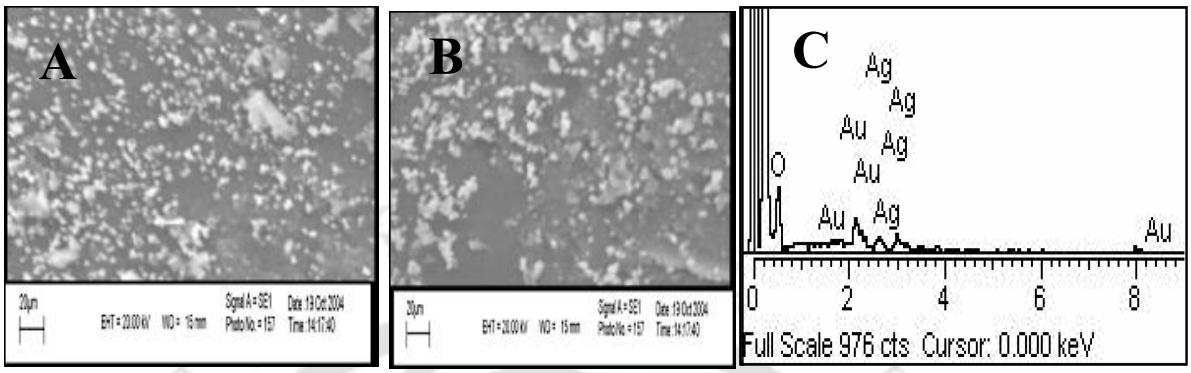

Figure 2.11 SEM of NPs stored resin beads recorded on the next day of sample preparation (A) and that after one month (B). EDX of one month old sample (C)

However, over one month there is no gross change in this pattern to suggest a possible further agglomeration of them on the surface of the resin beads. Energy dispersive X-ray analysis (not shown here) of both the samples were performed to confirm the presence of Ag species on the surfaces.

2.4 Conclusion

Herein we have been able to demonstrate reversible storage and retrieval of Ag nanoparticles in anion exchange resin. We also have shown that these NPs could be recovered and utilized for catalytic reduction of a dye. While being exchanged the Ag NPs were converted into their oxide forms in the resins. On the other hand these stored NPs were stable for more than a year in their chemical form as well as sizes.

2.5 References:

1. Sun, Y.; Xia, Y. *Science* **2002,** 298, 2176.
2. Mandal, S.; Selvakanan, P. R.; Roy, D.; Chaudhari, R. V.; Sastry, M. *Chem Commun.* **2002**, 3002.
3. Schauermann, S.; Hoffmann, J.; Johánek, V.; Hartmann, J.; Libuda, J.; Freund, H. J. *Angew. Chem. Int. Ed.* **2002**, 41, 2532.
4. Manna, A.; Imae, T.; Iida, M.; Hisamatsu, N. *Langmuir* **2001,** 17, 6000.
5. Morris, T.; Copeland, H.; Szulczewski, G. *Langmuir* **2002,** 18, 535.
6. Gao, S.; Lu, J.; Chen, N.; Zhao, Y.; Xie, Y. *Chem Commun.* **2002,** 3064.
7. Farmer, S. C.; Patten, T. E. *Chem. Mater.* **2001,** 13, 3920.
8. Yu, J. C.; Yu, J.; Ho, W.; Zhang, L. *Chem Commun.* **2001**, 1942.
9. Noack, V.; Eychmüller, A. *Chem. Mater*. **2002**, 14, 1411.
10. (a) Hu, M.S.; Chen, H.L.; Shen, C.H,; Hong, L.S.; Huang, B.R.; Chen, K.H.; Chen, L.C. *Nature Material* **2006,** 5, 102. (b) Yilmaz, O. F.; Chaudhary, S.; Ozkan, M. *Nanotechnology* **2006**, 17, 3662.
11. Dai, Z.; Kawde, A.-N.; Xiang, Y.; La Belle, J.T.; Gerlach, J.; Bhavanandan, V. P.; Joshi, L.; Wang, J. *J. Am. Chem. Soc*. **2006**,128, 10018.
12. (a) Liu, Juewen; Mazumdar, Debapriya; Lu, Yi. *Angew. Chem. Int. Ed*. **2006**,45,7955.

    (b) Sun, S.; Anders, S.; Hamann, H. F.; Thiele, J. U.; Baglin, J. E. E. ; Thomson, T.; Fullerton, E. E.; Murray, C. B.; Terris, B. D. *J. Am. Chem Soc.* **2002**, 124, 2884

    (c) Epifani, M.; Diaz, R.; Arbiol, J.; Comini, E.; Sergent, N.; Pagnier, T.; Siciliano, P.; Faglia, G.; Morante, J. R. *Adv. Funct. Mater*.**2006**,16,1488.

13. (a) Xu, L.; Zhou, W.; Kozlov, M. E.; Khayrullin, I. I.; Udod, I.; Zakhidov, A. A.; Baughman, R. H.; Wiley, J. B. *J. Am. Chem Soc.* **2001**, 123, 763 (b) Margeat, O.; Ciuculescu, D.; Lecante, P.; Respaud, M.; Amiens, C.; Chaudret, B. *Small* **2007,** 451.

(c) Jun, Y-w.; Choi, J-s.; Cheon, J. *Chem. Commum*. **2007**, 12,1203.

14. Martin, C. R. *Science* **1994**, 266, 1961.(b) Kim, H.-S.; Lee, H.; Han, K.-S.; Kim, J.-H.; Song, M.-S.; Park, M.-S.; Lee, J.-Y.; Kang, J.-K. *J. Phy. Chem. B* **2005**, 109, 8983.
(c) Chen, P.; Wu, X.; Lin, J.; Tan, K. L. *Scienc.* **1999**, 285, 91.

15. Pol, V. G.; Srivastava, D. N.; Palchik, O.; Palchik, V.; Slifkin, M. A.; Weiss, A. M.; Gedanken A. *Langmuir* **2002,** 18, 3352.

16. Sarathy, K. V.; Thomas, P. J.; Kulkarni, G. U.; Rao C. N. R. *J. Phys. Chem. B* **1999,** 103, 399.

17. Wang, T. C.; Rubner, M. F.; Cohen, R. C. *Langmuir* **2002,** 18, 3370.

18. Rong, M.; Zhang, M.; Liu, H.; Zeng, H. *Polymer* **1999**, 40, 616.

19. Zhang, J.; Coombs, N.; Kumacheva, E. *J. Am. Chem Soc.* **2002**, 124, 14512.

20. Sarma, T. K.; Chowdhury, D.; Paul A.; Chattopadhyay, A. *Chem. Commun*, **2002**, 10, 1048.

21. Gou, L.; Murphy. C. J. *Chem. Commum.* .**2005**, 5907.

22. Raimondi, F., Scherer, G. G., Ko¨tz, R.; Wokaun, A. *Angew. Chem., Int. Ed.* **2005**, 44, 2190.

23. (a) Keating, C. D.; Kovaleski, K.M.; Natan, M. J. *J. Phys. Chem. B* **1998**,102, 9404.

(b) Kneipp, H.; Itzkan, I.; Dasari, R.D.; Feld, M. S. *Chem. Rev*. **1999**, 99, 2957.

(c) Campion, A.; Kambhampati, P. *Chem .Soc. Rev.* **1998,** 27, 241.

24. (a). Kurita, A.; Kanematsu, Y.; Watanabe, M., Hirata, K.; Kushida, T. *Phys*. *Rev*. *Lett.* **1999**, *83*, 1582 (b). Santra. S.; Yang. H.; Holloway. P. H.; Stanley. J. T.; Mericle. R. A. *J. Am. Chem. Soc.* **2005**, *127*, 1656.

25. Jia, J.; Wang, B.; Wu, A.; Cheng, G .; Li, Z.; Dong, S.; *Anal. Chem*. **2002**, 74, 2217.

26. Hu, M.S.; Chen, H. L.; Shen, C.H,; Hong, L.S.; Huang, B.R.; Chen, K.H.; Chen, L. C. *Nat. Mater*. **2006**, 5, 102.

27. Ruiz, V.; Colina, A.; Heras, Ar_n.; pez-Palacios, J. L. *Small* **2006**, 2, 56.

28. (a) Kempa, K.; Kimball, B.; Rybczynski, J.; Huang, Z. P.; Wu, P. F.; Steeves, D.; Sennett, M;. Giersig, M.; Rao, D. V. G. L. N. D.; Carnahan, L.; Wang, D. Z.; Lao, J.Y.; Li, W. Z.; Ren, Z. F. *Nano Lett.* **2003**, 3, 13. (b) Jiang, S.H.; Smith, D.W.; Ballato, J.M.; Foulger, S. H. *Adv.Mater*. **2005**, 17,179.

29. Niemeyer, C.M. *Angew. Chem. Int. Ed*. **2001**,40,4128.

30. (a) Niemeyer. C.M.; Burger, W.; Peplies, J. *Angew.Chem.Int.Ed*. **1998**, 110, 2391.

(b) Niemeyer, C. M.; Burger, W.; Peplies, J. *Angew.Chem.Int.Ed.* **1998**, 37, 2265.

(c) Mirkin, C.A.; Letsinger, R.L.; Mucic, R.C.; Storhoff, J.J. *Nature* **1996**, 382,607.

31. Soppimath, K.S.; Tan, D.C.; Yang, Y.Y. *Adv.Mate*r. **2005**, 17, 318.

32. Levy, L.; Sahoo, Y.; Kim, K.S.; Bergey, E.J.; Prasad, P.N. *Chem. Mater*. **2002**, 3717.

33. Riboh, J. C.; Haes, A. J.; McFarland, A. D.; Ranjit, C.; Van Duyne, R. P. *J. Phys. Chem. B* **2003**, *107*, 1772.

34. Shafer-Peltier, K. E.; Haynes, C. L.; Glucksberg, M. R.; Van Duyne, R. P. *J. Am. Chem. Soc.* **2003**, *125*, 588.

35. Storhoff, J. J.; Elghanian, R.; Mucic, R. C.; Mirkin, C. A.; Letsinger, R. L. *J. Am. Chem. Soc.* **1998**, *120*, 1959.

36. Wang, Y.; Xie, X.; Wang, X.; Ku, G.; Gill, K. L.; O'Neal, D. P.;Stoics, G.; Wang, L. V. *Nano Lett.* **2004**, *4*, 1689.

37. El-Sayed, I. H.; Huang, X.; El-Sayed, M. A. *Nano Lett.* **2005**, *5*, 829.

38. Martin, C. R. *Science* **1994**, 266, 1961.

39. Shipway, A. N.; Willner, I. *Chem. Commun.* **2001,** 2035.

40. (a) Mei, Y.; Lu, Y.; Polzer, F.; B, M.; Drechsler, M. *Chem. Mater*. **2007**,19,1062. (b) Compagnini, G.; Scalisi, A. A.; Puglisi, O.; Spinella, C. *J. Mater. Res.* **2004**, *19*, 2795. (c) Mei, Y.; Sharma, G.;Lu, Y.; Ballauff, M.; Drechsler, M.; Irrgang, T.; Kempe, R. *Langmuir* **2005**, 21, 12229.

41. (a) Sivakumar, S.; Van Veggel, F.; C. J. M.; May, P. Stanley. *J. Am. Chem. Soc*. **2007**, 129, 620.(b) Fan, J.; Boettcher, S. W.; Stucky,G. D. *Chem. Mater*. **2006**,18,6391.

42. Zhang, J.; Coombs, N.; Kumacheva, E. *J. Am. Chem. Soc*. **2002**, 124, 14512.

43. Worden, J.G.; Dai, Q.; Shaffer, A.W.; Huo, Q. *Chem. Mater*. **2004**,16,3746.

44. Shaffer, A.W.; Worden, J.G.; Huo, Q. *Langmuir* **2004**, 20, 8343.

45. (a) Mayya, K. S.; Sastry, M. *Langmuir* **1998,** 14, 6344. (b) Kueles, P.J.; Snider, G.S. Williams, R.S.; *Scientific America*n, **2005**, 293, 72. (c) Cheng, K.L.; *Microchemical. Journal* **2006**, 82, 119.

3.1 Introduction

Nanoscale materials having interesting and different physico-chemical properties[1-3], have drawn considerable attention in recent years. This has lead to the development of newer techniques of generating different size and shaped nanomaterials[4-6], which have wide application potential in many fields ranging from sensors[7], optoelectronics[8], drug-delivery[9], catalysis[10] etc. However, in order to make good use of such smart nanomaterials in practical devices, one needs to find strategies to immobilize them on various types of solid surface[11]. Hence, newer methods of deposition of bulk and nanoscale metal particles on surfaces are continuously being developed owing to their significant practical application such as in electronics industry, displays, batteries and electrochemical sensors, Surface-enhanced Raman Scattering (SERS) -active surfaces[12-14]. On the other hand an important objective of nanotechnology is the miniaturization of sensors and actuators for chemical, mechanical and biological applications[15-17]. To achieve this objective a first requirement is to have metal or semiconductor nanoparticles (NPs) deposited on surfaces of the substrate. Attainment of these objectives using simplest possible ways with adaptability as required by the applications is a prime condition for future development in this direction. A constant and growing endeavor has been to find newer methods of synthesis of nanomaterials and ordered arrays of NPs on various surfaces under different experimental conditions, guided by their application potential [18-26].

The traditional method of vapor deposition of metals on various surfaces suffers from the inherent disadvantage of depositing bulk - metal - like materials on selective surfaces.

With regard to deposition of metal or semiconductor NPs on surfaces there are various techniques reported in literature prominent among them currently being used include photolithographic patterning[27], electrophoretic approach[28-29], chemical deposition using appropriate functionalization of the surface followed by deposition of NPs[30-31] and by functionalization of the NPs themselves in order to deposit on various surfaces[32-33]. Additionally, Langmuir – Blodegtt film or self – assembled films of monolayer of nanoclusters have also been deposited on surfaces[34-35]. Depositing on polymer surfaces provides unique flexibility to the deposited nanomaterials. Such polymer nanomaterials composite has created a separate unique place in nanoscience as polymer materials are increasingly being used for fabrication of low-cost devices with ease of production being an additional advantage. Deposition of nanomaterials especially on polymer microspheres find wide range of applications in various important processes such as microsphere based separation methods[36], carriers, catalysis[37], microsystems for molecular analysis[38] etc. Moreover making circuits with metal deposited in two dimensions is an important challenge in polymer electronics. This can be achieved by traditional physical deposition techniques or chemical methods of deposition of thin films or arrays of metal on the polymer films. In addition to traditional methods, there are a number of methods that have recently been developed in this regard. For example, Kumacheva and coworkers[39] have developed a method for obtaining periodic structures of hybrid nanocomposite materials with Ag or CdS deposited on the surfaces of nanosized diameter polymer spheres. Zhao et al.[40] have used viologen systems to obtain nanoscale metal coatings on polymer substrates in the presence of ultraviolet (UV) light. Horiuchi et al.[41] used a UV-photolithography based method for micropatterning of Pd nanoparticles (NPs) in a polymer. On the other

hand Andres et al.[42] has used organic interconnects to obtain two-dimensional superlattice of Au NPs. Also, several methods have been developed to obtain polymer-metal core-shell NP arrays consisting of metal NPs as the core and polymer as the shell[43-45] or polymer NPs as the core and metal NPs deposited on various surfaces[46,47] and bimetallic core-shell arrays on surfaces[48]. When metal salts, exchanged on polymer NPs, are reduced the dimensional restriction of the substrate would produce metal NPs on top of the surface. However, it is equally important technologically to have metal NPs and bulk particles deposited on polymer substrates that are not necessarily of nanometer dimensions. In other words, schemes for deposition of metal bulk and NPs on the surfaces of bulk polymers are necessary. It is here that chemical methods of deposition could play a superior role in obtaining three-dimensional deposition. However, none of the methods reported so far has introduced a general chemical method of deposition of bulk as well as NPs on polymer surfaces.

In this chapter we describe a simple generic route of depositing various metals either in their bulk form or in nano form in polystyrene resin surface, taking advantage of the ion exchange property on the resin. We have extended this method to two metals and even for depositing two metal and one semiconductor particles on the same resin surface. Further this method can be extended to deposit polymer-nanoparticles composite on the resin surface and use such beads in solid state catalysis or in sensors explained in detail in next chapter. The method is based on ion exchange of salt of metal with commercially available resin beads followed by reduction of the metal ions using $NaBH_4$ as the reducing agent. The choice of ion-exchange resin beads as the polymer was based on their ion-exchange properties, thermal stability and stability to work under various solvent, pH and ionic conditions. A general scheme of deposition of metal particles on the polymer surfaces is shown in Figure 3.1 with the deposition of Ag as an example.

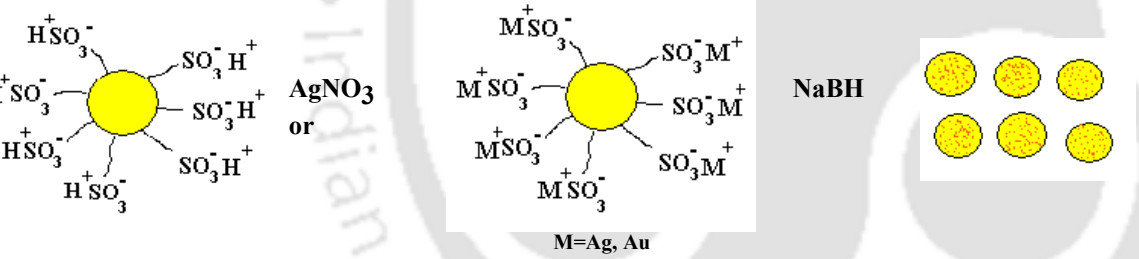

Figure 3.1 Schematic diagram showing the various steps for the metal (Ag, Au) particle deposition on the surface of a cation exchange resin bead. The last part of the scheme represents six such beads.

The sizes of the metal particles deposited could be controlled by controlling the concentration of the reducing agent. In this way we could deposit bulk metal particles of Au, Ag and Ni as well as NPs of Au and Ag on the surfaces of the resin beads. In addition, we were also able to deposit composite particles of Au-Ag, Au-CdS and

Au-Ag-CdS on the surfaces. The deposited materials were characterized by UV-vis spectroscopic, X-ray diffraction, scanning electron microscopic (SEM) and energy dispersive X-ray (EDX) measurements. Our observations suggest that the metal particles were deposited on the surface of the polymer beads. The bulk metal deposition appeared in the form of films on the surfaces. The typical thickness of such a deposition was about 5-10 μm. On the other hand the NPs were deposited in the form of scattered particles on the surfaces of the polymer beads. The deposited bulk particles as well as metal NPs were quite stable for months without any observable characteristic changes in their properties except for the case of Cu deposition, which was not stable in ambient condition for more than two hours.

3.2 Experimental Section

3.2.1 Activation of the cation exchange resin

3.0 g of commercially available cation exchange resin microbeads (Amberlite- IR 120, Merck) were at first kept in 10.0 mL 3.0 M HCl (Merck) solution for 1h. The beads were then washed thoroughly with water to remove the excess HCl. That was confirmed by checking the pH of the resultant water for which a value of 6.8 was obtained. This step is necessary to replace the Na^+ ions in the commercially available resin beads by H^+ ions and beads would then be ready for exchange with metal ions.

3.2.2 Deposition of Bulk Ag and Ag Nanoparticles

This was achieved by keeping the activated resin beads in 5.0 mL of 0.1 M aqueous $AgNO_3$ (MERK) solution for an hour. The solution was then decanted, which was followed by washing the beads with water to remove excess $AgNO_3$. They were then dried and finally treated with 5.0 mL of 0.5 mM $NaBH_4$ solution. The beads, whose color immediately turned silvery, were used for further analysis. The aqueous solutions mentioned above were made using Milli Q grade water (with resistivity value of 18.2 MΩ cm). In order to deposit Ag NPs, the procedure followed was the same as for the bulk except that for the final reduction of Ag^+ ions 5.0 mL of 0.2 mM $NaBH_4$ solution was used instead. The resultant color of the beads was golden yellow.

3.2.3 Deposition of metallic Au and Au nanoparticles

In the case of deposition of Au we observed that both cation and anion exchange resin beads could be used. Bulk metallic Au particles were deposited on anion exchange beads, while Au NPs were formed in cation exchange beads under identical reaction condition. This was required as the dark color of the anion exchange resin beads prevented us from visual or spectroscopic observation of the NP deposition. Therefore, we have used both kinds of resins for deposition of appropriate particles. It may be mentioned here that when grinded the color of the anion exchange resin beads became lighter and the formation of Au NPs could be observed. We, however, only report the results from cation exchange resin beads in this regard.

For bulk Au deposition, 3.0 g of anion exchange resin beads (Amberlite IR-400) were activated with 10ml of 1.0 M NaOH. The beads were then thoroughly washed with water to remove the excess alkali that was confirmed by checking the neutrality of the water

used. That was followed by keeping 0.5g of the above beads in 500 µL $HAuCl_4$ (Sigma-Aldrich, 17 W%) solution 1h. Then the excess salt was removed by washing with water. The beads were then treated with 1.0 mL 0.018 M $NaBH_4$ for 20 min. The beads turned shiny golden in color in 10 min, indicating the formation of bulk Au on the surface. In the case of deposition of Au NPs, 3.0 g of cation exchange beads (Amberlite IR-120) were activated using 10.0 mL of 3.0 M HCl, followed by washing the beads with water. 0.5 g of these activated resins were then treated with 500 µL of $HAuCl_4$ (Sigma-Aldrich, 17 W% in dilute HCl) for 1 h. After washing with water, the beads were then treated with 1.0 mL of 0.018 M $NaBH_4$ solution in order to reduce the metal salt to corresponding metal particles. The resin beads upon treatment with $NaBH_4$ turned purple in color indicating the formation of Au NPs on the surface.

3.2.4 Deposition of metallic Ni

3.0 g of activated cation exchange resin beads was kept in a 5.0 mL solution of 0.2 M $NiCl_2$ for 1 h. The beads were then washed to remove the excess salt. That was followed by keeping the beads in a 0.37 M $NaBH_4$ solution. The beads turned dark in color in 10 min indicating the formation of bulk Ni on the bead surfaces.

3.2.5 Deposition of metallic Cu

3.0 g of activated cation exchange resin beads were kept in 5.0 mL of 0.1M $CuNO_3$ for 1 h, which were then washed to remove the excess metal ions. Those beads were further treated with 5.0 mL of aqueous 0.26 M $NaBH_4$ upon which the color of the beads turned to that of characteristic metallic copper.

3.2.6 Au / Ag two metallic Particles deposition

0.5 g of the resin beads as activated earlier were kept in 500μL of 17.0 % $HAuCl_4$ for 1 h, which was followed by washing with sufficient amount of water. The beads were then treated with 1.0 mL of 0.018 M of $NaBH_4$ to generate Au NPs. They were then kept in a solution of 2.0 mL of 0.5 M HCl to remove some of the unreduced metal ions. They were further washed with sufficient amount of water followed by immersion in 1.0 mL of 0.1M $AgNO_3$ solution. The beads were again washed to remove excess Ag^+ ions. This was followed by treatment with 1.0 mL of 0.2 mM $NaBH_4$ to generate the Ag particles in addition to the remaining Au NPs.

3.2.7 Deposition of composite particles of CdS-Au.

To deposit composite particles 0.5 g of activated cation exchange resins were, at first loaded with CdS NPs, just by dipping them in 1.0 mL of 0.1 M $CdCl_2$ for half an hour. The beads were then washed properly with sufficient amount of water followed by treatment with 500 μL of 0.2 M Na_2S. The Au particles were then deposited by following the same procedure as above with some of the cation exchange sites were made available by keeping the beads in 2.0 mL of 0.5M HCl. The beads were then washed with copious amount of water, which was followed by treatment with 1.0 mL of 0.018 M $NaBH_4$. That generated bricked colored resin beads with plasmon peak characteristics to that of Au NPs.

3.3.8 CdS /Au/Ag NPs composite particle deposition:

In this case the first two steps followed were the same as given above in the section 3.3.7 for the deposition of composite CdS-Au particles. This was followed by keeping the 0.5g beads in 1.0 mL of 0.1M $AgNO_3$ solution for 1 h. They were again washed with plenty of water to remove excess Ag^+ ions. The beads were then reduced this time with 1.0 mL of 0. 2 mM $NaBH_4$ to generate the Ag particles along with the previously deposited CdS-Au particles.

3.2.9 XRD of the metal-coated beads

We observed that the metal-coated beads (especially NPs deposited beads) as prepared above did not provide good X-ray diffraction signal. In order to improve the quality of the signal the resin beads were grinded into fine powders, which were then activated with acid or base as appropriate. For example, 1.0 g of grinded resins was activated with 2.0 mL of 3.0 M HCl. This was followed by exchange with appropriate metal salts and then reduction by $NaBH_4$ as above. The beads (powder) were collected by centrifugation and cleaned by washing with water. This cycle was performed a few times to remove excess reagents from the beads. They were then air-dried to record room temperature XRD data using a Seifert powder X – ray diffractometer (XRD 3003 TT) having Cu - α source with wavelength 1.54 Å. The bulk metal deposited beads were recorded without grinding as the signal quality was good enough for analysis.

3.2.10 Diffuse reflectance UV-Vis measurements

The sample prepared for XRD studies were used for recording UV-Vis absorption spectra of the deposited metals on the bead surfaces. A Perkin Elmer (Lambda25) spectrophotometer was used in diffuse reflection mode for recording the data.

3.2.11 Scanning electron microscope (SEM) and Energy dispersive X-ray (EDX) studies:

The scanning electron micrograph and Energy dispersive X-ray studies were performed after sputtering the nanoparticles coated beads with Au. For these studies it was seen that single resin beads without grinding is enough to record the spectra. So spectra were recorded using single resin beads. Micrographs were recorded in a JEOL SEM (Model No. JSM 6700F) operating at 20 kV.

3.3 Results and discussion

Ion exchange resins are unique in their ability to function at all pH and under a variety of solvent conditions. When activated resins are dipped in a solution containing other ions, the mobile counter ions from the surrounding medium gets exchanged as a consequence of the phenomenon known as Donan equilibrium[34]. This phenomenon has traditionally been exploited in removing ions from solution, such as hardness removal from water. In the present set of experiments the H^+ ions of the activated cation exchange resin beads when dipped into appropriate solutions exchange with Cu^{2+}, Ag^+, Au^{3+}, Ni^{2+} or Cd^{2+} ions that are present in the salt solutions of the corresponding metal cations.

When the beads are further treated with a reducing agent such as an aqueous $NaBH_4$ solution the metal ions get reduced to their zero oxidation states. Upon reduction on the surfaces of the beads they deposit either in the form of bulk metal or NPs of the corresponding metal. Our experimental results suggest that the nature of particle size is primarily dependent upon $NaBH_4$ concentrations. For example, when cation exchange beads containing either of Cu^{2+}, Ag^{+} or Ni^{2+} ions were treated with excess amount of $NaBH_4$ the resultant depositions took place in the form of bulk metal. Photographs of bulk metal coated resin beads are shown in Figure 3.2.

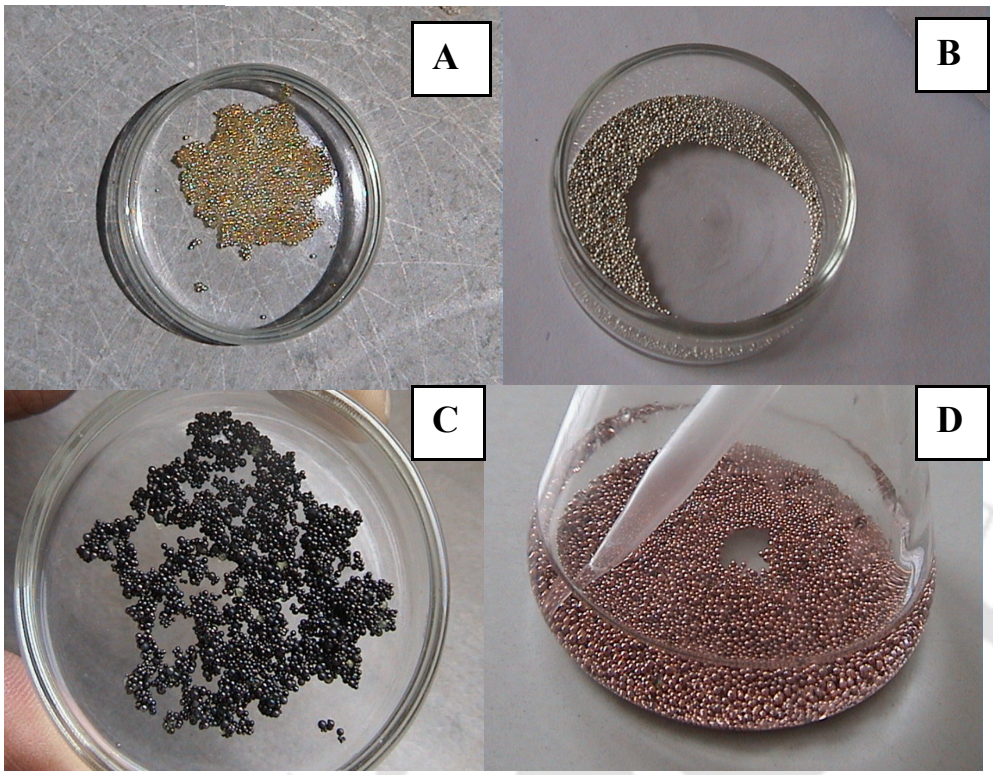

Figure 3.2 The photograph of cation exchange resin beads coated with bulk metals. (A) Blank resin (B) Silver (C) Nickel (D) Copper

As clear from Figure 3.2, the colors of the deposited metal correspond to the bulk metallic states of Ag, Ni and Cu. Blank resins are shown in Figure 3.2 A. The Ag coated beads looks shiny white (Figure 3.2 B), Au yellow (photograph not shown), Ni black (Figure 3.2 C) and Cu tarnish in color (Figure 3.2 D) indicating the generation of metallic depositions of Ag, Au, Ni and Cu respectively on the resin beads. One of the problems encountered in depositing bulk copper on the beads is that it was quite unstable and the resin turned to its original color after 1-2 h of keeping under ambient condition. Treatment of the same resins with $NaBH_4$ brought back the original color albeit unstable again.

3.3.1 X-ray diffraction (XRD) analysis:

Further investigation of the coated beads by X-ray diffraction (XRD) measurements revealed the presence of metallic states of each of the metal. For example, Figure 3.3A shows the XRD data, for Ag bulk metal thin films with peaks at $2\theta = 38.1^0$ and 44.8^0 corresponding to (111) and (200) planes respectively of Ag metal. Figure 3.3B shows the XRD for Au bulk deposit with diffraction peaks at $2\theta=38.5^0$, 44.1^0 corresponding to (111) and (200) planes respectively of Au metal. Figure 3.3C shows XRD for Ni bulk thin film with diffraction peaks at $2\theta = 44.8^0$ and 51.2^0 corresponding to (111) and (200) planes of metallic Ni. These peaks correspond to the deposition of metal in their zero oxidation states.

We were also successful in depositing metal NPs on polymeric resin beads. The approach adopted here was similar to that of bulk metal deposition. In this case the concentration of $NaBH_4$ used to reduce the metal ions was carefully controlled to generate NPs rather than bulk. For example, in order to deposit bulk Ag a solution of 0.5 mM of $NaBH_4$ was used. On the other hand a solution with 0.2 mM $NaBH_4$ was needed in order for the formation of AuNPs. Figure 3.4A and Figure 3.4B shows the X-ray diffraction peaks of the Au nanoparticles and Ag nanoparticles respectively. As can be seen clearly from the Figure 3.4A the peak centred at diffraction angle $2\theta=38.5$ is due to (111) plan for Au, similarly in Figure 3.4B the peak at $2\theta = 38.8$ corresponds to (111) plan of Ag nanoparticles.

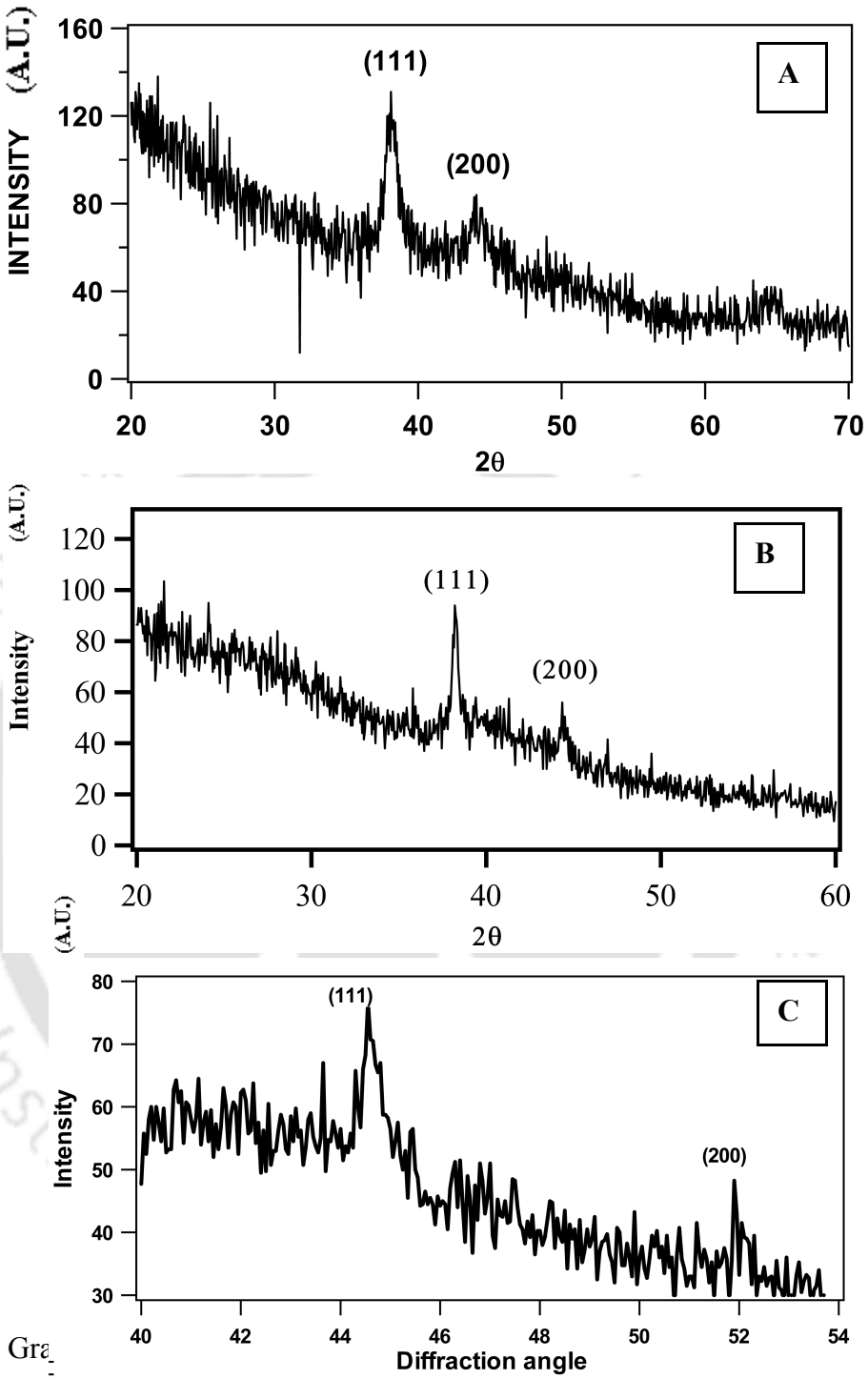

Figure 3.3 Gra ited on the surface of the resin beads in their bulk form. Intensity in each graph is in arbitrary unit.

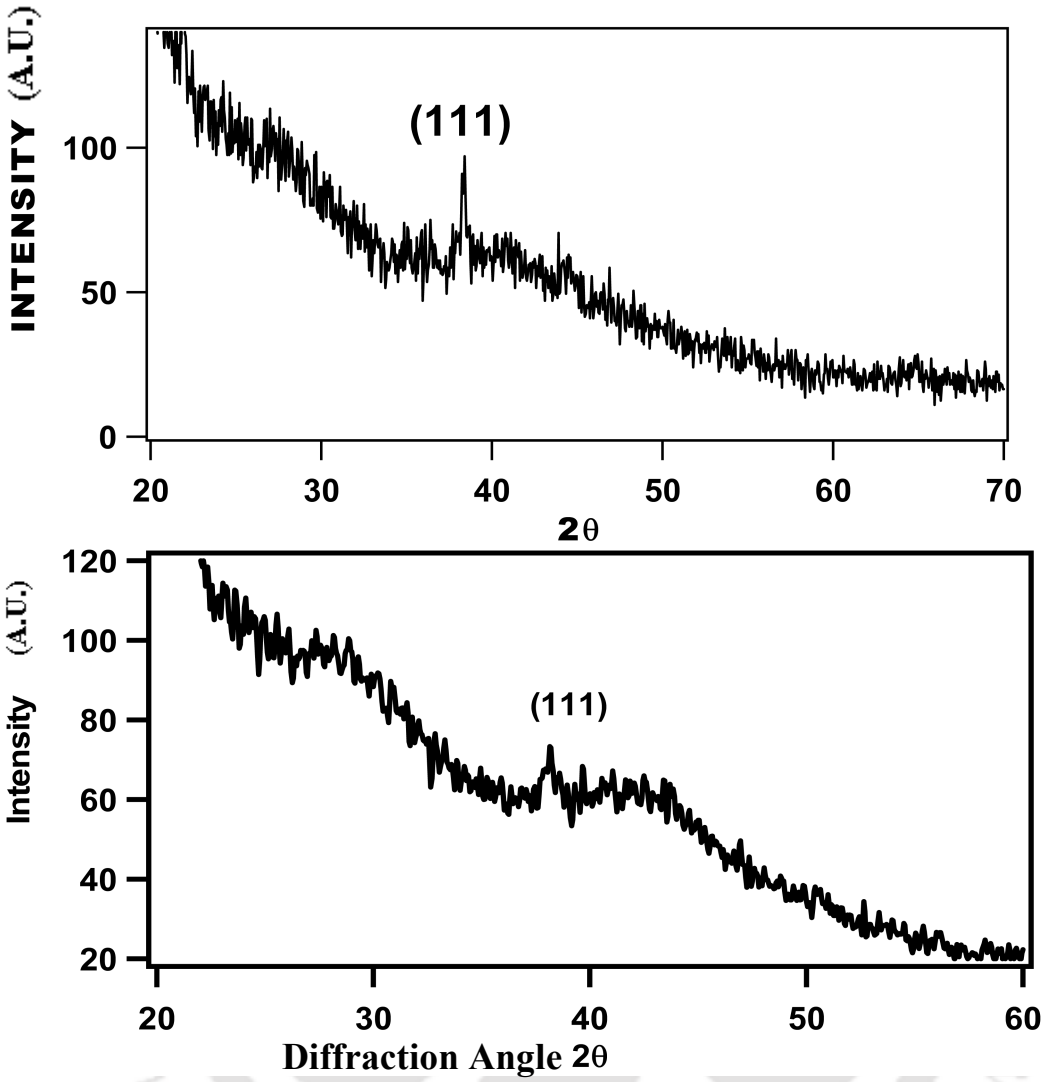

Figure: 3.4 X-ray diffraction pattern of the Au and Ag nanoparticles deposited on the resin surface (recorded with grinded resin to improve signal quality).

3.3.2 Diffuse Reflectance UV-Vis spectroscopic study

We investigated the yellow colored Ag and pink colored Au deposited beads by diffuse reflectance UV-Vis spectroscopy. Diffuse reflectance UV-Vis spectra of the Au and Ag nanoparticles deposited on the resin surface were recorded, on grinded resin powder to improve signal quality. The diffuse reflectance spectra are shown in Figure 3.5. Figure 3.5

A shows the Diffuse Reflectance UV-Vis spectra for Au nanoparticles loaded grinded resin, As can be clearly seen from Figure 3.5A, the plasmon oscillation of Au nanoparticles in resin is similar to that in solution occurring at 530 nm. Inset showing the photograph of the deposited nanoparticles in resin beads (ungrounded). Similarly, Figure 3.5 B shows the plasmon resonance peaks for Ag nanoparticles, occurring at 410 nm, and inset showing photograph of Ag nanoparticles deposited beads.

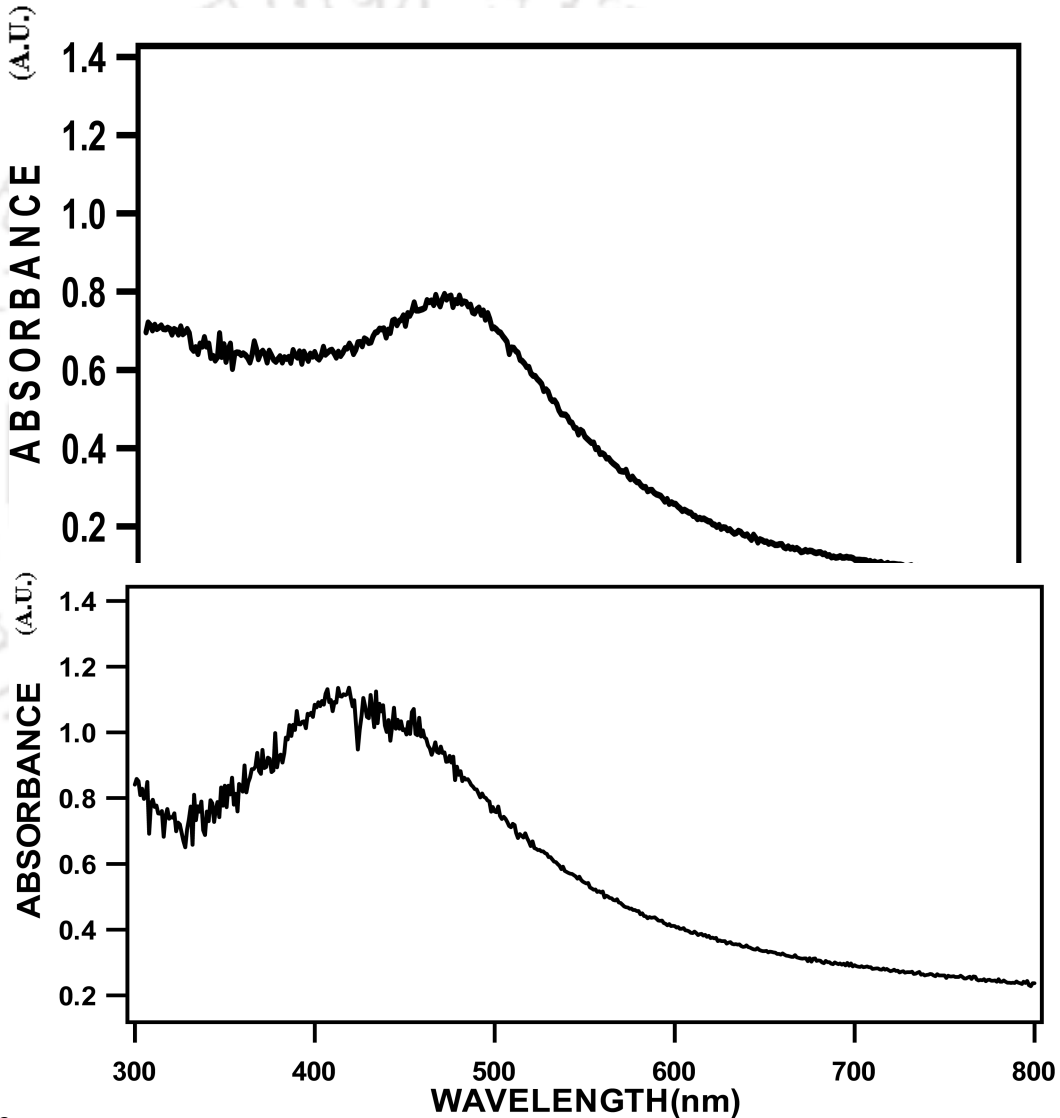

Figure 3.5 Diffuse reflectance UV-Vis spectra of the Au (A) and Ag NPs (B) and photographs of the deposited resin beads (insets).

The occurrence of the characteristic plasmon resonance of Au NPs absorption peak at 530 nm and for Ag deposited beads with a peak at 410 nm, indicates that, the metals were probably deposited as nanoparticles, with similar size range as in the solution. The deposition of Au and Ag in the zero oxidation states were further confirmed by powder

XRD pattern which are shown in Figure 3.4. It must be mentioned here that the present quality spectra could be observed only with deposition on the grinded version of beads, the details of which are described in the experimental section. The same samples used to record XRD are used in sample holder for solid sample in diffuse reflectance mode of UV-Vis spectrometer.

3.3.3 Scanning electron microscopic (SEM) study of single metal deposited beads

We further pursued the nature of deposition of NPs on the beads using SEM. Typical SEM micrographs for Au NPs and Ag NPs deposited on the polymer surfaces are shown in Figures 3.6. Figure 3.6 A and 3.6 B are SEM micrographs of Au NPs deposited beads recorded for two different resolutions. On the other hand Figure 3.6 C is of Ag NPs. As evident from Figure 3.6 A as well as 3.6 B, the deposition of Au NPs occurred with scattered spherical particles with sizes varying between 35 nm and 75nm. In the case with Ag NPs deposited on the beads (Figure 3.6 C) they were quite densely populated. They had widely different clusters of particle with sizes typically varying between 50 nm and 100 nm. It is noteworthy that both the Au and Ag NPs were deposited without the formation of thin films. They were rather formed with NPs character retained in the beads.

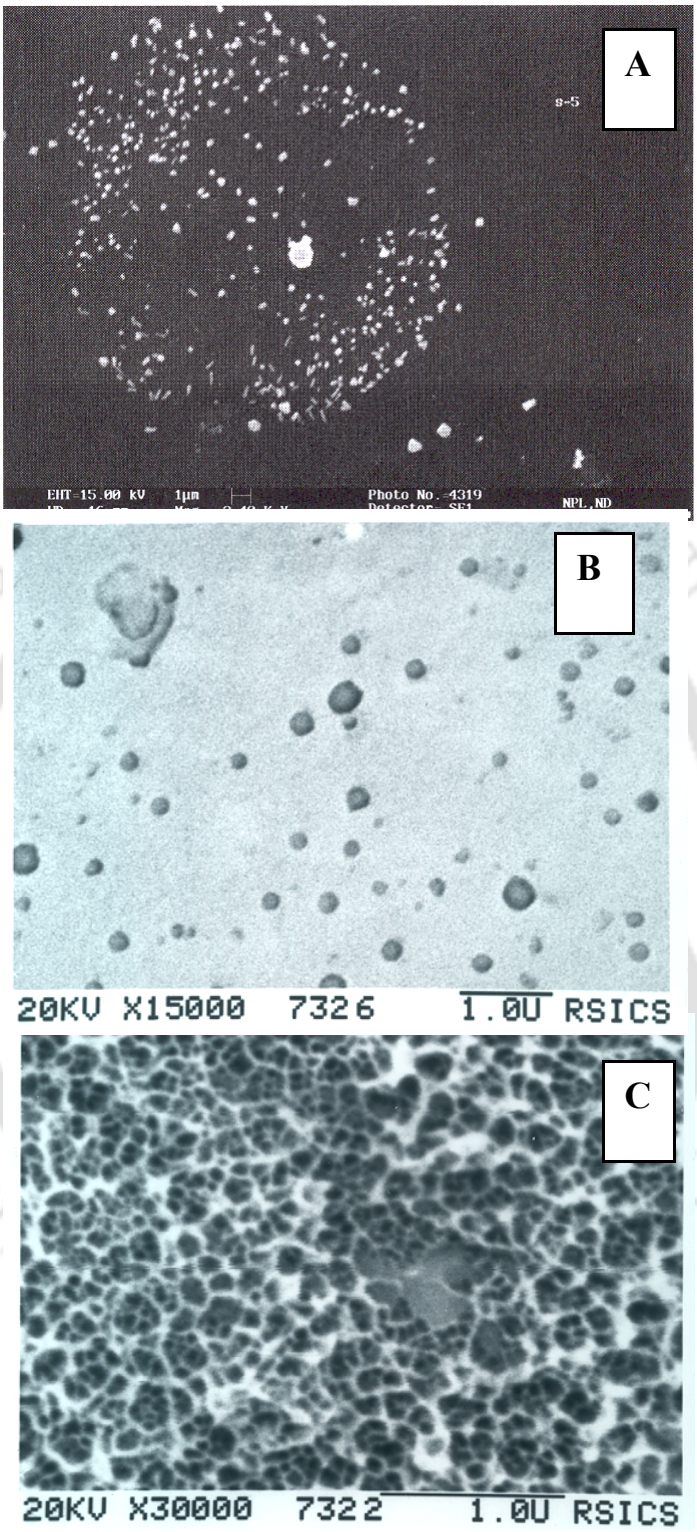

Figure 3.6 Scanning electron micrograph of the Au nanoparticles (Figures A and B) and Ag nanoparticles deposited on single cation exchange resin bead (C) .

3.3.4 Scanning electron microscopy (SEM) and energy dispersive X-ray (EDX) analysis of two metals and metal semiconductor deposited beads

We have successfully deposited particles of two metals in a single resin beads. Then we could deposite one metal and semiconductor particles also. This procedure we have extended to deposite one semiconductor or two metals and a semiconductor. The primary motivation behind these pursuits was to be able to obtain a general chemical method of deposition of multiple metallic or semiconductor species on the surfaces of polymer such that properties of each of these materials could be exploited in the final deposited surface of the polymer. The scheme followed in this deposition is based on the scheme of single metal deposition. A metal ion was first exchanged with the cation of the resin as before. The first metal ion was then reduced on the surface of the resin using the borohydride method described in the experimental section. In this way NPs of the parent metal ions were deposited on the resin beads. The resin beads were then treated with dilute HCl to activate the remaining unreacted exchangeable site, followed by keeping them in the ionic solution of the other metal ion. It was further treated with borohydride to reduce the second metal ion. For example, cation exchange resins were treated with $HAuCl_4$ to deposit Au NPs on the beads by reduction with $NaBH_4$. This was followed by treatment of the bead with dilute HCl and then the beads were added to either $AgNO_3$ solution or $CdCl_2$ solution and finally previously mentioned procedure was followed leading to further deposition of Ag NPs or CdS particles. We also successfully deposited two metal Au NPs, Ag NPs and one semiconductor CdS particles on the same bead. Such beads containing multiple components have potential of being used as multifunctional device for

catalysis etc. In general the deposited particles could not be detected either by UV-vis absorption or by XRD measurement as the signals were of poor quality except for the characteristic color due to deposition of Au NPs. However, they could be probed by SEM with EDX (energy dispersive X-ray analysis) that revealed the presence of various metallic and ionic species. As an example, the SEM micrograph of Au-Ag particles (Figure 3.7A) deposited could not really be observed clearly in the form of individual particles. On the other hands the particles could be seen clustered into lumps of deposition. The EDX studies showed the presence of both Au and Ag particles on the resin beads (Figure 3.7A'). We had recorded the UV-Vis diffuse reflectance spectrum of the beads where characteristic peak due to Au NPs only appeared (not shown here). This could be due to low deposition of Ag NPs.

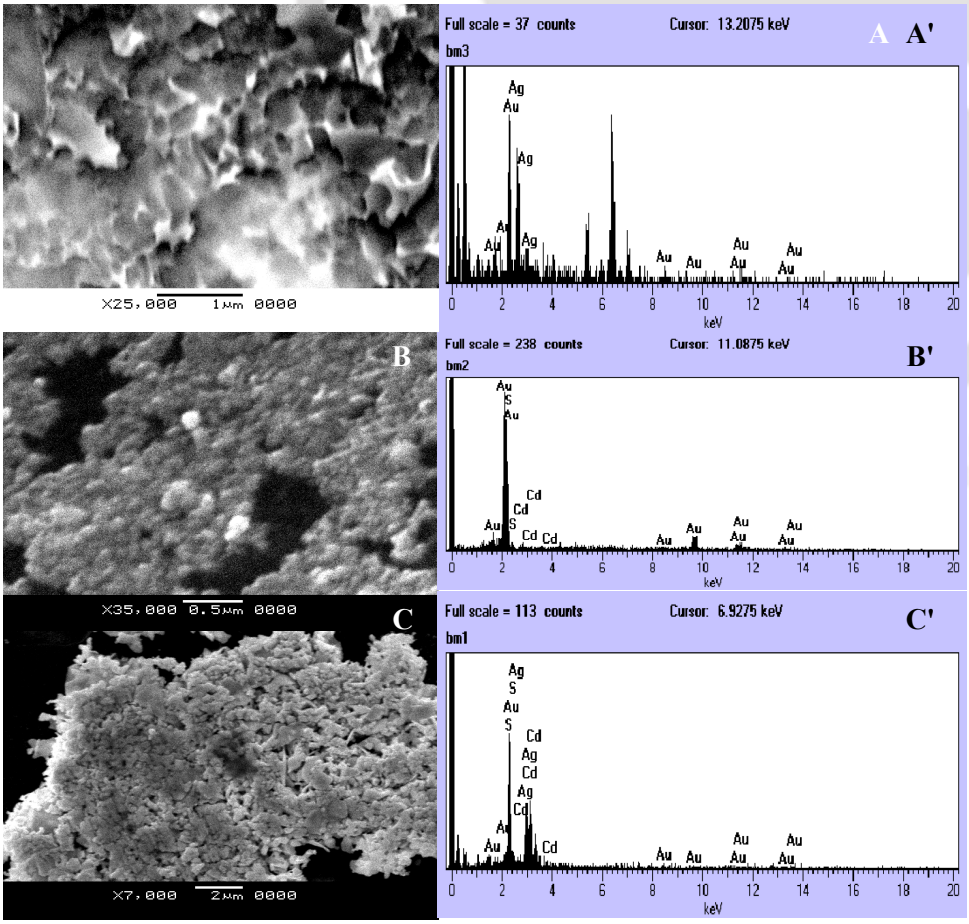

Figure 3.7 SEM micrographs and energy dispersive X-ray analysis of resin beads loaded with (A) and (A') Au/Ag particles; (B) and (B') Au/ CdS particles and (C) and (C') Ag/Au/CdS particles.

On the other hand, Au-CdS deposited on the beads showed distribution of particles of greater than 50 nm average sizes all over the beads (Figure 3.7B). EDX measurement at any arbitrary spot indicated the presence of both Au and Cd and S in that spot Figure 3.7B'). This means that both CdS and Au particles were evenly distributed all over the beads. Similar results were obtained with the deposition of Au-Ag-CdS particles which are shown in Figure 3.7C. The EDX spectra are shown in Figure 3.7C'. However, we could not for certain know the nature of deposition of the second or third species as the particle sizes could really not be discerned from the SEM pictures. They appeared rather clusters of particles with sizes much greater than hundreds of nanometers.

3.3.5 Determination of the thickness of the deposited films on resin surface

Finally, we would like to mention here about the nature of deposition of various particles on the surfaces of the polymer. In the case of deposition of bulk metal there is the possibility of the formation of a continuous thin film on the surface of a bead. In order to understand the nature of deposition we cut one such bead, with deposited metal, by a razor blade into two halves.

The cross section of the bead was studied by SEM and a micrograph is shown in Figure 3.8. As clear from the figure, there is the formation of a continuous thin film of metal deposited on the bead. The typical thickness of such films varied between 5 and 10 μm on the surface. Beyond this film there was no presence of any metallic species indicating that the bead might not be porous enough to deposit thicker film. The thickness

of the film may be due to a composite of metal and the polymer rather than the metal itself. This is quite plausible considering that the polymer bead would have enormous defects on its surface and thus generating thick film instead of thin film. On the other hand in the case of deposition of metal NPs or other composite it is not possible to have a continuous deposition of NPs. This is evident from SEM micrographs shown earlier (Figure 3.6) where the metal NPs were rather scattered on the surfaces of the beads.

A polymeric resin bead is not necessarily a porous material. Also, its surface will not be atomically flat. There will be a large number of defect sites on the surfaces. Thus the deposition of a monolayer of materials by simple reduction of the counter ion may not be feasible. Under our experimental condition the Na^+ ions of sodium borohydride may not be able to replace the cations in the resin and thereby could not bring the metal ions from the beads to the solution. On the other hand borohydride is a strong reducing agent and thus can easily reduce the cation to its corresponding zero oxidation state. This gives rise to the question about the mechanism of formation of metallic film or NPs deposition. At high concentration of $NaBH_4$ all or nearly all the metal cations present on the surface or in immediate vicinity may get reduced and form a film on top of the surface. The charge balance may be achieved by the attachment of Na^+ to the anions of the beads. On the other hand at a relatively lower concentration of $NaBH_4$ there is the possibility of incomplete reduction of the metal cations present in the beads thus forming NPs scattered on the surface rather than forming a film. This can also explain the deposition of two metals, one metal and one semiconductor or even three different species in a sequential manner. In other words, the unreduced parent metal cations would make rooms for further incorporation of a different cation and thus giving rise to the production of two-metallic or

metallic and semiconductor deposition on the beads. Additionally, there is the case of the reduction of Au^{3+} ions to their corresponding zero-valent states being possible using both cationic as well as anionic ion-exchange resin species and the nature of deposition was not dependent on the concentration of $NaBH_4$. In other words, one could use $AuCl_4^-$ in the form of the complex with over all negative charge as well as in the form of Au^{3+} for deposition on differently charged resins. Finally, we would like to mention here that the present method of generation of metallic and semiconductor NPs could have various applications, one of which is demonstrated in the next chapter.

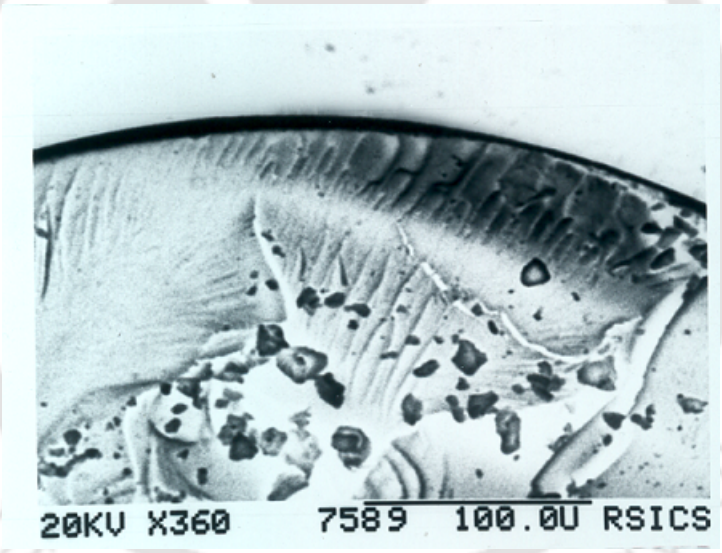

Figure 3.8 Scanning electron micrograph of metal coated bead (bulk metal) showing the thickness of the metallic film formed in the surface of the resin.

3.4 Conclusion

In this chapter, we have reported the syntheses of bulk as well as nanoscale metal on the ion-exchange resin beads. By controlling the concentration of the cation

(corresponding to the metal) and the reducing agent we could control the nature of the growth on the beads. The depositions were characterized by UV-vis spectroscopy, scanning electron microscopy and X-ray diffraction and energy dispersive X-ray analysis methods. These beads could be further used for other nanotechnology based applications, one of which is described in the proceeding chapter.

3.5 References

1. Eustis, S.; El-Sayed, M. A. *Chem. Soc. Rev*. **2006**, 35, 209.

2. Burda, C.; Chen, X.; Narayanan, R.; El-Sayed, M. A. *Chem.Rev*. **2005**, 105, 1025.

3. Chen, S.; Ingrma, R. S.; Hostetler, M. J.; Pietron, J. J.; Murray, R. W.; Schaaf, T. G.; Khoury, J.T.; Alvarez, M. M.; Whetten, R. L. *Science* **1998**, 280, 2098.

4. Lu, X.; Imae, T. J. *Phy. Chem. C* **2007**, 111, 2416.

5. Hussain, I.; Graham, S.; Wang, Z.; Tan, B.; Sherrington, D. C.; Rannard, S. P.; Cooper, A. I.; Brust, M. *J. Am. Chem. Soc.* **2005**, 127, 16398.

6. El-Sayed, M. A. *Acc. of Chem. Res.* **2004**, 37, 326.

7. Dai, Z.; Kawde, A.-N.; Xiang, Y.; La Belle, J. T.; Gerlach, J.; Bhavanandan, V. P.; Joshi, L.; Wang, J. *J. Am. Chem. Soc*. **2006**, 128, 10018.

8. Huynh, W. U.; Dittmer, J. J.; Alivisatos, A. P. *Science* **2002**, 295, 2425.

9. Kam, N. W. S.; Jessop, T. C.; Wender, P. A.; Dai, H. *J. Am. Chem. Soc*. **2004**, 126, 6850.

10. Narayanan, R.; El-Sayed, M. A. *J. Phys. Chem. B* **2005**, 109, 12663.

11. Shipway, A.N.; Kartz, E.; Willner,I. *Chem.Phys.Chem.***2000**,1,18.

12. (a) Shipway, A. N.; Lahav, M.; Blonder, R.; Willner, I. *Chem Mater* **1999,** 11, 13.

13. Lahav, M.; Gabai, R.; Shipway, A.N.; Willner, I. *Chem. Commun.* **1999**, 1937.

14. Freeman, R.G.; Hommer, M.B.; Grabar, K.C.; Jackson, M.A.; Natan, M. J *J. Phys. Chem.* **1996,** 100, 718.

15. Wohltjen, H.; Snow, A. W. *Anal. Chem.* **1998,** 70, 2856.

16. Cunningham, E.; Campbell, C. J. *Langmuir* **2003,** 19, 4509.

17. Velev, O.D.; Kaler, E.D. *Langmuir* **1999, 15**, 3693.

18. Malikkkova, N.; Pastoriza_Santos, I.; Schierhorn, M.; Kotov, N.A.; Liz-Marzan, L. M. *Langmuir* **2002**, 18, 3694.

19. He, H. X.; Zhang, H.; Li, Q. G.; Zhu, T.; Li, S. F. Y.; Liu, Z. F. *Langmuir* **2000,** 16, 3846.

20. Mayya, K. S.; Sastry, M. *Langmuir* **1999**, 15, 1902.

21. Chen, S.; Kimura, K. *Langmuir* **1999**, 15, 1075-1082.

22. Sun, Y.; Mayers, B.; Xia, Y. *Adv.Mater.* **2003**, 15, 641.

23. Zhang, J.; Coombs, N.; Kumacheva, E. *J. Am. Chem. Soc.* **2002,** 124, 14512.

24. Horiuchi, S.; Fujita, T.; Hayakawa, T.; Nakao, Y. *Adv. Mater.* **2003**, 15, 1449.

25. Maenosono, S.; Dushkin, C.D.; Saita, S.; Yamaguchi, Y. *Langmuir* **1999**, 15, 957.

26. Fan, H.; Yang, K.; Boye. D.M.; Sigmon, T.; Malloy, K.J.; Xu, H.; Lopez, G. P.; Brinker, C.J. *Science* **2004**, 304, 567

27. Lu, C.; Wu, N.; Jiao, X.; Luo, C.; Cao, W. *Chem. Commun.* **2003,** 9, 1056.

28. Hayward, R. C.; D. Saville, A.; Aksay, I. A. *Nature* **2000,** 404, 56

29. Chandrasekharan, N.; Kamat, P. V. *Nano Lett.* **2001,** 1, 67.

30. Schmitt, J.; Mächtle, P.; Eck, D.; Möhwald, H.; Helm, C. A. *Langmuir* **1999,** 15, 3256.

31. Hayes, R. A.; Bohmer, M.R.; Fokkink, L. G. J. *Langmuir* **1999**, 15, 2865.

32. Mayya, K. S.; Sastry, M. *Langmuir* **1999**, 15, 1902.

33. Andres, R. P.; Bielefeld, J. D.; Henders, J. I.; Janes, D. B.; Kolagunta, V. R.; Mahoney, W. J.; Osifchin, R.G. *Science* **1996,** 273, 1690.

34. Kim, F.; Kwan, S.; Akana, J.; Yang, P. *J. Am. Chem. Soc.* **2000**,122, 4360.

35. Collier, C. P.; Saykally, R. J.; Shiang, J.; Henrichs, S. E.; Heath, J. R. *Science.* **1997**, 277, 1978.

36. Deng, T.; Prentiss, M.; Whitesides, G. M. *Appl. Phys. Lett.* **2002,** 80, 461.

37. Seong, H.; Crooks, R. M. *J. Am. Chem. Soc.* **2002**, 124, 13360.

38. Vykoukal, J.; Vykoukal, D. M.; Sharma, S.; Becker, F. F.; Gascoyne, R. C.

Langmuir **2003,** 19, 2425.

39. Zhang, J.; Coombs, N.; Kumacheva, E. *J. Am. Chem. Soc.* **2002,** 124, 14512.

40. Zhao, L.; Neoh, K.G.; Kang, E.T. *Langmuir* **2003**, 19, 5137

41. Horiuchi, S.; Fujita, T.; Hayakawa, T.; Nakao, Y. *Adv. Mater.* **2003**, 15, 1449.

42. Andres, R. P.; Bielefeld, J. D.; Henders, J. I.; Janes, D. B.; Kolagunta, V. R.; Mahoney, W. J.; Osifchin, R. G. *Science* **1996,** 273, 1690.

43. Liu, Y. C.; Chuang, T.C. *J. Phy. Chem. B.* **2003,** 107, 12383.

44. Cao, H.; Xu, Z.; Sang, H.; Sheng, D.; Tie, C. *Adv. Mater.* **2001,** 13, 121.

45. Shin, H. J.; Hwang, I.W.; Hwang, Y.N.; Kim, D.; Han, S. H.; Lee, J.S.; Cho, G. *J. Phy. Chem. B.* **2003**, 107, 4699

46. Freeman, R. G.; Grabar, K. C.; Allison, K. J.; Bright, R. M.; Davies, J. A.; Guthrie, A.P.; Hommer, M. B.; Jackson, M.A.; Smith, P.C.; Walter, D. G.; Natan, M. J. *Science* **1995,** 267, 1629.

47. Jackson, J. B.; Halas, N. J. *J. Phy. Chem. B.***2001**, 105, 2743

48. Deng, T.; Prentiss, M.; Whitesides, G. M. *Appl. Phys. Lett.* **2002,** 80, 461

Au nanoparticles / polyaniline coated resin beads as colorimetric glucose sensor.

4.1 Introduction

One of the goals of nanotechnology is the multifunctional structure generation with nanoscale components working independently or in tandem when immobilized or fabricated on a substrate. Be it selective identification and destruction of cancer cells[1], site-selected drug release[2] or DNA microarrays generation[3] multifunctional structures with nanoscale materials bring forth the promise of nanotechnology to its best. Development in nanoscale science and technology has witnessed improved functions of materials by incorporating multiple components with varying electrical, optical and chemical properties. For example, Au deposition on TiO_2 nanoparticles (NPs) changes the band gap such that TiO_2 can photocatalyze reaction in the presence of visible light[4]. Also, self-assembled Au NPs monolayer when coated with aminosilane shows second harmonic generation due to coupled surface-plasmon resonance[5]. On the other hand, similar development in microfluidics has helped to carry out sequential reaction as well as product separation on the same chip[6]. An interesting aspect in multifunctional structure generation would be to have a component that would catalyze a chemical reaction while the other one would detect the formation of at least one of the products. For example, a metal catalyzed reaction could be performed by incorporating metal NPs on a substrate surface while the product of the catalyzed reaction could be identified by colorimetric, potentiometric or amperometric method as applicable. An important and useful example in this regard would be the simultaneous oxidation of glucose using Au NPs as catalysts and the detection of the product (gluconic acid) by any of the methods mentioned above. The method would be even more robust if both the catalyst and

the sensor (for example, colorimetric) could be immobilized on a substrate surface. This is especially important for two reasons – the first being the ease of recovery of the catalyst as well as the sensor; and the second reason being the use of the same system repeatedly a large number of times. There are a number of commercially available glucose sensing methods based on potentiometric[7], colorimetric[8] and amperometric[9] identification of a product. Moreover other methods such as Electrochemical[10] and micromechanical[11] glucose sensors have been developed lately, which have their specific advantages. The conventional sensors are based on the use of either an enzyme or a conducting polymer[12] appropriately functionalized for the purpose. The fundamental requirement of all the above methods is electricity. Also, the design of sensors is such that the sensor elements are generally for one-time use only. On the other hand there is no report on the simultaneous catalysis of the reaction by noble metal NPs and detection of the product gluconic acid colorimetrically. This would be of even greater advantage if both of them were embedded on a substrate surface and could be used repeatedly. The advantage could further be accentuated with the use of polymer as the substrate and sensor. We have recently demonstrated that metal NPs and conducting polymer composite could be generated in situ together and the properties of each of the components could be taken advantage in order to achieve better functionality. The compatibility of the two makes them more appealing for applications. For example, polyaniline- Au nanoparticle composite, when synthesized using a single reagent that reduces $HAuCl_4$ to Au nanoparticles and at the same time polymerizes aniline to polyaniline, first reported in our laboratory[13], possesses electrical conductivity considerably higher compared

to polyaniline alone. Similarly it was also demonstrated that a TiO_2 NP –polypyrrole composite is a better solid state photocatalyst than the NPs alone[14].

Encouraged by the success of research in nanomaterials[15-18] and polymers[19-20] and the promise of multifunctional structures with nanoscale components, we have successfully pursued the incorporation of Au NPs and PANI on the same surfaces of cation exchange resin beads and have used these beads for catalytic oxidation of glucose to gluconic acid and for simultaneous detection of the product of the reaction. We have chosen commercially available cation exchange resin beads as the substrate because of their thermal, environmental and chemical stabilities plus the ease of exchange of their cations with $HAuCl_4$ and anilinium chloride. The basic idea of the procedure is to exchange both $HAuCl_4$ and anilinium ions on the same cation exchange resin beads and then reduce Au^{3+} to Au NPs by $NaBH_4$ followed by polymerization of aniline using H_2O_2. The procedure resulted in the production of colored beads where the formation of PANI obscured the purple color of Au NPs that were formed initially. The beads were then treated with NaOH solution that converted the green colored beads into blue colored ones. They were then used to oxidize aqueous glucose in the presence of gaseous oxygen. The formation of the gluconic acid was indicated by the change in color of beads from blue to green. The product formation was further confirmed by FTIR spectroscopy. The formation of Au NPs on the beads was confirmed by UV-visible spectroscopy, X-ray diffraction (XRD) and scanning electron microscopic (SEM) measurements. As we know, this is the first report of having immobilized NPs on a substrate surface for use as catalyst, with the deposition of a polymer on the same substrate surface for

colorimetric sensing of the product formation. A schematic diagram of the processes involved in the synthesis as well as reaction and detection is shown in Figure 4.1. Also shown in Figure 4.2 is the reversible conversion between the two forms of PANI, namely the emeraldine salt (green) and emeraldine base (blue) effected by reaction with acid and base. Thus the Au NPs present in the beads catalyze the oxidation of glucose to gluconic acid resulting in the change of color of the beads from blue (emeraldine base) to green (emeraldine salt). Also, we found that the current method can test the presence of a minimum of 1.0 mM of glucose in water, which is comparable in sensitivity to the existing methods mentioned before.

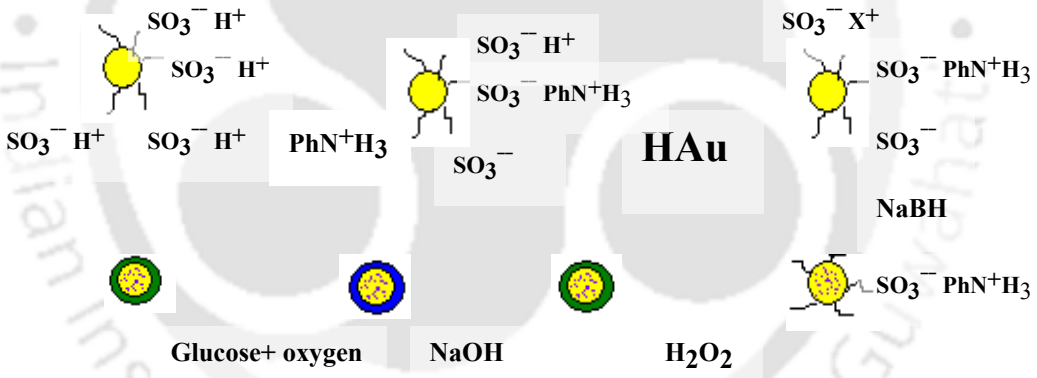

Figure 4.1 A Schematic diagram of various steps involved in the generation of Au nanoparticles and polyaniline on cation exchange resin beads, where X^+ is a cation generated from $HAuCl_4$, and their use for the oxidation of glucose and detection of the product formation.

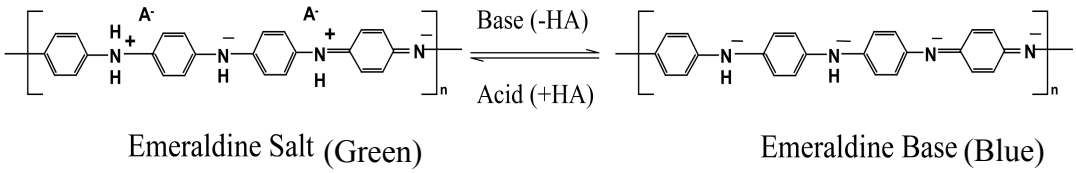

Figure 4.2 A representation of the reversible conversion between the two forms of PANI; namely the emeraldine salt (green) and emeraldine base (blue) in the presence of acid and base.

4.2 Experimental Section

4.2.1 Activation of the resin and incorporation of polyaniline and Au NPs

1.0 g of commercially available Amberlite-IR 120 cation exchange resin beads was activated with 5.0 mL 3.0 M HCl after which the beads were washed thoroughly with water to remove excess acid. This was followed by keeping the beads in a solution that had 10.0 µL of aniline dissolved in 5.0 mL of HCl. The beads were again washed with water, which was followed by treatment with 500.0 µL $HAuCl_4$ solution (Aldrich, 17 wt% of Au). Finally they were again thoroughly washed with water. An estimated exchange with H^+ of the beads was 2.1% of anilinium and 35% of Au species. This exchange was necessary in order for further use of the beads both as catalyst and sensor. Other ratio did not yield good results in terms of color change or catalysis as required in the experiments. The beads were then treated with 1.0 mL of 0.05 M $NaBH_4$ solution upon which the beads turned purple in color, indicative of the

formation of Au NPs. The beads were again washed with water. This was followed by treatment of the beads with 200 μL of 1% (v/v) H_2O_2 (diluted from original 30% solution from Merck India) which turned the color of the beads to green indicating the formation of PANI.

4.2.2 UV-vis spectroscopic studies

We noticed that the presence of Au NPs formed in normal sized beads (commercially available) could not be probed with good signal to noise ratio using UV-vis spectroscopy and X-ray diffraction. In order to alleviate the problem, we first grinded the beads (0.5 g) into finer powder using a mortar and a pestle and then loaded the powder with 250.0 μL of $HAuCl_4$ (17 wt%, Aldrich) followed by reducing them with $NaBH_4$ (1.0 mL of 0.05 M). The beads were then washed with water followed by centrifugation to collect the solid. They were then dried to record XRD and UV-vis spectrum. Similar procedure was followed for generation of Au-PANI composite coated grinded beads required for the recording of UV-Vis and FTIR spectra. UV-Vis spectra were recorded in a Perkin-Elmer (lambda 25) spectrophotometer in the diffuse reflectance mode.

4.2.3 FTIR studies

As mentioned above FTIR of the coarse resin beads yields peaks with poor signals, so we first grinded the resin beads as mentioned above. Then FTIR spectra were recorded in a Perkin-Elmar (Spectrum One A) spectrophotometer using KBr palate.

4.2.4 X-ray diffraction studies

It was found that in XRD also merely the coarse resin beads yields weak signals. So the same grinded powder as mentioned above (used for FTIR studies) was used and XRD measurements were made in a Seifert powder X – ray diffractometer (XRD 3003 TT) having Cu - α source with wavelength 1.54 Å.

4.2.5 Scanning electron microscopic studies

For scanning electron microscopic studies we could use the green beads as obtained in the experimental section 3.3 and mentioned above. Scanning electron microscopic (SEM) pictures of as-coated beads were recorded in a JEOL SEM (Model No. JSM 6700F) or LEO 1430 VP operating at 20 kV. Energy Dispersive X-ray (EDX) measurements were performed with Oxford INCA X-Sight instrument.

4.2.6 Glucose oxidation studies

For the study of oxidation of glucose, at first the regular green colored (Au NPs and PANI coated) beads were treated with 2.0 M NaOH, which converted the beads to the blue form. 5.0 mL of 0.106 M glucose, was taken in a conical flask, and 0.02 g of the AuNP-PANI composite beads (blue form) were added to it and the pH of the solution was maintained at 9.1 (using NaOH and HCl). Then the flask was fitted with a rubber stopper, and gaseous oxygen was allowed to flow through a syringe needle dipped in the solution. An outlet was also fitted

with the rubber stopper for the excess gas to come out. The progress of the reaction was monitored by observable color change of the beads from blue to green and then finally by FTIR spectroscopic measurement of the product after evaporation. In addition, polarimetric measurement of the product solution was performed using a Perkin Elmer polarimeter (model No 343), which uses sodium D-line at room temperature.

Also, we performed the similar experiment in the presence of Au NPs (only) on the beads without having PANI coated. The product however was identified using FTIR spectroscopy only.

4.3 Results and Discussion

We have already found a protocol for deposition of various metal nanoparticles on solid matrix, the details of which have been described in chapter 3. When cation exchange beads were treated with $HAuCl_4$ followed by reduction with $NaBH_4$, Au NPs could be deposited on the surfaces of the beads. The beads assume characteristic purple color of Au NPs. The Au NPs generated on the beads remain stable for months without any visible change in color. The details of the Au NPs-polyaniline composite beads and the results associated with them are described below.

4.3.1 UV-Vis spectrum

UV-visible spectrum of the beads after treatment with $NaBH_4$ but before treatment with H_2O_2, shown in Figure 4.3(A) consists of a peak at 540 nm that is characteristic of surface plasmon resonance of Au NPs. Also shown in the inset of Figure 4.3 (B) is the photograph of

a collection of beads coated with Au NPs (kept on a petri dish) with characteristic purple color of Au nanoparticles.

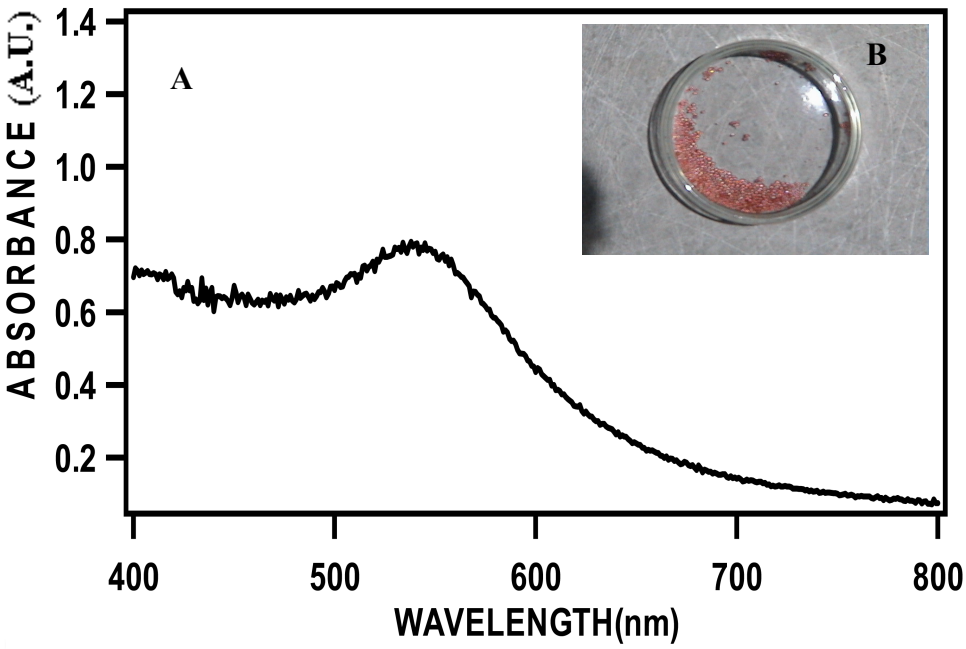

Figure: 4.3 (A). Diffuse reflectance UV-Vis spectrum of the grinded resin beads, and (B) (inset) photograph of the Au nanoparticles deposited resin beads.

4.3.2 X-ray diffraction studies of Au nanoparticles coated beads

X-ray diffraction studies were recorded with finely grinded resin beads deposited with Au nanoparticles. The XRD pattern of the beads is shown in Fig 4.4. As clear from the figure there is the presence of peak at 38.5^0, which corresponds to 111 face and another weak peak at 44.5^0 corresponding to 200 face thus confirming the presence of Au in the beads.

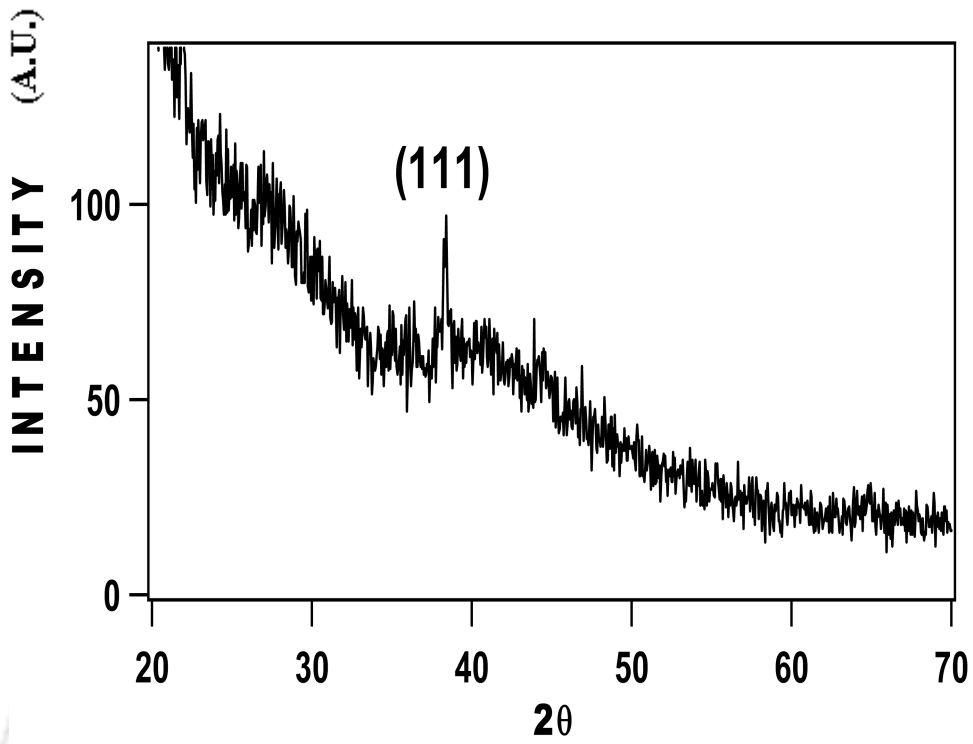

Figure 4.4: XRD pattern of the grinded Au nanoparticles deposited resin beads.

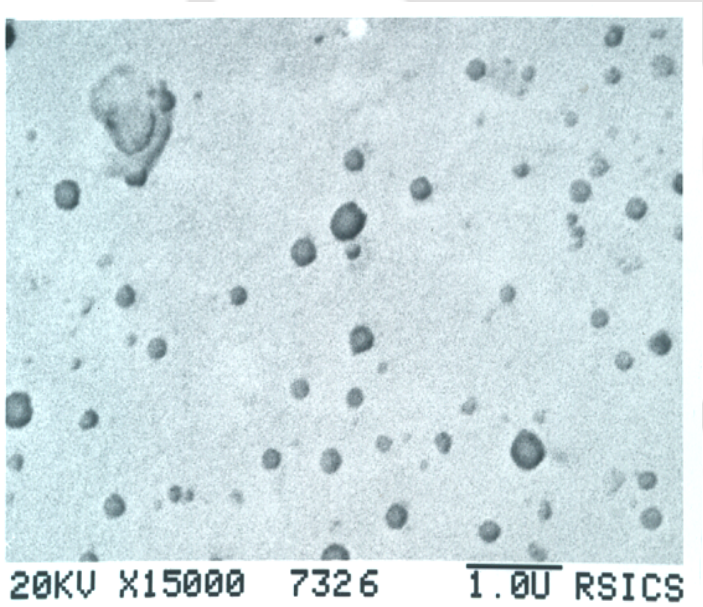

Figure: 4.5 Scanning electron microscopy image of the Au NPs deposited on the resin surface.

4.3.3 Scanning electron microscope studies of Au Nanoparticle deposited beads

To study surface morphology of the Au nanoparticles deposited on the surface of the beads, scanning electron microscopy (SEM) was used. Figure 4.5 shows the typical SEM image of the composite as deposited on a single bead. As clear from the figure there were NPs formed on the bead with the sizes ranging from 100 nm to 200 nm. The particles were isolated such that such there was no discernible agglomeration of them.

4.3.4 FTIR spectroscopic studies of the Au NPs-PANI composite beads

As a requirement of the experiments Au-NP and aniline deposited polymer beads were further treated with H_2O_2 for the generation of PANI. Although, green coloration of the bead was indicative of the formation of PANI on the surface of the beads, FTIR spectroscopy was pursued to ascertain the formation. The FTIR spectrum of the grinded beads was in a diffuse reflectance mode.

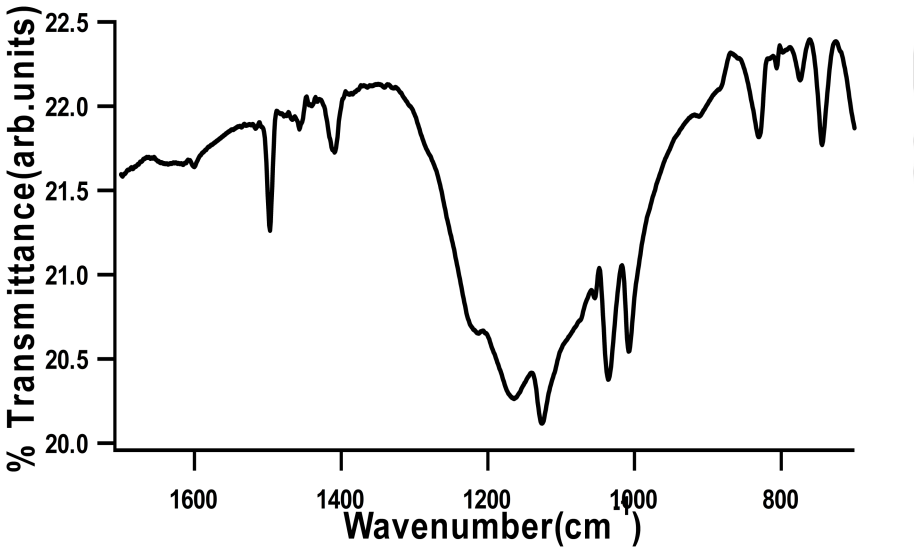

Figure 4.6 FTIR spectrum of the composite Au-PANI resin beads.

The FTIR spectrum of AuNP-PANI composite coated beads is shown in Figure 4.6. It can be clearly seen that spectrum contains strong peaks at 1417 cm^{-1} and 1500 cm^{-1}. The presence of these peaks indicates the presence of benzoid and quinoid ring vibration in the polyaniline backbone. The strong band at 1150 cm^{-1} is also a characteristic of conducting PANI. Thus PANI was indeed formed on the beads by the present method.

4.3.5 Diffuse reflectance UV-Vis spectrum of the composite

The UV-Vis spectrum of the AuNP-PANI composite beads was also recorded using the grinded resin beads in diffuse reflectance mode. A typical spectrum is shown in the Fig 4.7, which consists of peaks occurring at 800 nm and 400 nm. These peaks are characteristics of the emeraldine salt form of PANI. Thus both the FTIR and UV-Vis spectra confirm the deposition of conducting emeraldine salt form of PANI on the resins.

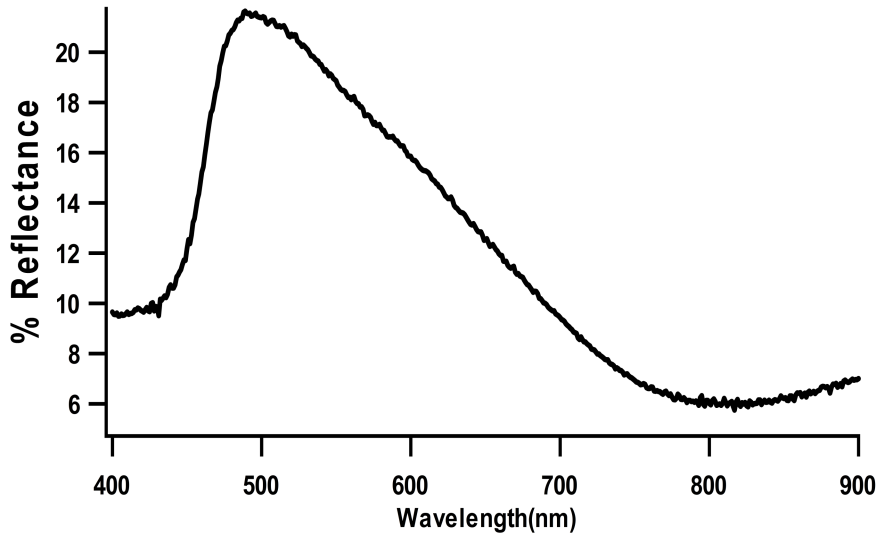

Figure 4.7 Diffuse-Reflectance UV-Vis spectrum of the Au-PANI composite deposited on the resin surface**.**

4.3.6 Scanning electron microscopy and EDX of the AuNP-PANI composite deposited on the resin beads

In an ordinary bead, upon exchange with the salt of Au and anilinium ion and subsequently when Au NPs were formed, the color of the beads turned purple, indicating the formation of Au NPs on the surface. On the other hand when the same beads were further treated with H_2O_2, the color of the beads turned light green due to the formation of PANI on the surface. To ascertain further that the process leading to polymerization did not change or remove Au NPs from the surface we performed SEM analysis of the beads after both Au NPs and PANI were generated. SEM micrograph and corresponding energy dispersive X-ray (EDX) analysis of a composite deposited resin bead (not grinded) are shown in Figure 4.8. The presence of individual Au NPs scattered over the bead could be seen as bright spots over a darks background (Figure 4.8 A). In addition, EDX graph shown in Figure 4.8 B clearly indicates the presence of Au in the bead. One could also see the presence of Cl in the composite bead as shown in the EDX spectrum in Figure 4.8 B.

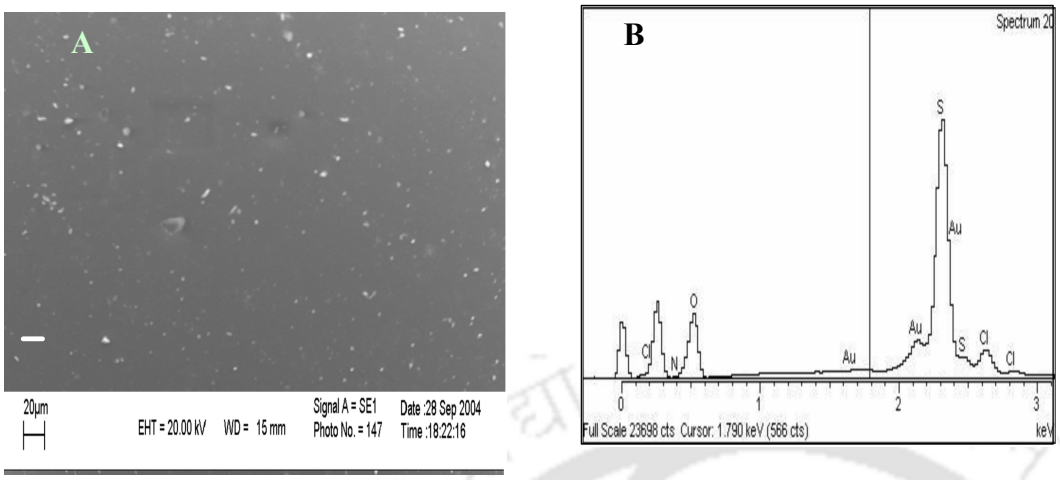

Figure 4.8 (A) Scanning Electron micrograph (SEM) and (B) Energy dispersive X-ray (EDX) of the AuNP-PANI composite deposited on the resin surface.

This probably indicates the presence of unreduced Cl-containing Au salt in the bead. On the other hand, the signal due to N is considerably low which is probably due to low initial loading of anilinium ions in the bead, essential for the generation of the composite on the beads.

4.3.7 AuNP-PANI beads as catalyst as well as sensors

After getting the beads with proper Au NP and PANI coating, we want to use it as a multifunctional device. For this purpose we had chosen to pursue the chemical reaction involving oxidation of glucose to gluconic acid. Glucose is known to get oxidized in the presence of O_2, and the reaction can be catalysed by Au NPs at alkaline pH[33]. The product of the reaction changes the pH of the solution from alkaline to acidic. Fortuitously, the change in pH renders the change in color of PANI from blue to green. Thus the formation of product as

a result of the reaction could be ascertained by the change in color of the PANI coated beads, while at the same time the Au NPs content of the beads acting as the catalysts of the reaction. In this regard, when 0.02g of the Au NPs and PANI composite coated beads were kept in 5 mL of 0.106 M glucose solution and O_2 was bubbled through the solution, the blue colored beads turned green in 20 min. The color change of the beads is as shown in the Figure 4.9. The pH of the solution changed from a value of 9.1 to 1.8. Polarimetric measurement showed that the specific rotation of the initial glucose solution decreased from value of $[\alpha]^{25}_D = 50^0$ to $[\alpha]^{25}_D = 20^0$ after 20 min of the progress of reaction. This is consistent with the formation of gluconic acid as the product of the reaction. We would also like to mention here that when the same PANI - only coated beads (without the presence of Au NPs or $HAuCl_4$) were used, which means that the reaction was carried out in the same condition as above except for the absence of Au NPs, then there was no change in color of the beads with blowing O_2, even long after 21 min. This shows that Au NP generated on the resin beads catalyzed the reaction in the presence of O_2.

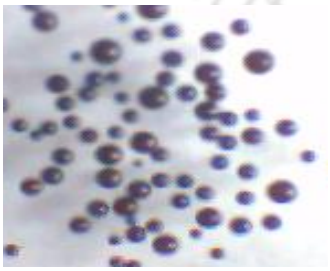

Glucose and oxygen

Au nanoparticles / polyaniline coated resin beads as colorimetric glucose sensor.

Figure 4.9 Photograph of the resin beads showing the change in colour during the oxidation of glucose to gluconic acid.

4.3.8 FTIR spectroscopic study of the reaction product

We have also pursued FTIR spectroscopic studies to confirm the product formed during the reaction. For this purpose we have separated the product, and allowed it to dry at room temperature. The spectra were recorded using KBr palate. The spectra are shown in the Figure 4.10. As evident from the spectra, an additional peak, occurring at 1650 cm^{-1} typically corresponding to C=O stretch of an acid, is present in the product (Figures 4.10B and 4.10 C) from the reaction of glucose with O_2 in the presence of both Au NPs and Au NPs plus PANI containing beads, in comparison to the peaks of the reactant glucose (Figure 4.10 A). This would mean that gluconic acid was formed as a result of the reaction in both the cases. It is also interesting to note the accompanying change in color of the beads from blue to green (in the case of Au NPs and PANI coated beads) as a result of the reaction and is shown in Figure 4.9. This also supports that acid product was formed due to the reaction in the presence of composite coated beads.

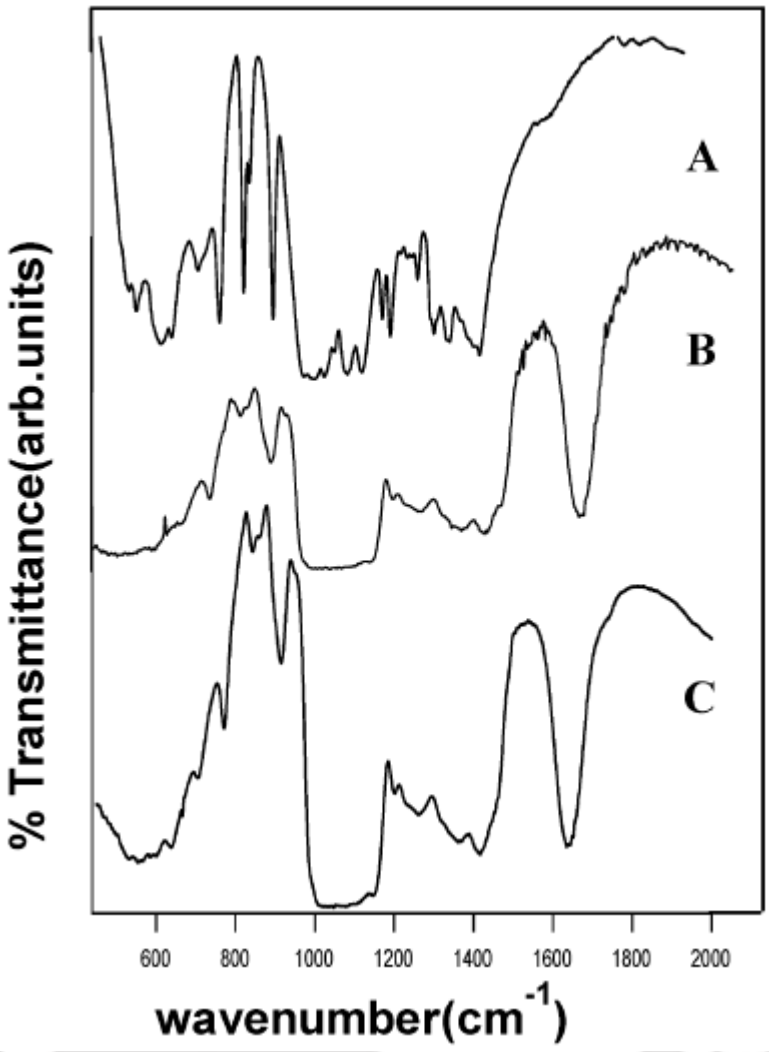

Figure: 4.10 FTIR spectra of the (A) Glucose; (B) the dried product of oxidation of glucose formed in the presence of Au NP (only) coated beads: (C) the dried product of oxidation of glucose formed in the presence of Au NP –PANI composite coated beads.

4.3.9 Sensitivity limit

Further, we would like to point out here that we have found that the minimum concentration of glucose needed for visual observation of color change with the same amount of beads was 1.0 mM. This sensitivity is comparable to all the existing methods of glucose testing.

When cation-exchange resin beads are treated with $HAuCl_4$ and when exchange happens, it is normally likely that $AuCl_4^-$ will not exchange with the protons in the activated beads. However, there is the likelihood of reduction of $AuCl_4^-$ by the sulfate or other groups of the resins. The attached species may further be reduced by $NaBH_4$ to generate Au NPs. The following observation would support the above proposition. When $HAuCl_4$ (acidic) was added to an aqueous solution of sodium dodecyl sulfate (SDS) and the solution was kept for two days the solution turned purple in color with UV-Vis spectrum consisting of characteristic absorption of Au NPs at 530 nm. Thus if sulfate group attached to an aliphatic organic chain could reduce $HAuCl_4$ to Au NPs, it may also be possible for the $-SO_3^-$ groups of the resin beads to reduce $HAuCl_4$ into an intermediate species which can further be reduced by $NaBH_4$. The presence of Cl as observed in the EDX spectrum corroborates the idea of one or more of the Cl containing Au species to be attached to the resin beads. Once attached, they can appropriately be reduced on the surface by a suitable reducing agent such as $NaBH_4$. The reduction of cationic species such as a gold salt to Au NPs when embedded in a polymer is

well-known, especially in the presence of UV light[34]. Hence, the idea of attaching an Au salt to a polymer resin followed by chemical reduction to Au NPs, hitherto unknown, is well-suited with the present level of knowledge in this field. Finally, the potential for the use of the same beads for multiple uses makes the work appealing and promising.

4.4 Conclusion

In brief, we have introduced a new method of generation of Au NPs and PANI on the surfaces of cation exchange resin beads and then used the beads for catalytic oxidation of glucose at the same time detection of product formation by the change in color due to the presence of PANI on the beads. We have been able to measure the presence of a minimum of 1.0 mM glucose in aqueous solution using the present method. This could form the basis of introduction of even a larger number of species in sequence or simultaneously. Incorporation of multiple nanoscale materials would improve the sensitivity of the elements exhibiting multifunctionality

4.5 References

1. Levy, L.; Sahoo, Y.; Kim, K.S.; Bergey, E.J.; Prasad, P.N. *Chem. Mater*. **2002**,14,3717.
2. Ravi Kumar, M.N.V. *J. Pharm. Pharmaceutical. Sci*. **2000**, 362, 234.
3. Niemeyer, C. M.; Ceyhan, B.; Hazarika, P. *Angew. Chem. Int. Ed.* **2003**, 42, 5766.

4. Rajeshwar, K.; Tacconi, N. R.de.; Chenthamarakshan, C.R. *Chem. Mater*. **2000,** 13, 2765.

5. Hayakawa, T.; Usui, Y.; Bharathi, S.; Nogami, M. *Adv. Mater***. 2004**, 16, 1408.

6. Seong, G. H.; Crooks, R. M. *J. Am. Chem. Soc*.**2002**, 124, 13360.

7. Shoji, E.; Freund, M. S. *J. Am. Chem. Soc.* **2002**, 124, 12486.

8. Marvin, J. S.; Hellinga, H. W. *J. Am. Chem. Soc.* **1998**,120, 7.

9. Cui, G.; Kim, S. J.; Choi, S. H.; Nam, H.; Cha, G. S.; Paeng, K. *J. Anal. Chem.* **2000**, 72, 1925.

10. Lin, Y.; Lu, F.; Tu, Y.; Ren, Z. *Nano Lett*. ***2004***, 4, 191.

11. Pei, J.; Tian, F.; Thundat, T. *Anal. Chem*. **2004**, 76, 292.

12. Hoa, D. T.; Kumar, T. N. S.; Punekar, N. S.; Srinavasa, R. S.; Lal, R.; Contractor, A. Q. *Anal. Chem.* **1992**, 64, 2645.

13. Sarma, T. K.; Chowdhury, D.; Paul, A.; Chattopadhyay, A. *Chem.Commun*. **2002**, 1048.

14. Chowdhury, D.; Paul, A.; Chattopadhyay, A. *Langmuir* **2005**, 21, 4123.

15. Maier, S.A.; Brongersma, M.L.; Kik, P.G.; Meltzer, S.; Requicha, G.; Atwater, H.A. *Adv. Mater*. **2001**, 13, 19.

16. Kamat, P. V. *J. Phys. Chem. B* **2002**, 106, 7729.

17. Murray, C.B.; Sun, S.; Doyle, H.; Betley, T. *Mater. Res. Soc*, **2001**, 26, 985.

18. Guczi, L.; Peto, G.; Beck, A.; Frey, K.; Geszti, O.; Molnar, G.; Darocz, C. *J. Am. Chem. Soc*. **2003**, 125, 4332.

19. (a) Hall, N. *Chem.Comnun*. **2003**,1 (b) MacDiarmid, A. G. *Angew. Chem. Int. Ed.*

2001, 40, 2581. (c) Shirakawa, H. *Angew. Chem. Int. Ed*. **2001**, 40, 2574.

(d) Heeger, A. J. *Angew. Chem. Int. Ed.* **2001**, 40, 2591.

20. (a) Sonmez, G.; *Chem. Commun.,* **2005**, 5251.

5.1 Introduction

In the last few decades, considerable efforts have been made to downscale the feature size of building blocks in various microelectronics, optical and magnetic devices. These are necessary in order to incorporate complex functions in a single device and also to increase the speed of currently available devices. The primary approach in such device fabrication has been through the 'top-down' lithographic technique especially developed for the applications in semiconductor industries. In addition, recent developments in soft lithographic[1] techniques such as replica molding[2-3], microcontact printing[4] are creating platforms for providing cost effective patterns over large area of substrate surfaces. On the other hand, chemists and biologists prefer the 'bottom up' routes in systematic generation of superstructures for better and system-specific performances. Additionally, scanning probe microscopy (SPM) [5] based techniques use a combination of top-down and bottom-up approaches in the systematic depositions of colloidal materials over substrate surfaces. Further, SPM-based methods are also used in pattern generation in combination with chemical, biochemical, electrical, magnetic and mechanical methods.

Along with the development of various techniques for generating nanopattern, the importance of generating colored pattern has also been realized. Lithography in color with either sub-micron scale features or with components utilizing properties of nanomaterials occupies a special place with potential for applications in diverse fields such as in displays, lasers, sensors, information storage and electronic papers [6-15], high-density optical information storage[16],miniaturized optical devices[17],and in biological staining[18]. Although,

one looses the resolution when information is stored and retrieved in color compared to its monochromatic counterpart (due to limits imposed by diffraction), the advantage of storing information in "true" color cannot be overstated. Our laboratory had for the first time introduced the idea of lithography in color with the basis that even though the resolution will be inherently compromised while retrieving information in color (due to the limited range of wavelength) the advantage, however, lies with the information in color being stored as it is[19]. Subsequently there have been other reports in this regard[20]. In all the methods developed so far the materials that have been used were either of no tunable (optical) properties or of limited tunability. Thus there is a need for incorporation of materials in the patterns that have tunable optical properties. Among the materials that are of great potential use in this regard, semiconductor nanoparticles (NPs), whose optical properties are governed by quantum mechanical laws and thus the name quantum dots (Q dots), are drawing considerable attention for various applications. Due to their size dependent optical properties [21] they are promising candidates for wide range optoelectronic, photovoltaic, and biological sensing[22-26] device applications. They have also been used as single photon source, in semiconductor lasers and in non linear optical devices[27-30]. Along with developing ways of generating high quality monodispersed NPs[31], pattering them on various surfaces is also important. Such arrays would be useful in multiple color light emitting diodes (LEDs)[32], pixels for field emission displays[33], multichannel chemical sensors[34] etc. Several approaches, such as crystal growth on patterned surface by metal organic chemical vapor deposition, (MOCVD)[35], interference photolithography[36], plasma etching[37] and microcontact printing[38], have been developed to

fabricate them. Alexander. M. Bittner[39] and his coworkers have developed a direct printing method based on dendrimer stabilized CdS nanoparticles. Luis. M. Liz Marzan and coworkers[40] use photoactivation of semiconducting NPs to generate multicolor patterns. However, the pattern formed on the substrate surface was unstable in the presence of light. In this chapter we report a new method of generation on films embedded with quantum dots based on a combination of top-down and bottom-up approaches and demonstrate one of its potential applications by imprinting patterns in one and two colors. The method is based on chemical reaction of a gaseous species with another species present in a polymer film where the pattern is generated by exposing a selected area of the film to the reacting gas by using a transmission electron microscopic (TEM) grid as a mask. The TEM grid, placed on the surface, blocks the chemical reaction on that (unexposed) part of the surface thereby producing a regular and predetermined pattern due to the formation of NPs on selected parts of the surface. The present method that we report herein has three objectives. The first being a new method of lithography using a combination of top-down and bottom-up approaches, where the TEM grid contributes the top-down part and the molecular reaction leading to lithographic pattern generation contributes the bottom-up approach of it. The second objective is to develop a simple, yet powerful method for structured pattern formation on an arbitrary surface using the objective of photolithography but the principle of molecular lithography at various length scales of the pattern with single or multiple functional components. The third objective is the development of a new and versatile form of lithography for the storage of information in color. Although the present report is about lithography in color, the principle behind the method would make it possible to be extended to patterning a large number of

materials on various substrate surfaces, which would possibly make the method more general. The present method should be able to generate structural patterns from a small to a very large area substrate surface, which is useful for applications at various length scales.

5.1.1 Our strategy

Our objective was to generate pattern with quantum dots in polymer films. For this purpose we used a TEM grid as the mask, and gas solid reaction to generate pattern on the unmasked parts of the film. As shown in Figure 5.1, the Cd^{+2} ions were embedded uniformly in the polymer film, and the film with TEM grid was exposed to H_2S for a particular duration to obtain uniform pattern.

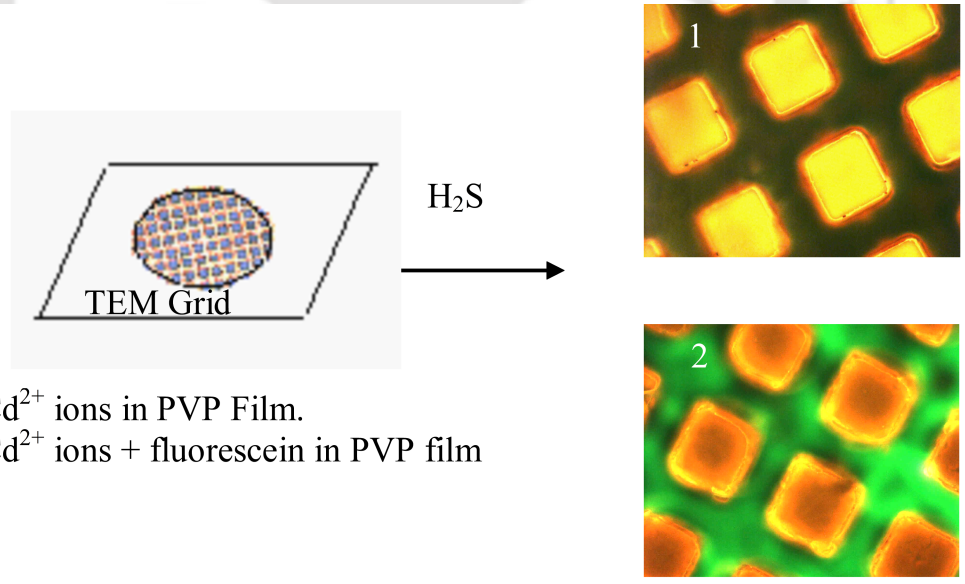

1. Cd^{2+} ions in PVP Film.
2. Cd^{2+} ions + fluorescein in PVP film

Figure 5.1 Generation of pattern using TEM grid as mask and reaction of Cd^{2+} embedded in the film with gaseous H_2S. In the right top (1) is shown the optical micrograph of the fluorescent pattern against PVP as the dark background; while at right bottom (2) is the fluorescent CdS pattern against fluorescein dye in the PVP film. (The scale bar is 20 μm)

We have used the chemical reaction of Cd^{2+} ions, present in a polyvinyl pyrrolidone (PVP) polymer film, with gaseous H_2S to produce fluorescent yellow/orange colored CdS NPs[41,42] in the form of rectangular grid patterns that follows the pattern of the TEM grid. In addition, we have extended this principle for pattern generation in two colors by starting with a fluorescent dye incorporated in all parts of the film and then selectively converting the Cd^{2+}, present in the unmasked part of the grid, into CdS thereby producing a regular pattern of two colors occurring due to CdS and the dye. Further, we have been able to demonstrate the versatility of the method by generating patterns with PbS NPs on the surface using the same principle. Interestingly, by superposition of two grids on the film (and using the same as a mask) we have achieved several patterns other than square patterns and also the best line resolution of 1 μm.

5.2 Experimental section

In a typical experiment 0.05 M cadmium acetate was prepared in 10 mL of ethanol and 0.074 g of polyvinyl pyrrolidone (Aldrich, MW ca 29,000) was separately dissolved in 2.5 mL of ethanol. 200 μL of each of the above solutions were mixed together. Then 40μL of this

solution (mixture) was placed on a microscope glass slide (typically 5 mm x 5 mm) and a thin film was formed upon evaporation. The typical thickness of a film was measured to be about 5 μm. In actual experiments a 3 mm diameter copper TEM grid (400 Mesh) was placed on top of the evaporating film 15 min after the liquid was placed on the slide at room temperature. The slide was then placed inside a 50 mL glass vial that was covered with a *parafilm*. H_2S gas, generated from an ordinary Kipps apparatus, was then blown through the container for half an hour through a *microtip*. The film could be observed to turn yellow in color and was subsequently taken out for further analysis following removal of the grid using a pair of forceps. In a typical experiment it took about 30 min of exposure of H_2S gas to obtain a good imprint. A longer exposure tended to either blurs the pattern or turned it into black. Lower exposure time did not generate a complete and reproducible pattern.

It may be mentioned here that we had done other experiments by varying the time of placing of the TEM grid on the film. We found that if the time of placement was earlier than the above (i.e. the film was far from dry), the TEM grid could not be lifted from the film after H_2S exposure without damaging the film. This is typically about much less than 15 min after deposition of the film. On the other hand if the grid was placed much after 15 min the seal was not sufficiently good to have preferential pattern formation at the exposed sites only. It may further be mentioned here that on exposure to H_2S, the TEM grid becomes black in color (from initial copper color), probably due to the formation of copper sulfide. However, our observations suggest that this did not affect the production of patterns as desired. For example, we had used nickel grids and we observed the same results in that case too. Also, the

same grid could be used repeatedly for a few times (typically three times without damage during lift-off) for pattern generation.

5.2.1 Bicolor pattern generation

For the pattern generation in two color, the procedure was the same as above except that 200μL of 4.5×10^{-4} M fluorescein solution in ethanol was mixed with 400 μL of the mixture prepared as above. The procedures for subsequent placing of the TEM grid followed by exposure to H_2S gas were exactly the same as above.

5.2.2 Patterns with PbS

In the case of generation of pattern with PbS NPs, the experimental procedure was same as the one used for bicolor generation. In a typical experiment, 0.05 M lead acetate (Merck) solution was prepared in 10 mL of ethanol and 0.074 g of polyvinyl pyrrolidone (Aldrich, MW ca 29,000) was separately dissolved in 2.5 mL of ethanol. 200 μL of each of the above solutions were mixed together. Then, 200μL of 4.5×10^{-4} M fluorescein solution in ethanol was mixed with 400 μL of the above mixture. This was followed by placing 40μL of this solution (mixture) on a microscope glass slide (typically 5 mm x 5 mm) and a thin film was formed upon evaporation. A TEM grid was placed before complete evaporation (15 min after the liquid was placed on the glass slide). The exposure to H_2S and subsequent removal of the grid were same as in the case of CdS generation.

5.2.3 Double-Grid Mask

We have also generated patterns with two TEM grids by aligning one atop the other in order to achieve higher resolution. In these experiments, two grids were first aligned under an optical microscope, followed by transferring to the film and subsequently pressing using hydraulic press (at 5 ton for 30 s on a 5 mm x 5 mm film) and then carefully transferred to the film as before (with single grid). The covered film was then exposed to H_2S gas as before and finally the grids were lifted using the procedure described above for single - grid experiments.

5.2.4 Fluorescence Microscopy studies

In order to observe the pattern formation on the film, the TEM grid was carefully removed from the film and the film on the glass slide was used for observation using a Karl Zeiss epifluorescence microscope (Axioskop2 MAT). The sample (film) was excited with light of three different wavelengths. For ultraviolet excitation, the wavelength was in the range of 365 nm and was collected by a band pass filter beyond 390 nm. For blue excitation, the wavelength was in the range of 450 – 490 nm and the emission was collected by a band pass (high) filer beyond 515 nm. For green excitation, the wavelength was in the range of 536-554 nm and the emission was collected by a band pass (high) filter beyond 565 nm.

5.2.5 Spectroscopic Studies

UV-vis and fluorescence spectroscopic studies were performed by placing the film in the sample compartment of the spectrophotometer. A Perkin-Elmer lambda25 UV-vis spectrophotometer and a Varian Cary Eclipse fluorescence spectrophotmeter were used for the

studies. For the spectroscopic, X-ray diffraction and TEM studies (below), we used the plain film sample without covering with a TEM grid.

5.2.6 X-ray diffraction studies

To further characterize the particles formed on the film, and to measure the particle size, X-ray diffraction of the sample was recorded using a Seifert powder X – Ray diffractometer (XRD 3003 TT) with Cu - α source at wavelength 1.54 Å and the data were recorded at room temperature. As a larger size film was required for the measurement, the whole film (3mm x 3mm) was exposed to H_2S gas without the use of the grid and once the yellow color formation was observed after 30 min of exposure to the gas, the film was used as it is for XRD measurement.

5.2.7 Transmission Electron Microscopic Studies

In order to perform TEM studies of the NPs generated in the process, the entire film (1.5 mm x 1.5 mm) was dissolved in 3 mL ethanol followed by diluting the solution to 10 mL. One drop of the diluted solution was placed on a TEM grid (carbon coated copper grid) and was allowed to dry under the ambient condition. The grid was then placed under a JEOL (Model 1200 EX) transmission electron microscope operating at an accelerating voltage of 120 KV for further observations.

5.2.8 Atomic Force microscopy (AFM) measurements

Atomic force microscopic measurements were made of as-prepared film with patterned CdS NPs on it, using a Veeco Multimode AFM. The recording was done in tapping mode.

5.3 Results and Discussion

When a TEM grid is placed on a polymer film that is more of a paste than a completely dried film then parts of the film can essentially be blocked from being exposed to the impending gas molecules, especially if the exposure is for a relatively shorter duration. When the Cd^{2+} ions, present in the polymer (PVP), reacted with H_2S they produced CdS particles. Thus in the final film a regular patterns of CdS particles would form on the film following the TEM grid pattern. Systematic studies were performed to find the optimum concentration of Cd^{2+} in the film and it was found that the TEM grid to be placed after 15 min after the liquid was placed on the slide at about 25^0 C. Further studies shows that to obtain highly fluorescent film 30 minutes exposure to H_2S gas is sufficient. With increasing exposure time more that reduces the fluorescence intensity of such pattern while lesser exposure time leads to incomplete pattern formation. A typical fluorescence microscopic image of one such film is shown in Figure 5.2. As clear from the figure, the above method produced regular square, apparently two-dimensional boxes of yellow colored patterns against a dark background. Each yellow colored box in Figure 5.2 has the dimensions of about 48 μm x 48 μm, which are equal to those of the holes in the TEM grid. The yellow color formation indicates that CdS NPs were possibly generated in the film. This observation indicates that during exposure of the polymer film to H_2S, and masked by the grid, the molecules could only react with the Cd^{2+} ions present in the open part (unmasked region) of the film and there is no evidence to

suggest that H_2S penetrated through the grid mask. The placing of the grid on the film, when the polymer was not completely dry, made an effective seal where H_2S could not penetrate through the side (covered parts) even though it reacted with Cd^{2+} present in the unmasked parts by penetrating along the depth of the film. This is consistent with our observation that when the grid was placed on a dried film (i.e. after 15 min of film formation) the seal was not good and CdS formation (fluorescence) could be observed even in the masked part where H_2S moved laterally also.

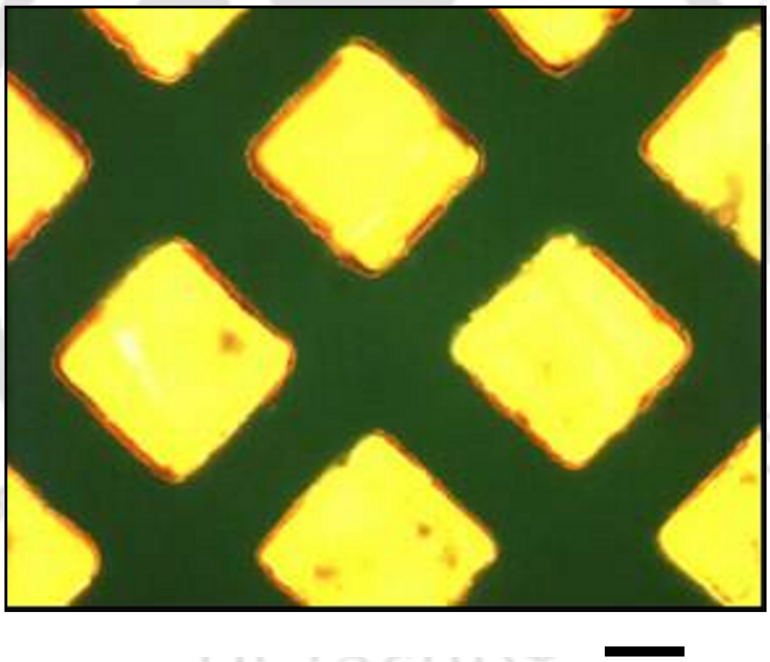

Figure 5.2 A typical fluorescence micrograph of the CdS nanoparticles patterned on PVP films using the present method of imprinting. The scale bar is 20 μm.

5.3.1 UV-Visible spectroscopic study

UV-Vis spectrum of the film (prepared in the absence of a TEM grid) showed a broad peak with a maximum at around 410 nm Figure 5.3 (a), which is characteristic of CdS NPs present in the matrix. The intensity and wavelength maximum varied from sample to sample and is known to be very sensitive to the size and shape of the NPs formed. In the present set of experiments, the particle sizes of CdS were rather small with a narrow distribution, as shown later from the TEM measurements.

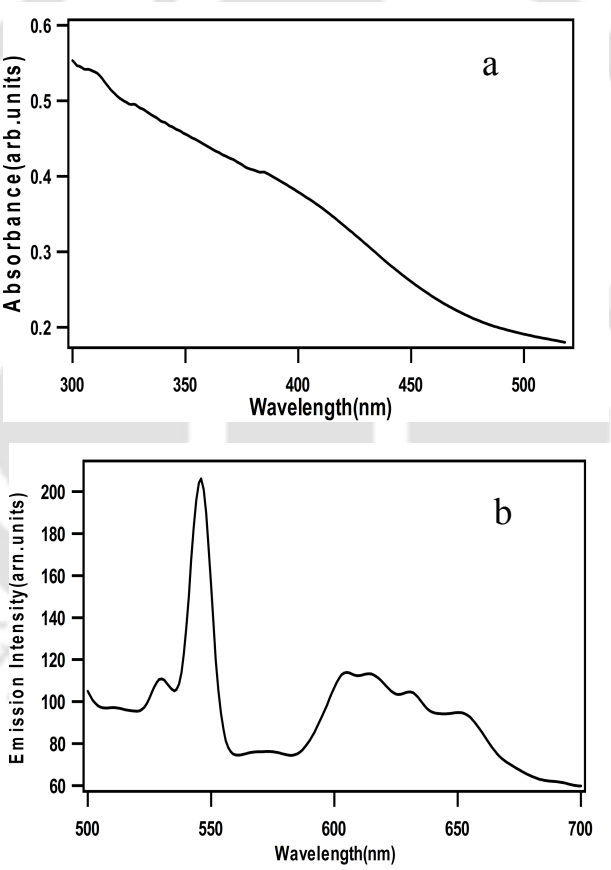

Figure 5.3 Absorption (a) and emission (b) spectra of a typical CdS / PVP film at room temperature. For fluorescence, excitation wavelength was set at 415 nm.

Fluorescence spectrum of the same film when excited at 415 nm consisted of two sharp peaks at 535 nm and 545 nm and a broad peak with several humps spanning 580 – 680 nm Figure 5.3 (b). The sharp peaks are known to represent the band gaps and are thought to occur due to recombination of electron-hole pair. On the other hand the broad peaks in the longer wavelength region are due to radiative charge recombination of the surface trap states and these may be the primary color seen under the microscope. Lackowicz et al[42] have reported similar observations in their Cd^{2+} enriched CdS NPs, which may well be the case in the present system. This is consistent with our observation of yellow/orange boxes on the film. Both the UV-vis and fluorescence spectra together support that CdS NPs were probably formed, which gave rise to color in the film.

5.3.2 X-ray diffraction study

We further pursued X-ray diffraction (XRD) studies to probe the formation of CdS NPs and to get an idea of the particles sizes. For this experiment we had allowed the entire film containing Cd^{2+} ions without the presence of a TEM grid, to be exposed to H_2S gas, as the XRD experimental setup requires a larger film than to be obtained using a TEM grid. All other conditions of the experiment were kept the same. An XRD plot shown in Figure 5.4 indicates the formation of CdS particles grown primarily in the (111), (220) and (311) lattice planes with a relatively smaller and sharper peak representing growth in the (200) plane. Particle sizes, when calculated using Scherrer[43] formula, Crystallite Size $D_{crystallite} = k\lambda/\beta\cos\theta$, Where k =0.8-1.39 (usually close to 0.9), λ= is the wavelength of the radiation λ_{Cu}

= 1.54056 Å, β - FWHM (full width at half maximum) in radians, θ - the position of the maximum of diffraction. The particle size were found to be typically 11 nm, 15 nm and 16 nm corresponding to the graphs in (111), (220) and (311) planes respectively. Thus XRD studies demonstrate that the present procedure of exposure of Cd^{2+} containing film to H_2S gas resulted in the formation of CdS NPs.

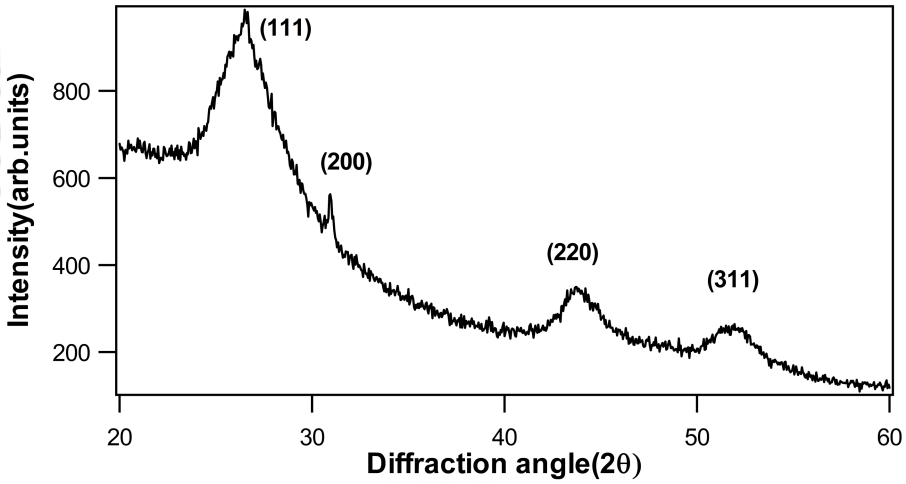

Figure 5.4 X-ray diffractogram of CdS deposited on the PVP film. The principal Bragg-diffraction lines are identified.

5.3.3 Transmission electron microscopic study

Further, the formation CdS NPs was supported by the observation of the particles under a TEM. For this the film was dissolved in ethanol prior to sample preparation. A typical micrograph is shown in Figure 5.5. As clear from the figure, the particles formed were spherical and had diameter of about 4 nm. A sample plot of particle size distribution indicates that there were greater than 90% of the population with sizes of 4 nm (small) and the rest were distributed between 5-7 nm (large) and some were also less than 4 nm diameter. Thus the present method of CdS formation using a gas-solid reaction generated primarily NPs of small sizes and of narrow size distribution.

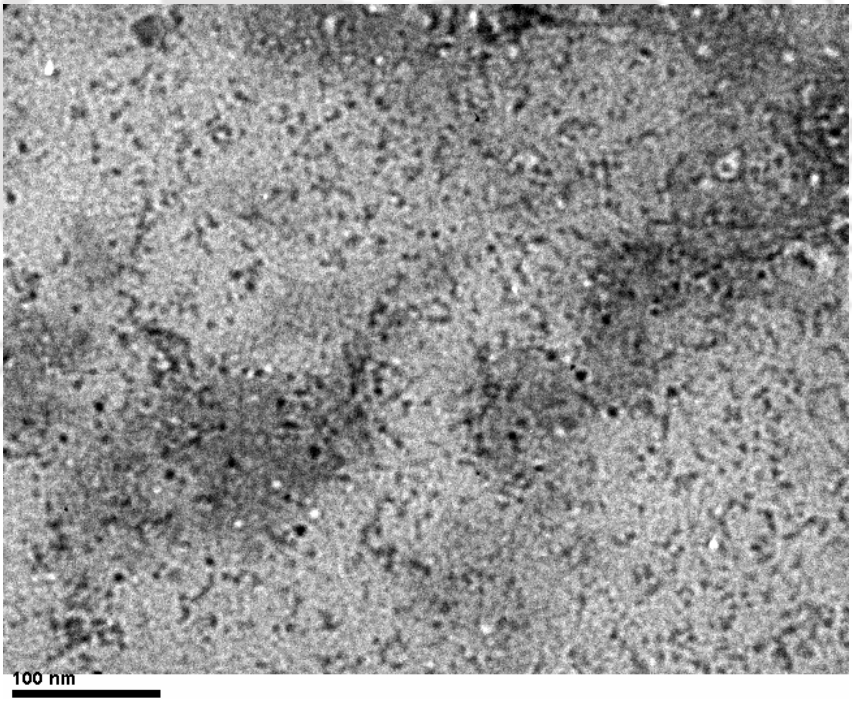

Figure 5.5 A typical transmission electron micrograph of CdS nanoparticles produced in the film.

5.3.4 Effect of TEM grid on the film

It is important to note here that the procedure followed in this protocol in placing and subsequently lifting of the TEM grid after exposure did not damage the basic uniformity of the film structure in terms of distribution of CdS NPs covered boxes. In other words, the production of uniformly patterned surface covered with CdS NPs could be possible using the present method, thus keeping the integrity of the film intact. This can be appreciated if one notices the uniformity of distribution of CdS deposited boxes in the film in Figure 5.1. It may further be mentioned here that upon exposure to H_2S the TEM grid becomes black in color (from initial copper color), probably due to the formation of copper sulfide. However, our observations suggest that this did not affect the production of patterns as desired. For example, we had used nickel grids and we observed the results similar to those mentioned above. This indicates that even though the exposed top part of the copper grid reacted with H_2S, it did not affect the pattern formation used in our method. Further, since the masked parts contain color characteristic of the background (PVP or the dye in case of two color experiment) it can be assumed that the reaction of TEM grid with H_2S did not affect the final desired outcome. Also, we did not observe any effect of possibly trapped H_2S on the features.

For example, we have recorded the fluorescence micrograph of a sample with an interval of 1 year (the first measurement was performed within 1 hour of preparation) and we did not observe any significant change either in feature size or shape. In addition, we have observed no difference in features between the one observed before the removal of TEM grid and after the removal of the same. Also, we have found that in most of the cases the TEM grids can be

reused for a few cycles (three to four times). However, sometimes the grid did get damaged (as a result of being bent or broken) during lifting and hence could not be reused.

5.3.5 Atomic Force Microscope study

In order to better understand the formation of CdS on the film we pursued atomic force microscopic (AFM) study of a part of the film. This is shown in Figure 5.6 (a). As evident from the figure there are the formation of walls around the centre of the box, and which is in between the centre of the box and the grid-lines. This "hill" formation probably occurred during the placing of the grid on the film (due to the weight of the grid) before it was completely dried. In other words, it is due to material transfer from the covered part of the film to the open part of the film when the TEM grid is placed on it. Thus when relatively less amount of gas is blown over the film, the Cd^{2+} ions present in the top "hilly" portions react much more than the bottom "crater" portions. Also, the three-dimensional hill-like structures would have much more exposed surface area for reaction with the impending gas than those of the two-dimensional film at "crater" parts of the film. This essentially leads to the formation of colored rims at the beginning of exposure. Upon further exposure to H_2S, the Cd^{2+} ions from all parts of the box get converted to CdS leading to apparent yellow colored box formation.

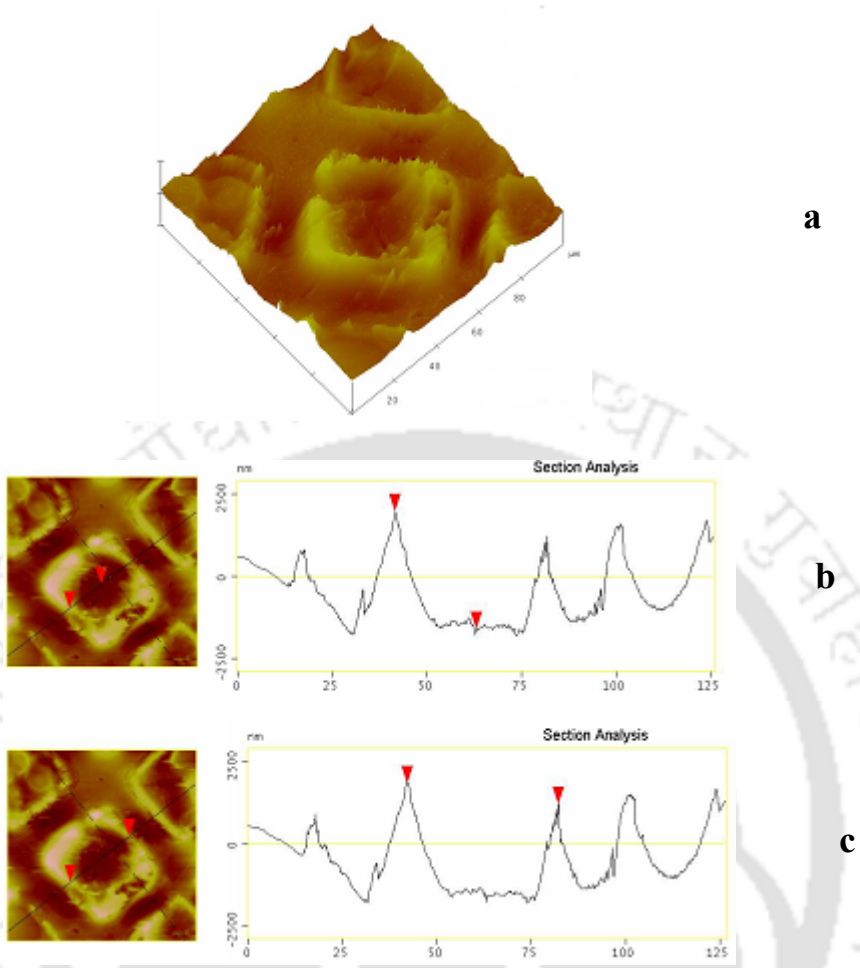

Figure 5.6 (a) AFM of a selected area of a typical film with CdS imprinted using the present method. (b) Section analysis for measuring the height of the "hill" from the "valley". (c) Section analysis for measuring the dimension of each box.

It may be mentioned here that the AFM picture (Figure 5.6 a) shows that each yellow colored box in Figure 5.1 is in reality a three-dimensional structures with "hilly" rims and a "valley" at the centre. The intense fluorescent color from the CdS present in the film blurs the three-dimensional structure and makes them appear like a two-dimensional box. Further, in

certain cases the placing of the grid on the film results in the formation of non-uniform heights of the film-rim, which leads to deposition on the "hilltop" and thus formation of structures other than the rim.

5.3.6 Effect of H_2S gas on the film with time

We also noticed that exposure of the film to H_2S for a shorter duration than mentioned above did not produce a continuous box but generated a structure, which is essentially a rim in the box. A typical deposition of CdS on the film from a 15 min of H_2S exposure (compared to a regular exposure of 30 min shown in Figure 5.1) is shown in Figure 5.7. As can be seen from the figure for most of the boxes the initial depositions appeared to have occurred at the periphery rather than at the center. There is also a box or two where the CdS was formed on one side of the box than the other. It is expected that a film with uniform distribution of Cd^{2+} would produce NPs distributed uniformly over the film. However, the present observation apparently indicates something other than the above.

The occasional presence of lines in Figure 5.7 in some of the boxes is probably due to cracks formed during the drying process, which are clearly visible at low concentration of CdS deposition but are not discernible at higher deposition (Figure 5.2). In other words, the brighter lines are the "hilly" portions between the depressed (cracks) parts and thus react easily with the gas and thereby produced fluorescence at an early exposure. AFM measurement confirms that the size of each box is 48 μm x 48 μm (Figure 5.6 (b). It also suggests that a typical height of each "hill" is about 3.6 μm when measured from the center of the box Figure 5.6 (c). This height would certainly be a function of the fluidity of the polymer film as decided by the time of placing the grid on it. However, as the typical film thickness is

on the order of 5 μm, the hills and valleys generated (with height difference of 3.6 μm) in the structures do not affect the overall continuity of the film. Also, the TEM grid used were ordinary copper grid without any preferential coating on a side. In other words, the side of the grid used did not matter in creating the seal and imprinting the lithographic pattern by preferential CdS formation in the film. The color difference of CdS in Figure 5.1 and Figure 5.2 is probably due to particle sizes formed under two different local reaction conditions. Also the gradient of color could possibly be due to presence of different sizes of CdS NPs, which gives rise to different fluorescence color due to their size differences, even under excitation by the same light. This is further corroborated by the observation of formation of particles of different sizes from TEM measurements (Figure 5.5). Further, it may be mentioned here that CdS NPs formation on the film surface may not be limited to surface plane.

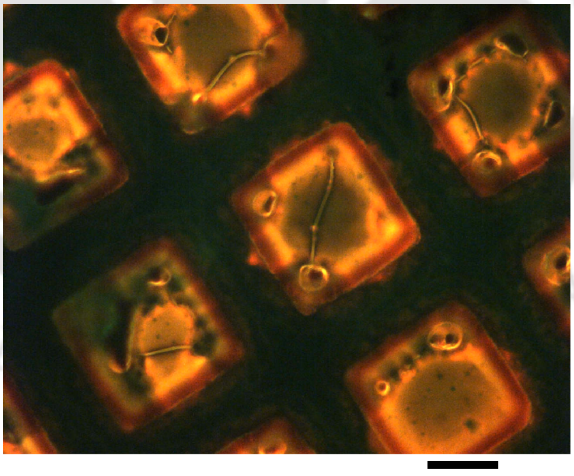

Figure 5.7 Exposure of the film to H_2S for 15 min only resulted in incomplete conversion resulting in non-uniform distribution of particle formation. A typical fluorescence micrograph is shown here. The scale bar is 20 μm.

As clear from Figure 5.6 (a), the exposed area of the film is not two dimensional and thus CdS would form in all the exposed three dimensional surfaces of the film. In addition, the film may be sufficiently porous for the H_2S to enter inside the film and form a three dimensional network of CdS NPs. However, the exact depth of the CdS formation in the film would depend on the porosity of the film as well as the time of exposure to the gas.

5.3.7 Bicolor pattern of CdS and PbS

We were further interested in extending this technique to achieve lithographic patterning using fluorescent materials of two different colors on the same film where CdS NPs would be one of the fluorescent materials. The idea is that CdS would be produced by the reaction of H_2S with Cd^{2+} in the exposed part of the film, whereas the unexposed part of the film would retain its original fluorescence due to the dye. This would be even better if the reaction of H_2S with the dye reduces the fluorescence due to the dye. For this experiment we began with a dye (fluorescein) incorporated in the film at the time of film preparation by dissolving the dye in the solution mixture, the details of which have already been included in the experimental section. The film was deposited on a glass slide in the same way as before and a TEM grid was placed on it as before. The film was then exposed to H_2S gas as earlier and the TEM grid was subsequently removed. We observed that a regularly patterned film with two distinct colors containing two differently fluorescent species could be obtained in this way. A typical picture is shown in Figure 5.8 in which the distinct yellow-orange (CdS) boxes of 48 μm x 48 μm sizes are uniformly distributed against the background of green colored

fluorescence from the dye present in the film (when excited by blue light). There are two important things that need to be mentioned here. First of all the color due to the emission of CdS could be obtained even in the presence of fluorescence of the dye which is present all over the film. Also, the intensity and green color of the background (unexposed parts) due to the dye did not get changed significantly even if the film was exposed to H_2S although selectively. This also means that H_2S did not generally migrate (diffuse) into the region outside the open grid boxes. We noticed that when the TEM grid covered film was exposed to H_2S for a shorter time (10 min) there was the presence of black spots at the center of the boxes (similar to those in Figure 5.7) indicating that the reaction of H_2S with the dye and Cd^{2+} diminished the intensity of green fluorescence of the dye.

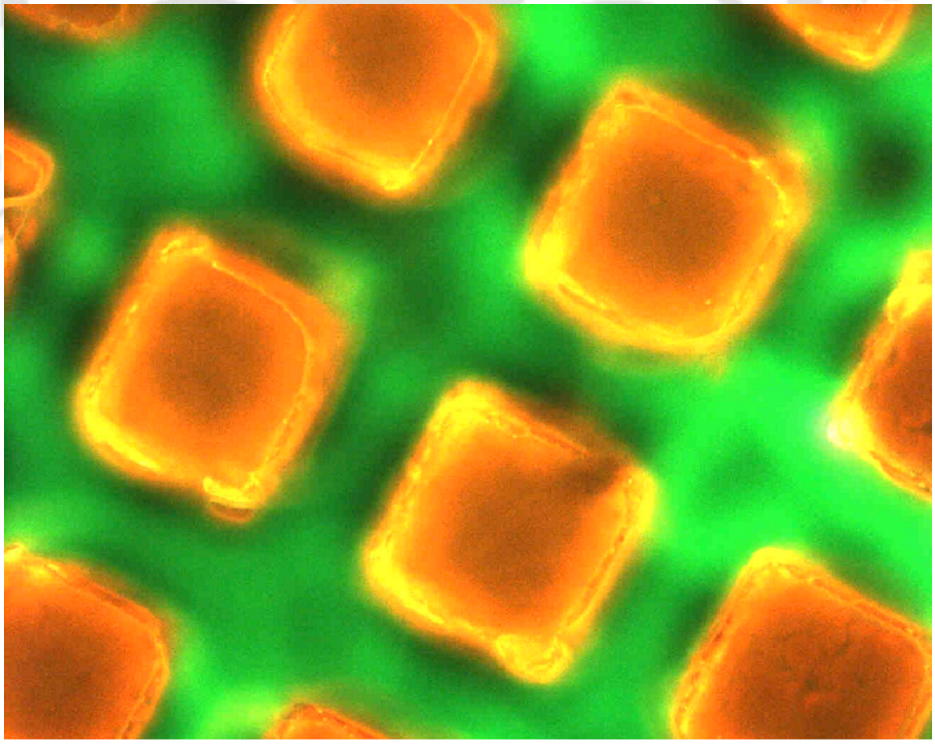

Figure 5.8 Fluorescence micrograph of a section of the polymer film consisting of rectangular boxes of CdS nanoparticles against the background of a dye. The scale bar is 20 μm.

Further, even though the fluorescent dye is present in the background, the formation of CdS NPs on the selected parts of the film and the fluorescence from the NPs resulted in the creation of two color pattern formation on the film. In addition, when a blank film with the dye only and no Cd^{2+} was exposed to H_2S gas the color of the fluorescence diminished significantly after an exposure of more than 20 min. Thus the reaction of H_2S with Cd^{2+} and the dye present in the film served the twin purpose of diminishing the fluorescence of the dye and formation of CdS NPs that are highly fluorescent.

In order to show the feasibility of the present approach for patterns with other materials on the film, we have pursued and obtained patterned films of PbS on PVP surface using the same method as mentioned in the (experimental section 5.2.2), except that we had started with lead acetate in the film rather than Cadmium-acetate and the grids used were either a nickel grid or a copper grid. A typical pattern appeared to be similar to that for CdS NPs (not shown here). However, since PbS emits in the near infrared region the contrast of color with PVP only film was not good. On the other hand when the fluorescein dye was incorporated in the film the green background fluorescence from the dye (when excited by blue light) provided a good contrast for the dark colored patterned due to PbS NP formation. We show a typical fluorescence micrograph of one such film, obtained using two grids together as the mask in Figure 5.9, when excited by blue light. As clear form the figure the typical dark rectangular patterns due to the formation of PbS NPs, could be seen against the background of PVP with

dye. Similarly a film, without the presence of the grid when exposed to H_2S gas generated a film that consisted of PbS nanocrystals as evidenced by XRD spectrum shown in Figure 5.10. The diffraction planes identified in the figure match with those of PbS. The average particle size calculated from the spectrum was 20-24 nm.

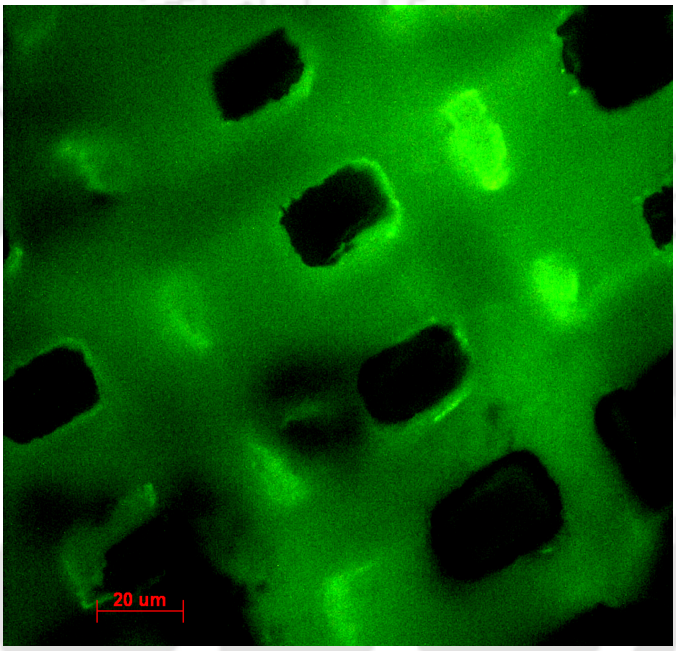

Figure 5.9 Fluorescence micrograph of the PbS pattern formed against background of fluorescein dye.

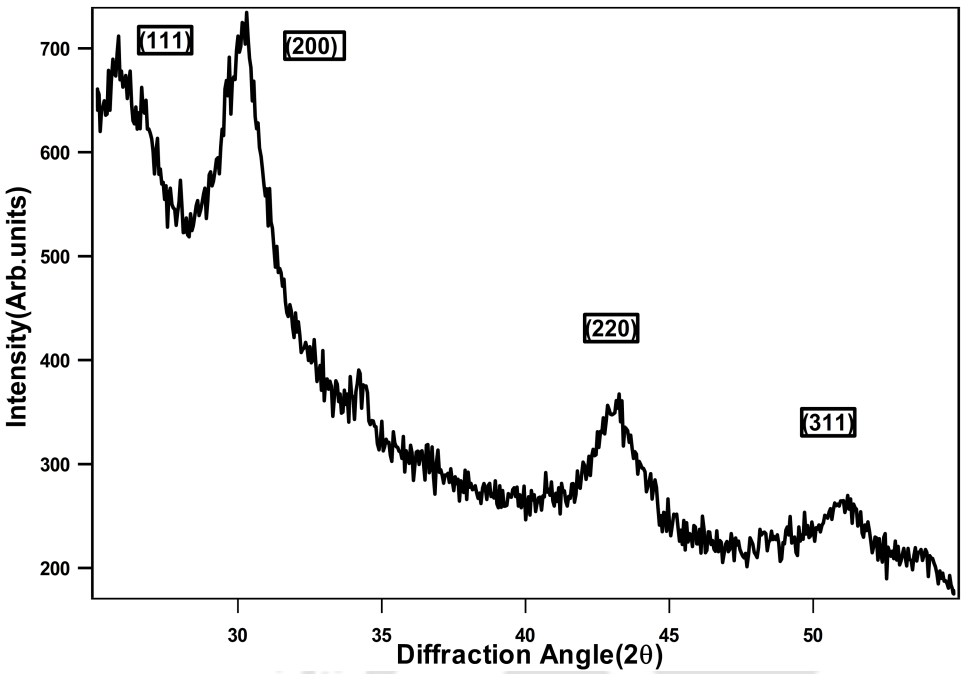

Figure 5.10 X-ray diffractogram of PbS deposited on the PVP film. The principal Bragg-diffraction lines are identified.

5.3.8 Pattern of various shape

We further pursued experiments to obtain structures of various sizes and shapes on the films. This was achieved by superposition of two TEM grids, where the patterns on each grid (holes) were kept at an angle with the other. This would produce a double-grid with a large number of patterns (holes) of different shapes and sizes. This is shown in the figure below

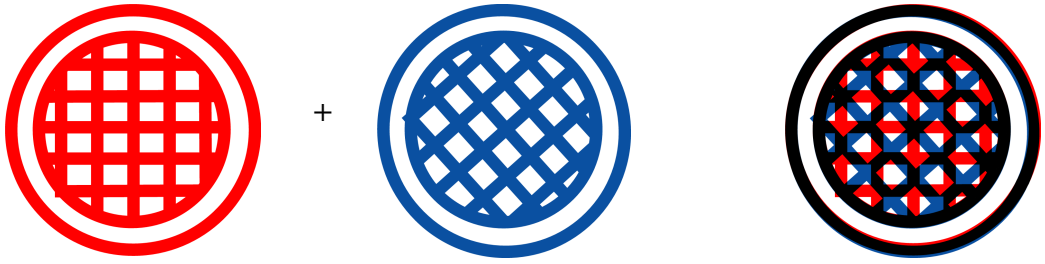

Figure 5.11 Schematic diagrams depicting the generation of patterns of various shapes using two grids.

When this double-grid was placed on the film containing either Cd^{2+} or Pb^{2+} ions with dye and was then exposed to H_2S gas, a large number of patterned structures could be obtained as seen through a fluorescence microscope. Figures 5.12 A, 5.12 B and 5.12 C show typical examples of patterned CdS NPs on the film when excited by blue light, and generated using the present method. The dark lines present in between the bright ones are due to valley formation as explained before. Similar example of PbS NPs generated on a dye containing film using two grids was already shown in Figure 5.9 while the picture was obtained by exciting the film with blue light. As clear from all the figures there are a variety of structures, that could vary from being rectangular in shape to simple line to a triangular and other shapes, could be generated using the present method. Thus it is possible to obtain various structured patterns on the film with quantum dots as one of the fluorescent materials. Another interesting aspect of the method here is that even though we have used two separate TEM grids we were able to obtain clear patterns when superimposed on each other and embedded in a film. In other words, there was no clear diffusion of H_2S gas through these 'holes' that would have otherwise marred the features we have observed.

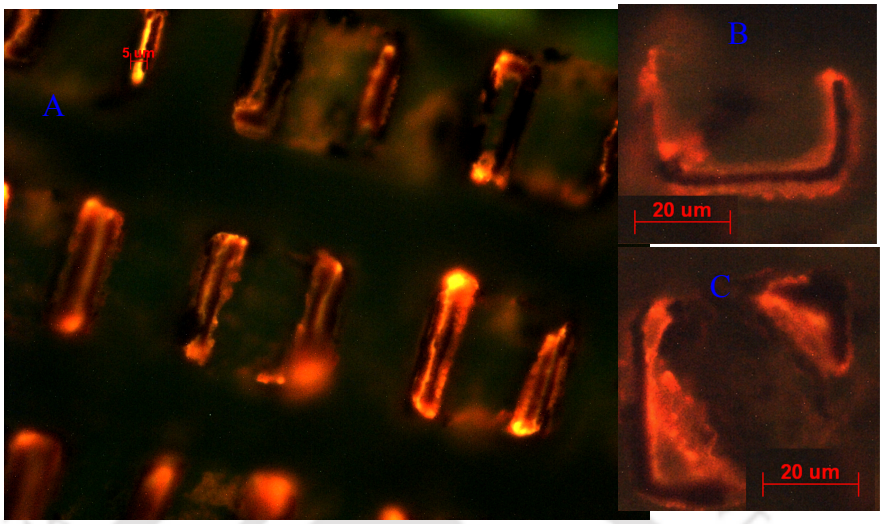

Figure 5.12 Fluorescence micrographs of CdS patterns formed using two grids. **A** shows the parallel line patterns (scale bar is 5 µm), while **B** and **C** are other angular shapes generated using two grids (scale bar is 20 µm).

5.3.9 Pattern with the best possible resolution

Finally, we also pursued experiments in order to achieve highest possible resolution of imprints of NPs on the film. We have used a two grid mask system as described above and used Cd^{2+} in the film without the presence of the dye. The result from three single lines obtained in the film (yellow colored line observed when excited by blue light) is shown in Figure 5.13. As clear from the figure the best resolution obtained in the present set of experiment is 1µm (top right one). Thus by suitably placing the grids (one atop the other) we could obtain a resolution of 1 µm in the patterned generation of CdS on PVP film. Even though the highest resolution we have achieved using the present method in combination with

TEM grids and polymer is 1 μm, the principle could possibly be extended to reach near theoretical resolution.

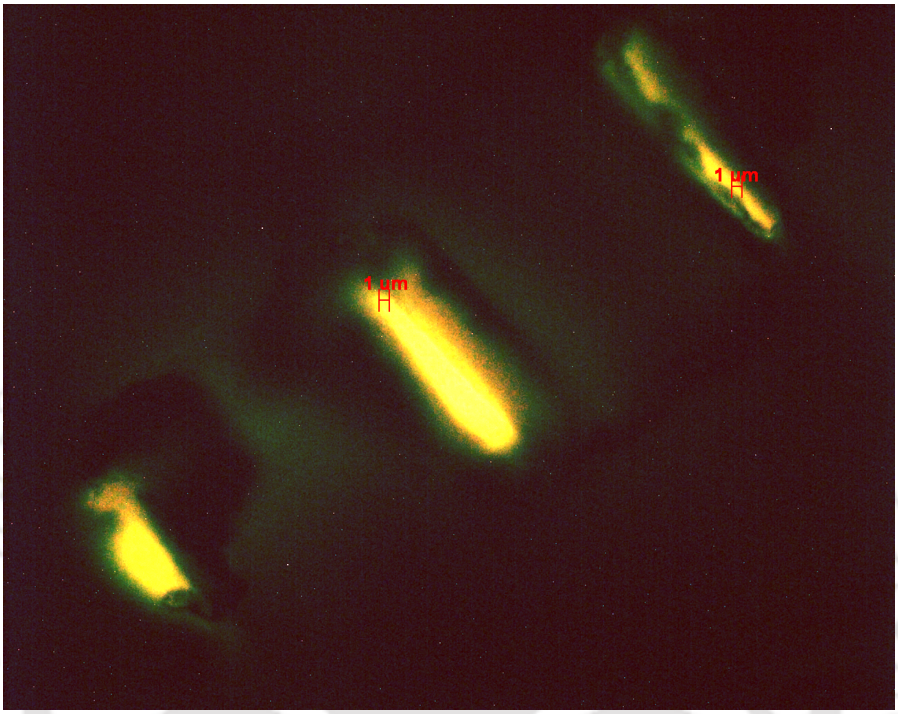

Figure 5.13 Fluorescent micrograph of CdS NPs formation with highest resolution achieved herein using a two-grid mask. The film was excited with blue light. The minimum line width in top right is 1 μm.

5.3.10 Wavelength dependent studies

Further, we have pursued excitation of the bi-colored patterned film with light of three different wavelengths. The results are shown in Figure 5.14. Figure 5.14 (A) shows the fluorescence micrograph of the film when excited by blue light (wavelength 450-490 nm). As clear from the picture the orange emission in the form of square patterns appeared from the exposed parts of the film along with green fluorescence from the background (dye containing

film). When the same film was excited by UV-light (wavelength 365nm) we observed light red patterns on the film against bluish scattered background.

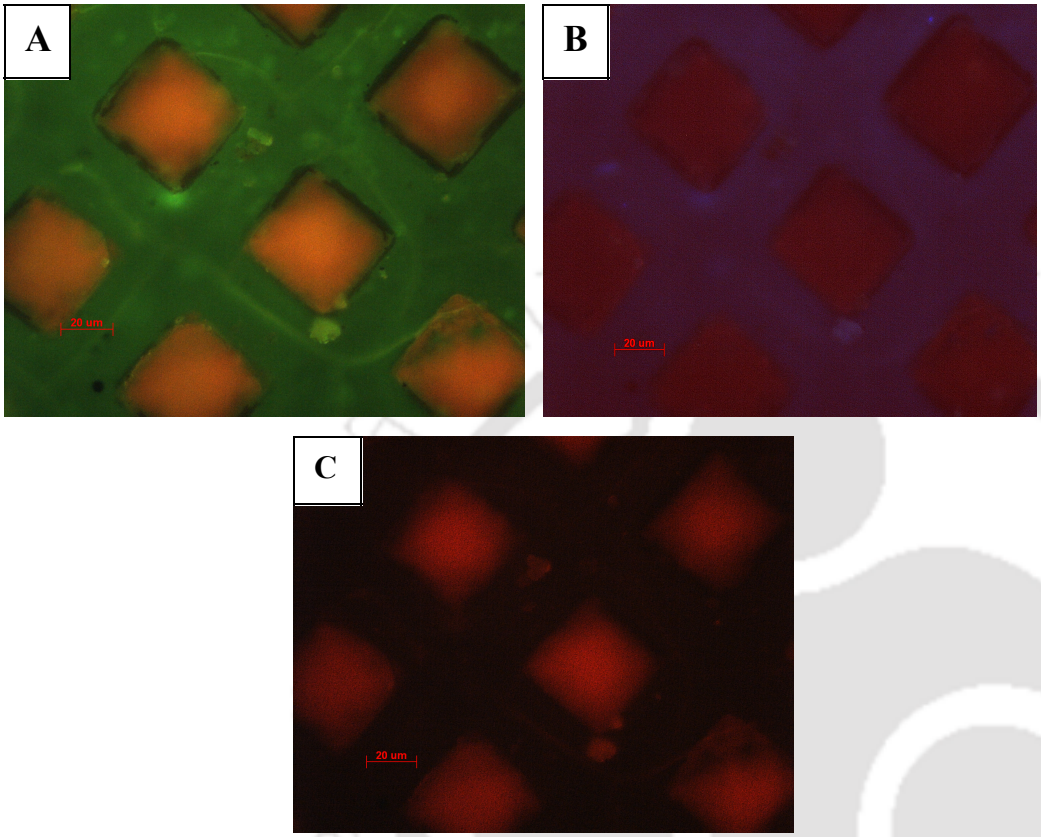

Figure 5.14 Fluorescence micrograph of a Fluorescein CdS in PVP film, excited at two different wavelengths. Micrograph in **A** was recorded when the film was excited using light at 450-490 nm, while that in **B** was recorded using light of wavelength 365 nm and **C** was recorded using light of wavelength 536-554 nm.

In other words, the emission was weak red fluorescence from the CdS NPs and no fluorescence could be observed from the dye containing background. Finally, when the film was excited by green light (wavelength 536-554 nm) no clear emission from any part of the

film could be observed. The excitation as well emission (observed herein) of both the dye and CdS NPs are sensitive to the wavelength of light and the above observations support that even though the whole part of the film is excited by light, because of sensitivity of light absorption as well as emission due to the chemical constituents in the film, patterned sections could be viewed in the presence of other parts by suitably adjusting the wavelength of excitation. In other words, by suitably choosing the excitation wavelength of light, it is possible to have fluorescent patterns either from both the constituents (patterned) on the film; or one of the two constituents can be made fluorescent while the other material would not fluoresce.

5.4 Conclusion

In this chapter, we have reported the development of a new form of lithography that involves a reaction between a gas and an ion embedded in a polymer film. The principle is based on a combination of top-down and bottom-up approaches in which a TEM grid was placed on a PVP film containing Cd^{2+} ions, which was then exposed to H_2S gas. This led to the generation of a fluorescent yellow pattern due to the formation of CdS nanoparticles on exposed parts of the film. Also, we have used the same method to generate patterns in two colors by starting with a green fluorescent dye incorporated into the film and following the same procedure in which patterned yellow-orange CdS NPs were distributed over the background fluorescence of the dye. Additionally, we have shown that the placing of the grid on the film (before it was dry) created an effective seal; however, the structure of the film became three dimensional with the presence of "hills" and valleys. Also, we have shown that film patterned with PbS NPs could be generated in the same way. Finally, we have been able

to generate patterns of different shape and sizes using a two grid mask and we have been able to achieve a resolution on the order of 1 μm. We have used fluorescence microscopy, UV-vis and fluorescence spectroscopy, transmission electron microscopy, atomic force microscopy, and X-ray diffraction methods for the characterization of the products and patterns. This method could possibly be a fairly general method of generating patterned materials on 2D and 3D substrates.

5.5 References:

1. Zhao, X. M.; Xia,Y.; Whitesides, G.M. *J. Mater. Chem.* **1997**, 7, 1069.

2. Xia,Y.; McClelland,J.J.; Gupta, R.; Qin,D.; Zhao.X.M. Sohn, L.L.; Celoyya,R.J.; Whitesides, G.M. *Adv .Mater*. **1997**, 9,147.

3. Xia, Y.; Kim, E.; Zhao, X .M.; Rogers, J.A.; Prentiss, M.; Whitesides, G.M. *Science* **1996**, 273, 347.

4. Xia,Y.; Whitesides, G.M. *Langmuir,* **1997,** 13, 2059.

5. Lee, K. B.; Park, S. J.; Mirkin, C. A.; Smith, J. C.; Mrksich, M. *Science* **2002**, 295, 1702.

6. Xia,Y.; Whitesides ,G. M. *Angew. Chem. Int. Ed.* **1998,** *37*, 550.

7. Ginger, D. S.; Zhang, H.; Mirkin,C. A. *Angew. Chem. Int. Ed*. **2004**, *43*, 30.

8. Lin, X. M.; Parthasarathy, R.; Jaeger, H. M. *Appl. Phys. Lett.* **2001,** *78*, 1915.

9. Chou, S. Y. ; Keimel, C.; Gu, J. *Nature* **2002,** *417*, 835.

10. Crook, R.; Graham, A. C.; Smith, C. G.; Farrer, I.; Beere, H. E.; Ritchie, D. A. *Nature* **2003**, *424*, 752.

11. Haynes, C. L.; Van Duyne, R. P. *Nano Lett.* **2003**., *3*, 939.

12. Grosso, D.; Boissiere, C.; Smarsly, B.; Brezesinski, T.; Pinna, N.; Albouy, P. A.; Amenitsch, H.; Antonietti, M.; Sanchez, C. *Nauture Materials*. **2004**, 3, 787.

13. Hua , F.; Lvov, Y.; Cui, T. *Thin Solid Films* **2004**, *449,* 222.

14. Jung, Y. J.; Wei, B.; Vajtai, R.; Ajayan, P. M.; Homma, Y.; Prabhakaran, K.; Ogino, T. *Nano Lett.* **2002***, 3,* 561.

15. Wei, B.; Vajtai, R.; Jung, Y.; Ward, J. ; Zhang, R.; Ramanath, G.; Ajayan, P. M. *Nature* **2002,** *416,* 495.

16. Liu, Z. F.; Hashimoto, K.; Fujishima, A. *Nature* **1990**, 347, 658.

17. Yang, P.; Wirnsberger, G.; Huang, H. C.; Cordero, S. R.; McGehee, M. D.; Scott, B.; Deng, T.; Whitesides, G. M.; Chmelka, B. F.; Buratto, S. K.; Stucky, G. D. *Science* **2000**, 287, 465.

18. Takayama, S.; Ostuni, E.; LeDuc, P.; Naruse, K.; D. Ingber, E.; Whitesides, G. M. *Nature,* **2001**, 411, 1016.

19. Chowdhury, D.; Paul, A.; Chattopadhyay, A. *Nano Lett.* **2001**, 1, 409.

20. Campbell, C. J.; Fialkowski, M.; Klajn, R.; Bensemann, I. T.; Grzybowski, B. A. *Adv. Mater*. **2004**, 16, 1912.

21. Cheng, H.-M.; Lin, K.-F.; Hsu, H.-C.; Hsieh, W.-F. *Appl. Phys. Lett.* **2006**, 88, 61909/1 (b) Jacobsohn, M.; Banin, U. *J. Phys. Chem. B* **2000**, 104, 1 (c) Nakashima, P. N. H.; Tsuzuki, T.; Johnson, A. W. S. *J. Appl. Phys*. **1999**, 85, 1556

22. A. P. Alivisatos, *Science* **1996**, *271*, 933.

23. Bawendi, M. G.; Steigerwald, M. L.; Brus, L. E. *Annu. Rev.Phys. Chem.* **1990**, *41*, 477

24. Chestnoy, N.; Harris, T. D.; Hull, R.; Brus, L. E. *J. Phys. Chem.* **1986**, *90*, 3393.

25. Henglein, A. *Top. Curr. Chem.* **1988**, *143*, 113.

26. Steigerwald, M. L.; Brus, L. E. *Acc. Chem. Res.* **1990**, *23*, 183.

27. Kako, S.; Santori, C.; Hoshino, K.; Goetzinger, S.; Yamamoto, Y.; Arakawa, Y. *Nature Materials* **2006**, 5, 887.

28. Sellin, R. L.; Kaiander, I.; Ouyang, D.; Kettler, T.; Pohl, U. W.; Bimberg, D.; Zakharov, N. D.; Werner, P. *Appl. Phys. Lett.* **2003**, 82, 841.

29. (a) Chang, W.-H.; Chen, W.-Y.; Chang, H.-S.; Hsieh, T.-P.; Chyi, J.-I.; Hsu, T.-M. *Phys. Rev. Lett.* **2006,** 96, 117401/1 (b) Malko, A.; Baier, M. H.; Karlsson, K. F.; Pelucchi, E.; Oberli, D. Y.; Kapon, E. *Appl. Phys. Lett.* **2006,** 88, 081905/1. (c) Fattal, D.; Diamanti, E.; Inoue, K.; Yamamoto, Y. *Phys. Rev. Lett*. **2004**, 92, 037904.

30. Gong, H.-M.; Wang, X.-H.; Du, Y.-M.; Wang, Q.-Q. *J.Chem. Phys.* **2006,** 125, 024707/1 (b) Wang, X.; Du, Y.; Ding, S.; Wang, Q.; Xiong, G.; Xie, M.; Shen, X.; Pang, D.. *J. Phys. Chem. B* **2006,** 110, 1566.

31. Kim, J.; Lee, J.-K. *Adv. Functional Mater.* **2006**, 16, 2077. (b) Lucey, D. W.; MacRae, D. J.; Furis, M.; Sahoo, Y.; Cartwright, A. N.; Prasad, P. N. *Chem. Mater*. **2005** , 17, 3754.

32. Milliron, D. J.; Hughes, S. M.; Cui, Yi.; Manna, L.; Li, J.; Wang, L.-W.; Alivisatos, A. Paul. *Nature* **2004**, 430, 190.

33. Ren, Z. F.; Huang, Z. P.; Wang, D. Z.; Wen, J. G.; Xu, J. W.; Wang, J. H.; Calvet, L. E.; Chen, J.; Klemic, J. F.; Reed, M. A. *Appl. Phys. Lett*. **1999**, 75, 1086.

34. Meldrum, A.; Buchanan, K.S.; Hryciw, A.; White, C.W. *Adv.Mater*.**2004**,16, 31.

35. Birudavolu, S.; Nuntawong, N.; Balakrishnan, G.; Xin, Y. C.; Huang, S.; Lee, S. C.; Brueck, S. R. J.; Hains, C. P.; Huffaker, D. L. *Appl. Phys. Lett.* **2004,** 85, 2337.

36. Nesterov, S. I.; Myagkov, D. V.; Portnoi, E. L. *Int. J. Nanosci.* **2004**, 3, 59.

37. Sikorski, C.; Merkt, U. *Phys. Rev. Lett*. **1989**,2164.

38. Xu. X.C.; Chi, L.F.; Fuchs, H. Eur. *J. Inorg. Chem*, **2005**, 3729.

39. Wu, X, C.; Bittner, A.M.; Kern, K. *Adv Mater*, **2004**, 16, 413.

40. Wang,Y .; Tang, Z.; Correa-Duarte, M. A.; Liz-Marzán, L. M.; Kotov N. A. *J. Am. Chem. Soc*. **2003**, 125, 2830

41. Spatz, J. P.; Chan, V. Z.-H.; MSßmer, S.; Kamm, F.-M.; Plettl, A.; Ziemann, P.; MSller, M. *Adv. Mater*. **2002**, 14, 1827.

42. Xia,Y.; Whitesides ,G. M. *Angew. Chem. Int. Ed.* **1998,** *37*, 550 – 575.

43. Lakowicz, J. R.; Gryczynski, I.; Gryczynski, Z.; Nowaczyk, K.; Murphy, C. J. *Anal. Biochem.* **2000**, 280, 128-136.

44. Nair, P. S.; Radhakrishnan, T. ; Revaprasadu, N.; Kolawole, G. A.; O'Brien, P. *Chem. Comm.*, **2002**, 564

6.1 Introduction

The synthetic schemes developed over the last two decades or so, for nanoscale materials with tunable optical[1], chemical[2], electronic[3] and mechanical properties have created a platform for further development in devices consisting of nanoscale functional units[4,5].An important requirement for the fabrication of functional device is to have organized and well-defined structures on two and three-dimensional substrate surfaces. The structures could be made of arrays of nanoparticles (NPs)[6] patterned on solid surfaces, with the scope of utility of the nanoscale properties of the patterned materials as the functional units. The last few decades have witnessed significant growth of a number of methods of imprinting nanoscale materials or structures on substrate surfaces. The methods are roughly divided into two generic categories – the top-down approach and the bottom up approach. The top-down approach involves systematic reduction of dimensions of bulk materials till they reach nanoscale. Lithographic principles involving light, electron and ion beams have been the primary work horses in this approach .On the other hand the bottom up approaches with systematic organization of atomic and molecular materials into zero, one, two and three-dimensional functional structures have opened up far superior avenues that would otherwise have been difficult if not impossible- to achieve using the top down approaches[7, 8]. The combination of two approaches – the self-assembly approach using the principles of chemistry and biology and the top-down approach- in fabricating devices is itself a natural extension of the two[9-11]. For example combining chemical lithography mediated by Ag NPs, where Au NPs has been adsorbed on lithographically patterned surface and further using

visible laser to reduce selective part of the surface, well-defined patterns have been obtained[12]. Arrays of nanoparticles (NPs) when organized in a desired fashion are expected to generate devices such as photonic crystals[13], laser diodes, sensors[14], and magnetic storage devices[15] with enhanced sensitivity and capacity [16, 17]. The principles used so far in fabricating such structures have been primarily based on lithography using light[18] micro-contact printing[19], focused ion beams[20], electrons beams[21] and also dip-pen lithography[22] and other scanning probe microscopy (SPM) techniques. Also, Si surfaces have been patterned with Au using lift-off electron beam lithography, and the resulting patterns were then amplified by surface initiated polymerization[23, 24]. Further, photolithography has been coupled to molecular self-assembly to produce functional micropatterns for application in bioscience[25]. However, the primary objective of systematic arrangements of NPs, especially hybrid NPs, on a surface still remains to be fulfilled.

An ideal scenario would be the combination of the properties of NPs and those of electroactive and photoactive polymers with patterned imprint on substrate surfaces. In that situation the NPs would provide the size-dependent optical, chemical and electronic properties and the polymer would provide the mechanical flexibility, electrical conductivity and also photoluminescent or electroluminescent properties. Several methods have been developed in our laboratory in the generation of polymer-NP composite materials with superior performance[26-28]. Also, A.G.Macdiarmid and co-workers have reported a simple method of "line-patterning" of polypyrrole films[29] on transparency sheet surface. On the other hand,

R.A.de. Barros[30] and co-workers reported a versatile method for writing with conducting polymers using a conventional Deskjet Printer. Further, polyaniline (PANI) microstructures have been fabricated on ITO, glass and silica surfaces using microcontact printing and electrochemistry[31]. Patterned hydrophobic and hydrophilic surfaces have also been used to deposit films of PANI and polypyrrole[32]. However, fundamental limitation of using PANI due to low solubility in most solvents poses a barrier for various applications.

In this chapter, we report a new method of imprinting predefined patterns of composite of Au and Ag NPs on a glass substrate (surface), where we have used the principle of soft lithography[33], redox reactions and simple assembly of NPs in a confined space at a higher temperature in order to achieve the desired patterns. The patterns could be in the form of parallel lines of NPs separated by a distance on the order of 1 μm, or they could be cross lines with separations of the above order. These composite metallic lines have further been used as a template to deposit Au NPs-PANI composite in a patterned fashion. The initial deposits of Au-Ag NP composite particles were characterized by UV-vis spectroscopy, X-ray diffraction and scanning electron microscopic (SEM) techniques to ascertain the nature of the materials and structures of the patterns. It was found that final structures retain the characteristic optical properties of a combination of Ag and Au NPs. SEM studies revealed that in the final patterned structures, the NPs remain separated with characteristic dimensions on the order of 50 nm or less. Interestingly, confocal laser scanning microscopic (CLSM) evidences suggest three dimensional natures of the patterns. Atomic force microscopic evidences indicated the deposition of polymer-NPs composite in organized patterns following the metallic lines. A

schematic representation of the process leading to the pattern generation on glass is shown in Figure 6.1.

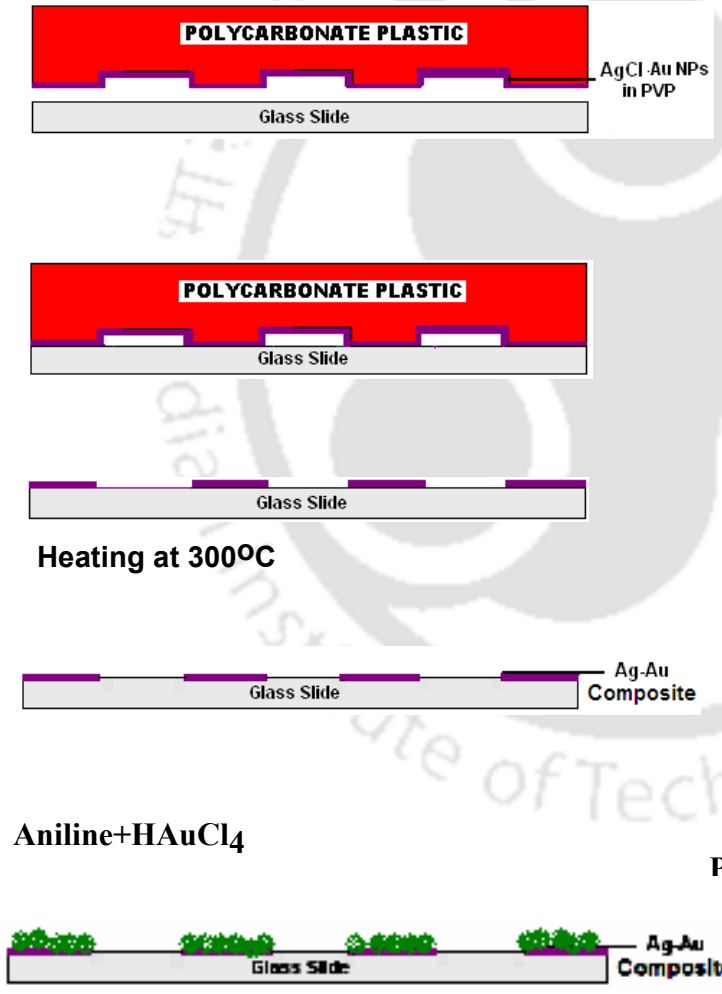

Figure 6.1: Schematic representation of the procedure depicting different steps leading to formation of patterned surface with Ag-Au composite nanoparticles, followed by patterned depositions of polyaniline as composite.

6.2 Experimental Section

6.2.1. Preparation of the Ink: In a typical experiment three stock solutions were initially prepared. They were (a) 0.076 g of Polyvinyl pyrrolidone (Aldrich, MW ca 29,000) in 2.5 mL of ethanol; (b) 2.9 x 10^{-2} M $AgNO_3$ (E. Merck India) in 5 mL of ethanol; and (c) 1.7 x 10^{-3} M $HAuCl_4$ in 5 mL ethanol (prepared by diluting 10 μL of $HAuCl_4$ (Aldrich, 17 wt%) to 5 mL). 200 μL portions of each of the above solutions were then mixed together which resulted in a purple color solution. The purple colored solution was further used as the ink for stamping patterns as described later.

6.2.2. Preparation of the stamp and stamping: We used an ordinary compact disc (CD) component - both the alumina and the poly carbonate parts – as the stamp. This is based on a previously reported procedure[34]. In brief, the components of the CD were washed thoroughly (after dismantling) using methanol and then air dried prior to use as the molds for stamping. This was followed by inking the stamp with the purple solution as prepared above. 20 μL of

the solution was pipette out using a micropipette and put it on to the stamp, which was then allowed to partially dry for 3 min and then washed with ethanol to remove the excess ink. Then the stamp were placed on a 5 mm x 5 mm glass slide and appropriate pressure was applied onto them which resulted in partial transfer of the ink to the glass slide as observable by the development of interferences fringes on the slide. In typical experiments, we used the polycarbonate parts of the CD because of the ease of use. However, it was found that the aluminum parts also provided good patterns.

In a similar way, cross patterns were generated, using identical stamps and inks, by pressing the inked mold twice in sequence, and at angle to the original direction, onto the glass slide.

6.2.3. Burning polymer off from the glass slide: The stamped glass slides were heated in Muffle furnace to burn the polymer completely. It was found that heating at 300 ^{0} C for 30 min removed the polymer, leaving behind patterns of Au-Ag on the surface. The absence of the carbon-containing polymer was confirmed by energy dispersive X-ray spectroscopy (EDS).

6.2.4 Optical microscopic studies: After transferring the pattern of the mold to the glass slides, the slides were monitored with Karl Zeiss epifluorescence microscope (Axioskop2 MAT) in normal view (reflection) mode.

6.2.5 UV-Visible spectroscopic studies: UV-vis spectra of individual slides, coated with patterned polymer plus inorganic components or just the inorganic components (for post-heated samples), were recorded by placing the slide in the sample compartment of a Perkin-Elmer lambda 25 UV-vis spectrophotometer. Ordinary microscope (glass) slides were used as the reference for the measurements.

6.2.6 X-ray diffraction studies: In order to further characterize the films X-ray diffraction patterns of individual slides were recorded using a Bruker D8 X-ray diffractometer. As the sample required is large, the sample used were plain thin films of dimensions 25 mm x 25mm prepared without stamping. Both the preheated and post-heated samples were recorded under identical conditions.

6.2.7 Scanning electron microscopic studies: Scanning electron microscope measurements were performed with a LEO VP 1430 instrument operating at 20 KV, and the EDS measurements were performed with an Oxford INCA –X-sight instrument. The samples were coated with 10Å of gold film before recording of the micrographs.

6.2.8 Confocal laser scanning microscopic studies: Confocal laser scanning microscopic (CLSM) studies were carried out with a Karl Zeiss LSM510 Meta instrument consisting of an inverted microscope. The incident laser excitation wavelength used for the measurements was 488nm. The three-dimensional pictures were recorded in Z-stacking mode.

6.2.9 Deposition of PANI: To deposit polyaniline on the Au-AgNP composite lines, the glass slides with well-defined pattern of Ag-AuNP (after heating) were dipped in a solution containing 15 mL of water, 2 mL (3M) HCl, 120 µL distilled aniline and 50 µL of $8.3x10^{-3}$ M $HAuCl_4$ for 4 h. Deposition of PANI on the glass slides could be observed by appearance of green color in the slides. To remove the excess PANI, the glass slides were put in a beaker (with water) and sonicated for 5 mins. The slides were then dried in the air for further analysis.

6.2.10 Atomic force microscopic studies: To find out the nature of PANI deposited on the lines, the glass slides after deposition of PANI were observed under VEECO nanoscope IV (a). The images were recorded in contact mode.

6.2.11 UV-visible study of the PANI deposited films: To confirm the presence of PANI on the lines, and to know whether the deposited PANI retained reversibility of its optoelectronic properties in terms of conversion between the two forms, upon treatment with acid and bases, we prepared sample of PANI deposited on Au-AgNP composite containing glass without patterning. A large sample was required for spectroscopic studies. The procedure of deposition was otherwise same as used in experimental section 6.2.9. Initially green colored deposition was observed. UV-vis spectrum of the slide was recorded. The slide was then treated with 1 M NaOH solution for 1 min. The color of the slide turned blue. The UV-vis spectrum of the slide was then recorded. Microglass slides were used as the blank for recording the spectra. We had to sometime use two slides containing the same form of PANI,

placed together in the sample compartment of the spectrophotometer, in order to obtain better quality spectra.

6.3 Results and Discussion

6.3.1 Optical microscopic Studies

When a thin fluid film of the polymer-NP composite "ink" is placed on the CD mold and then evaporated, the "hill" parts of the mold retain the "ink" at higher positions than the "valley" parts where ink goes into a dip upon evaporation. Afterwards, when the mold is placed on a glass slide then the composite ink from the "hill" portions is transferred to the surface providing a regular pattern of parallel lines of the composite materials imprinted on the surface. The separation of lines on the imprint would follow the separation of "hills" in the mold. That is also what we have observed in the present case. Figure 6.2(A) shows optical micrograph of a typical transfer due to imprinting. As clear from the figure, the quality of transfer is quite good as the lines are continuous with width the same as the original mold (about 0.8 μm) and well separated without splashing. Also, the separation between the lines followed that of the mold (about 1 μm). We also noticed that when the slide was heated at 300^0C for 30 min to remove the polymer content, the lines retained their characteristics as clear from Figure 6.2(B)

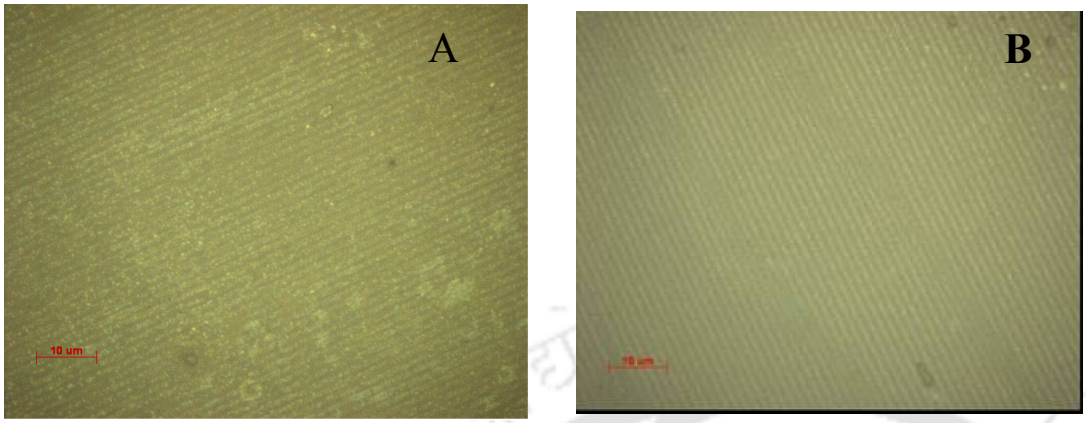

Figure 6. 2 Optical micrographs of the stamped sample (A) before and after (B) heating.

6.3.2 UV-visible spectroscopic and X-ray diffraction Studies

UV-vis spectrum (Figure 6.3A) of the deposited materials consisted of a peak at 535 nm which is characteristics of Au NPs present in the film. Thus the initial deposition consisted of Au NPs in the composite structures. X-ray diffraction measurement of the deposited structures showed (Figure 6.3B) peaks at 32.13^0, and 46.13^0 (2θ values) which are assigned to be the diffraction from (200) and (220) planes of AgCl. Also present was a weak peak at 38.02^0 due to diffraction from (111) plane of Au. Thus the present method can produce uniform parallel line patterns of composite materials where the Au NPs are present as the "active" optical components with the additional presence of AgCl. It must be stated here that the presence of $AgNO_3$ was essential in PVP for the formation of Au NPs. We observed that in the absence of $AgNO_3$, when $HAuCl_4$ alone was present in the PVP solution, no coloration was observed for after a week, indicating the lack of formation of Au NPs in the medium.

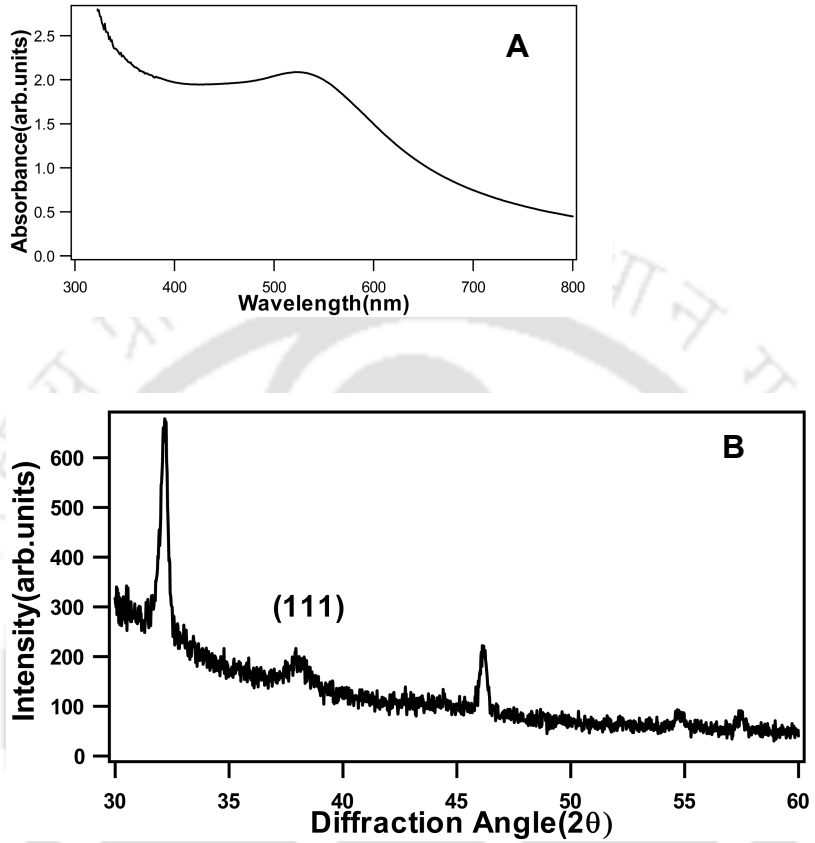

Figure 6.3 UV-Visible spectrum of the sample before heating (A), and XRD patterns of the same sample (B).

Further, the samples were heated at 300^0C to remove the polymer. For the UV-vis and XRD studies larger samples were required and hence simple composite films were evaporated without patterns. All other conditions were the same as with the patterned lines. UV-vis spectrum of the post-heated slide Figure 6.4(A) consisted of a broad peak which in itself

appears to be the superposition of two peaks one at 430 nm, which is characteristic of Ag NPs, while the other one was near the original peak of Au NPs occurring at 565 nm.

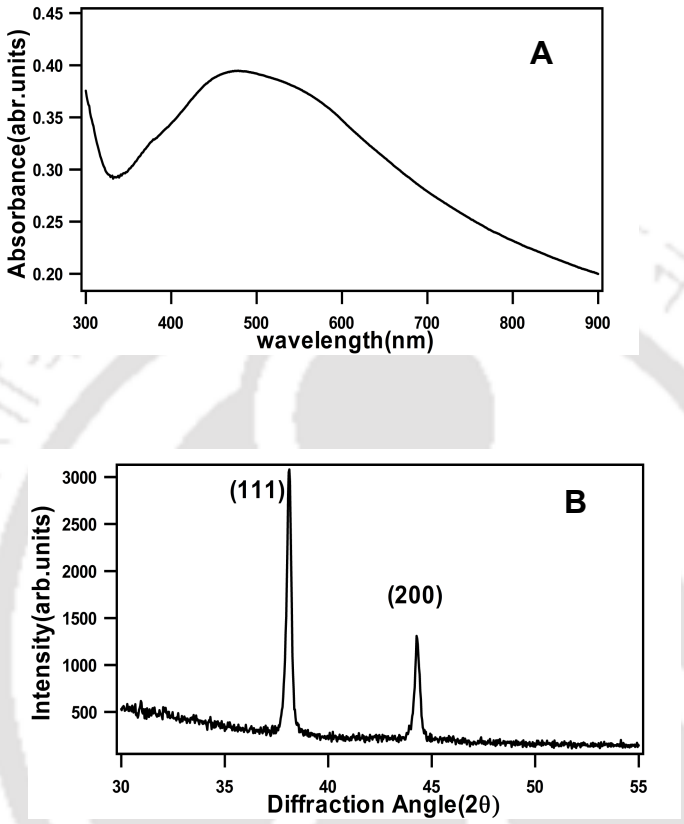

Figure 6.4 UV-visible spectrum of the sample after heating (A), and XRD pattern of the corresponding sample (B).

This indicates that in addition to Au NPs the structures consisted of Ag NPs after heating. The particles could be made of Au-Ag alloy or a combination of individual Au and Ag NPs dispersed in/on the glass. The Ag NP formation was further confirmed by X-ray diffraction measurements which showed two prominent peaks- one at 38.12^0 and the other at 44.27^0, that are characteristic of Au and Ag NPs. It is also interesting to note that all other peaks due to

AgCl, that were present before heating, had vanished upon heating. This means that burning off /decomposition of the polymer at an elevated temperature accompanied conversion of AgCl to Ag NPs which increased the intensities of the (XRD) peaks at 38.12^0 and at 44.27^0. This is also consistent with the UV-vis spectrum of heat treated sample slide[35].

6.3.3 Confocal Laser Scanning Microscopic Studies

The patterned glass slides were further studied by CLSM, both before heating and after heating. The CLSM pictures are shown in Figure 6.5. The micrograph of the sample before heating, Figure 6.5(A) consisted of parallel lines of about 1 μm width with the separation between two lines of 1.5 μm. The dimensions of these lines and their separations match well with those measured by optical microscopy as mentioned above. The three-dimensional nature of the imprints could easily be seen from the micrograph. Also, interesting to note is the fact that the lines are continuous indicating a good quality transfer of lines from the mold to the substrate surface. In addition it is important to note the heights of the lines are nearly uniform with little defect. The corresponding micrograph of the heated sample is shown in Figure 6.5(B). It is interesting to note that the sharp lines changed to less sharp but clear lines upon heating. The dimensions of the lines and their separation did not get affected though due to heating. However, along the lines unevenness is clear. The lines seem to be broken, which is probably due to the presence of composite NPs and possible absence of polymer.

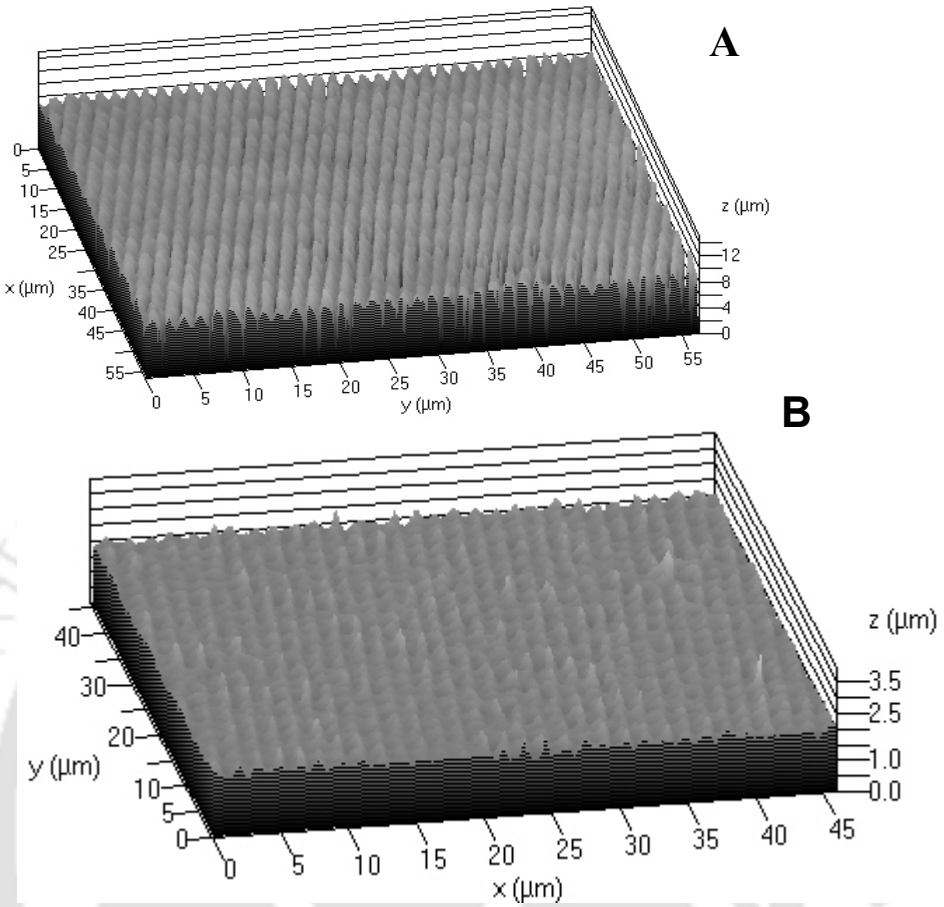

Figure 6.5 CLSM micrographs of the patterned surface before heating (A) and after heating (B).

6.3.4 Cross Pattern Generation

We also pursued the possibilities of cross-pattern generation of the NP composites using the present method. When the mold was used for the second time after the first imprint, before the film was completely dry and without the use of any "ink", cross-pattern formation could be observed as per the separation of "hills" in the mold. A confocal micrograph of a typical pattern is shown in Figure 6.6 (A). The film consisted of AgCl and Au NPs as before

and the content was not further probed as it was deemed not necessary. As clear form the figure well separated patterns could be made with separation between the lines on the order of the sizes of the "valleys" (first imprint) in one direction, while the separation is equal to "hills" (second imprint) in the other direction. In the first imprint the materials are imprinted on the substrate from the top of the "hills" when placed on the substrate surface. On the other hand the second imprint merely removes the composite upon pressing of the mold. This means the separation between the lines follows the width of the "hills". This is how cross-patterns were created with two different periodicities. It is also possible that while pressing for the second time the mold not only removes the materials from the places where "hills" of the mold impresses upon the surface but also moves them up along the "valleys". In other words, the original imprints were chiseled out by the second pressing and parts of the materials from the imprints might have moved up along the "valleys" of the mold during second pressing. When the imprinted composite patterns were heated as before at 300^0C for 30 min, the polymer component was removed as before and imprints with Au and Ag NPs were left on the glass slide. Confocal micrograph of a typical such imprint of cross patterns is shown in Figure 6.6(B). As clear from the figure, the general patterns of NPs with distribution of arrays of them follow that of the original imprint before heating. The separation between the particles in the arrays follows typically that of the separation of the "hills" and "valleys" in the original mold in either direction of the arrays. It may be mentioned there that individual imprints of arrays are not singular NP of either of Ag or Au. Each dot in the arrays represent materials that are made of Au and Ag NPs, whose separation and number depend on the exact initial concentration of $HAuCl_4$ and $AgNO_3$ that finally turn into NPs. However, each dot in

the arrays represents a collection of NPs well separated such that their NP character is not lost.

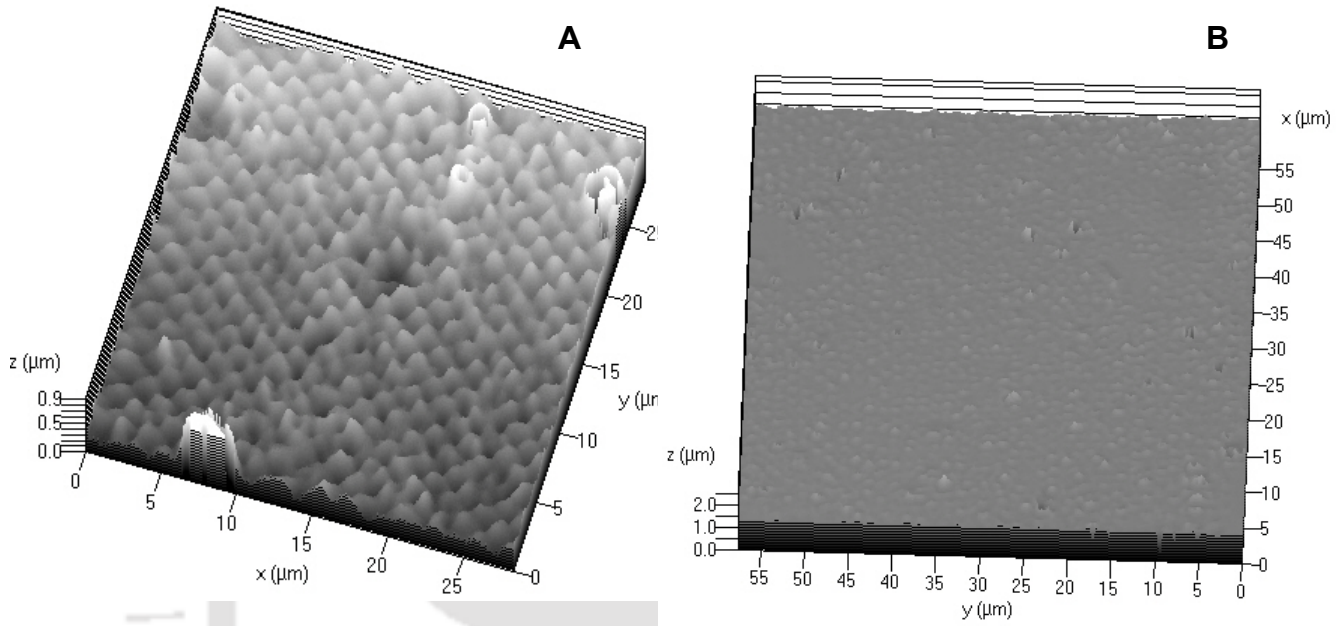

Figure 6.6 Confocal micrographs showing the cross pattern before heating (A), and after heating (B).

6.3.5 Scanning Electron Microscopic Studies

In order to ascertain the nature of the particles in the lines and to determine the sizes of the particles, on individual lines after heating, the glass slides were studied by SEM. A typical micrograph of a slide with only parallel line patterns before heating is shown in Figure 6.7(A). As clear from the figure, the NPs could be seen deposited along the lines according to the

dimensions of the imprint. Also, important to note is that there is uniform distribution of NPs along the lines. This indicates that the NPs were present homogeneously in the original

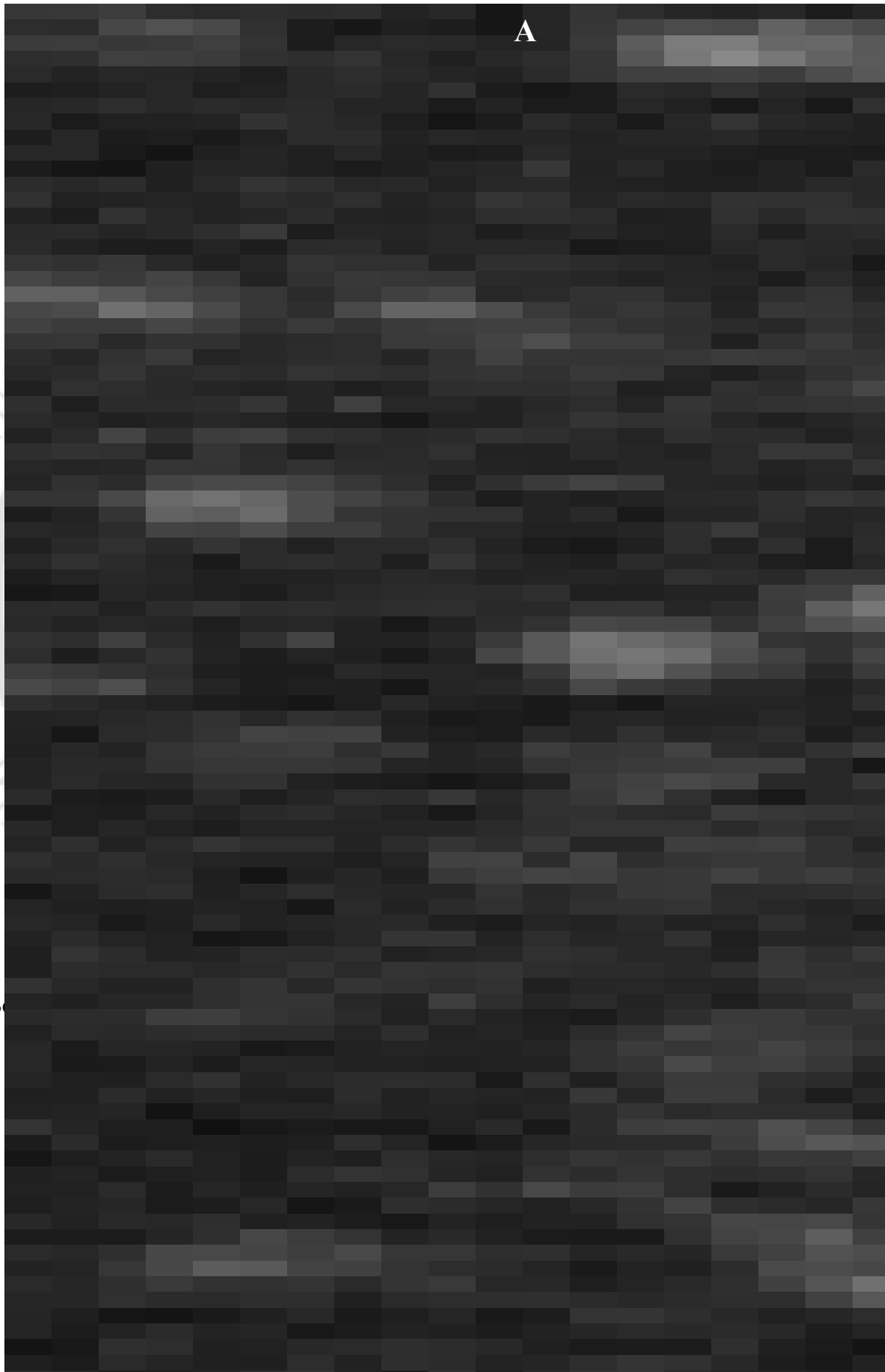

Figure 6.7 S

heating (B).

Sub-micron s

==========

mixture (ink)

X-ray (EDX)

the presence

heating at 30

converted to

SEM image i

from the figu

as it was befo

little amount

after heating.

NPs along its

The process o

of the particl

note here.

6.3.6 Deposi

We were furt

along the line

is important

as electrode a

fashion coul

polymerizati

Sub-micron s

==========

coated with

PANI-metal

Ag-Au NPs

experimental

green color o

water for 10

AFM. A typ

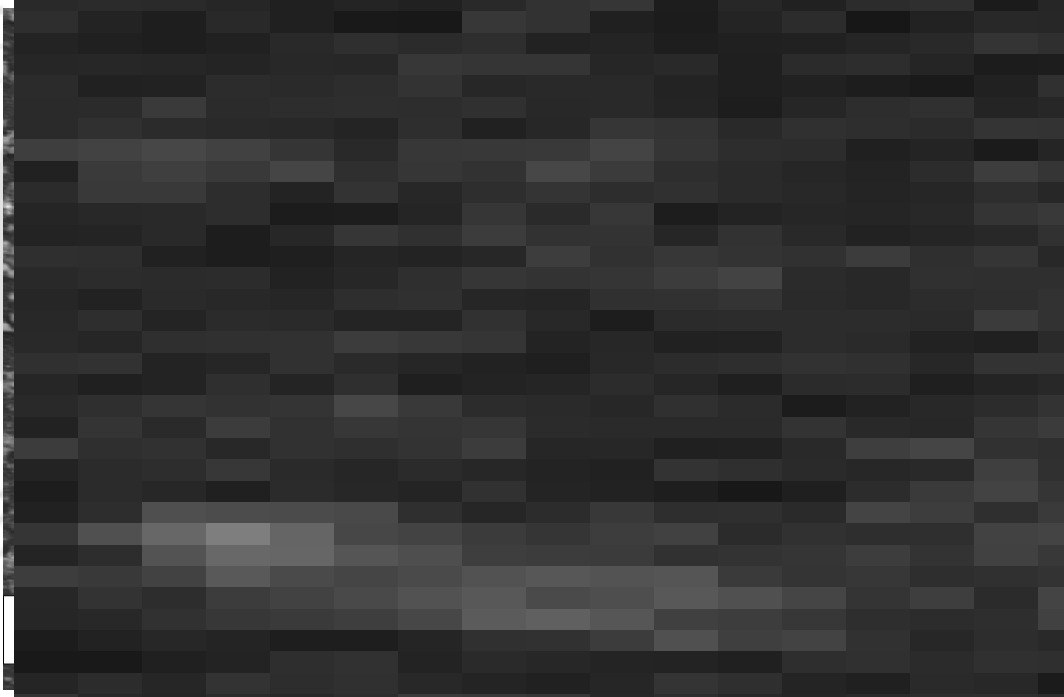

Figure 6.8 S

As clear fro

Au-Ag comp

Sub-micron s

==========

about 0.8-1.2

the original

actually be c

polymer depo

6.3.7 Atomic

The PAN

view (height

deposits of P

on the slide

the original p

clearly indica

be about 100

lines could b

predefined fa

the depositio

slide and NP

Au NPs were

could not be

be "sticking"

ultrasonic wa

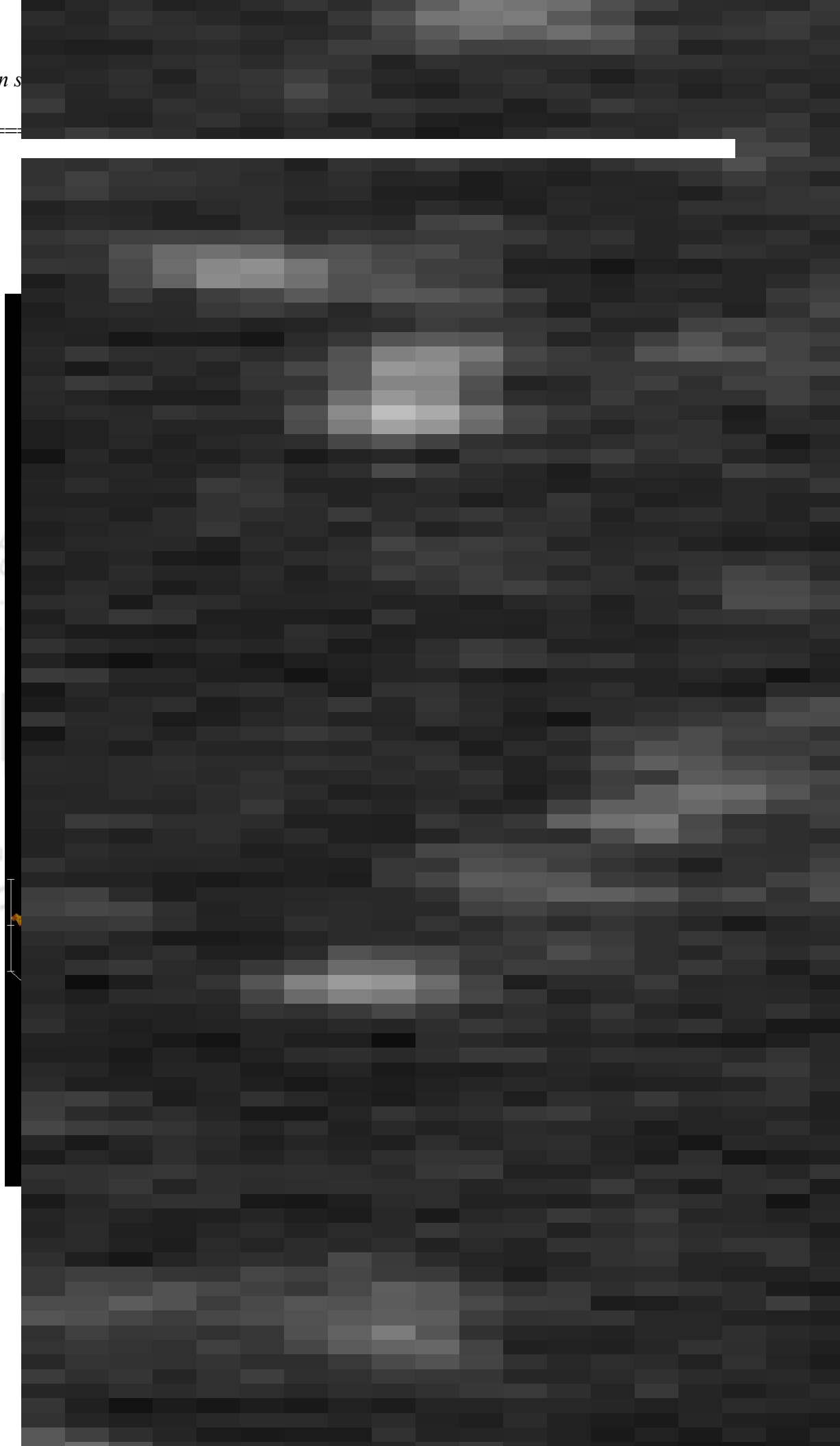

Sub-micron s

==========

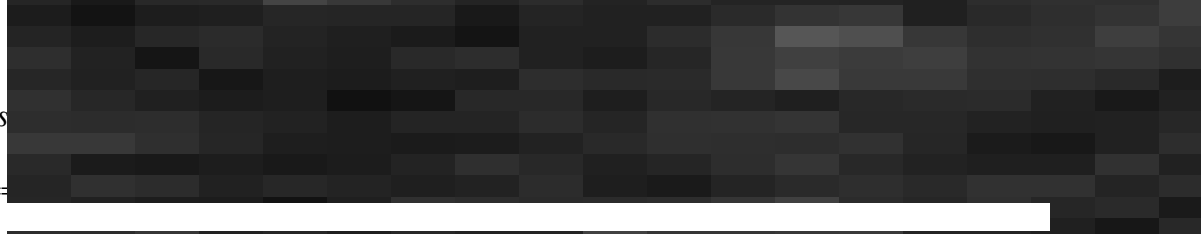

Figure 6.9 (*A*

Ag-Au comp

6.3.8 Retenti

Finally, we

acid-base pro

subject to aci

solution. Dif

In order to c

without patte

to make a thi

6.2.9 and 6.2

any specific

measurement

solution cont

appearance o

cleaned usin

deposits on t

characteristic

emeraldine s

were then tre

Sub-micron s

==========

slides turned

peak at 400 r

when further

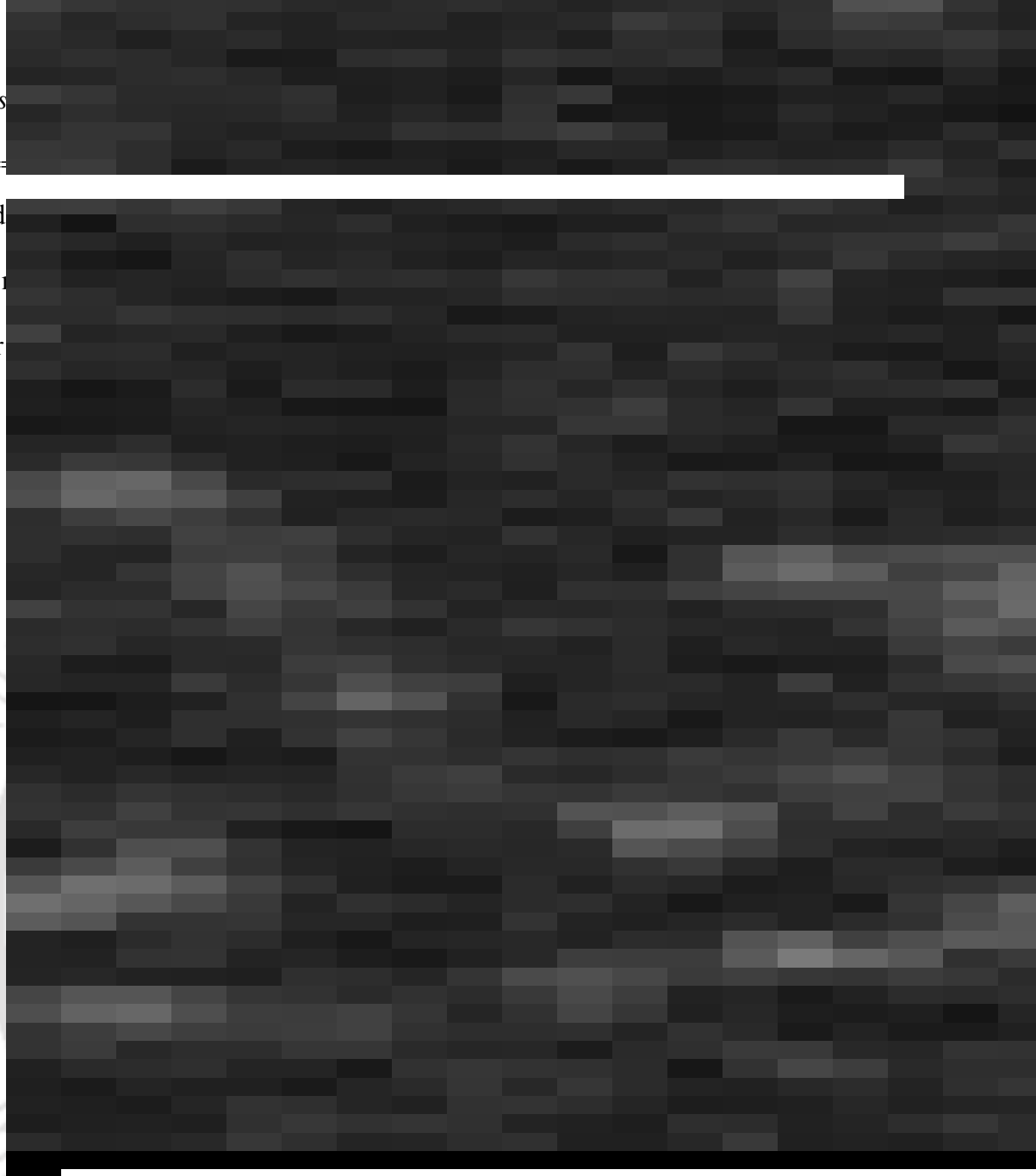

Sub-micron s

==========

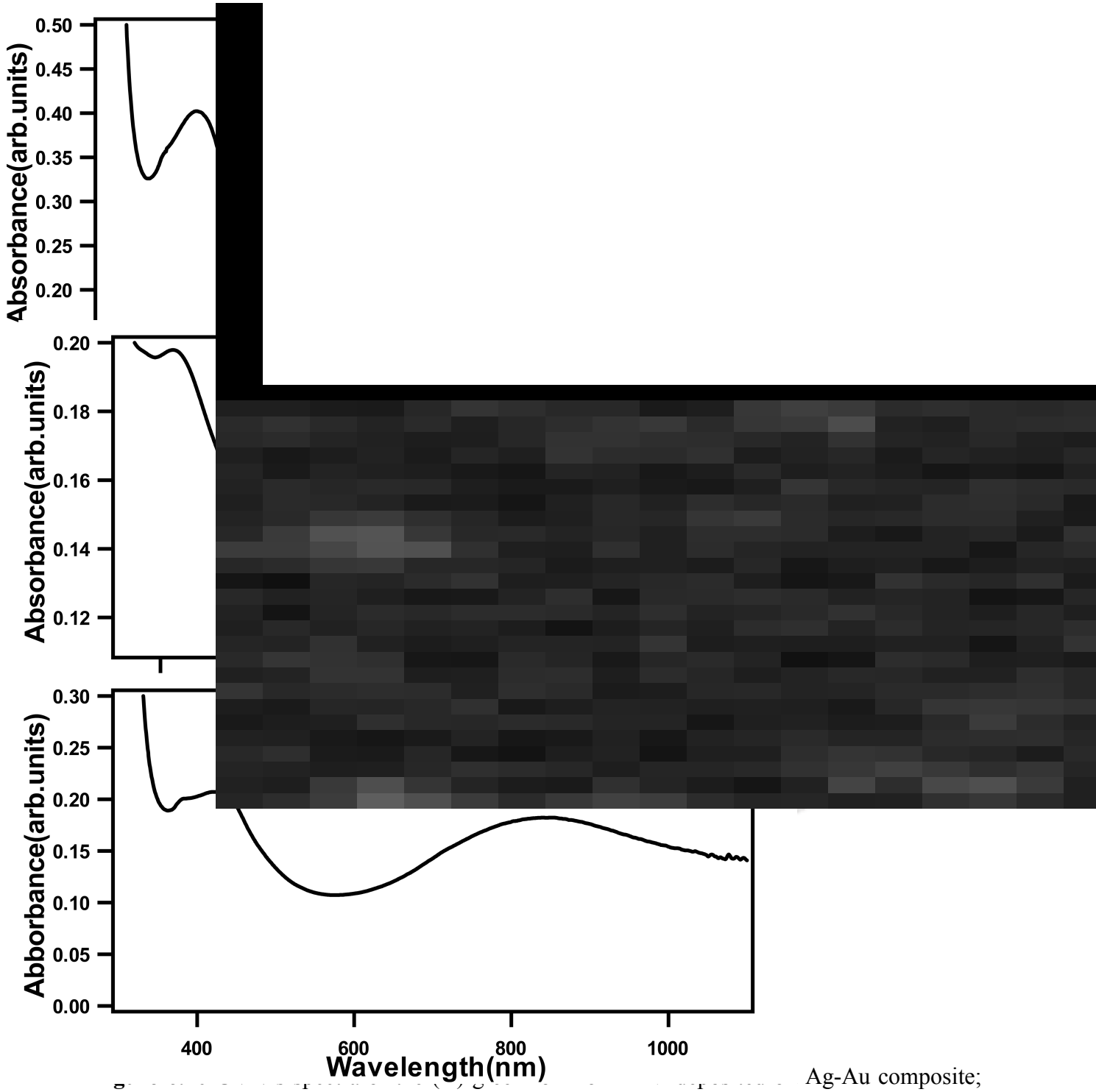

Ag-Au composite;

(B) blue form of PANI obtained upon treating with base; and (C) green form of PANI

recovered from the blue form upon treatment with acid. Multiple (identically prepared) slides were also used to obtain better quality spectra.

420 nm and 875 nm confirming the conversion into emeraldine salt form. The present observations are important as we have a thin film deposit of PANI on glass slides, with the full retention of acid-base characteristics as well as the color characteristic of the polymer. These films could be useful for applications where conducting polymer-metal NPs could act as electrodes, sensors and actuators.

6.4 Conclusion

In this chapter, we have reported the development of a new method of generation of patterned array deposits of Au-Ag composite NPs. The method is based on a soft-lithography approach where initial metal NPs-polymer composite was used as ink to imprint line patterns on glass slides using a mold. The burning off of the polymer left composite NPs as per the original line patterns on the glass slide. The sizes and shapes of the NPs did not apparently change. On the other hand, AgCl present in the original ink got converted into Ag NPs. Further, PANI could be deposited on the slides along the patterns of the NPs. In addition, the deposited PANI retained its acid-base characteristics. Analytical measurements were used to confirm the depositions and to characterize the NPs and the polymer. AFM measurements indicate the depositions of think lines of PANI with heights on the order of 50 nm. These three-dimensionally patterned polymer-metal NP composite structures may be useful in optoelectronic devices, photonic devices, fuel cell electrodes and optical coatings.

6. 5 References:

1.Huang, X.; Li, J.; Zhang, Y.; Mascarenhas, A. *J. Am. Chem. Soc*. **2003**, 125,7049.

2. Antonietti, M.; Goltner, C. *Angew. Chem.Int. Ed*.**1997**, 36,911.

3. Velasco-Santos, C.; Martinez-Hernandez, A. L.; Fisher, F. T.; Ruoff, R.; Castano, V. M. *Chem. Mater*. **2003**,15, 4470.

4. B. Bhushan (editor) "*Handbook of Nanotechnology",* Springer-Verlag Berlin Heidelberg **2004**.

5. Goddard III, W.A.; Brenner,D.W.; Lyshevski, S.E.; Iafrate,G.J. "*Handbook of Nanoscience, Engineering, & Technology"*, CRC press, **2003.**

6.(a) Zhang, L.; Hong, L.; Yu, Y.; Bae, S.C.; Granick, S*, J. Am. Chem. Soc.* **2006,** 128, 9026.(b) Sander, M. S.; Tan, L.S. *Adv. Funct. Mater.* **2003**, 13, 393.

7. Talin, A. A.; Hunter, L.L.; Leonard, F.; Rokad, B. *Appl. Phys. Lett*. **2006**, 89, 153102/1.

8. Deguchi, S.; Mukai, S-a.; Tsudome, M.; Horikoshi, K. *Adv. Mater* **2006**, 18, 729.

9. Shipway, A. N.; Katz, E.; Willner, I. *Chem. Phys. Chem*. **2000,**1, 18.

10. Hulteen, J. C.; Treichel, D. A.; Smith, M. T.; Duval, M. L.; Jensen T. R.; Van Duyne, R. P. *J. Phys. Chem. B* **1999,** 103, 3854.

11. Xia, Y.; Whitesides ,G. M. *Angew. Chem. Int. Ed*. **1998,** 37, 550.

12. Kim, K.; Lee, I. *Langmuir* **2004**, 20, 7351.

13. (a) Imahori, H.; Mitamura, K.; Shibano, Y.; Umeyama, T.; Matano,

Y.; Yoshida, K.; Isoda, S.; Araki, Y.; Ito, O. *J. Phys. Chem. B* **2006**, 110, 11399. (b) Mafouana, R.; Rehspringer, J.-L.; Hirlimann, C.; Estournes, C.; Dorkenoo, K. D. *Appl. Phys. Lett*. **2004**, 85, 4278.

14. (a) Willner, I.; Baron, R.; Willner, B. *Adv. Mater*. **2006**,18, 1109.(b) Astruc, D.; Daniel, M.-C.; Ruiz, J. *Chem. Commum.*. **2004**, 2637.

15. Yu, M.; Liu, Y.; Moser, A.; Weller, D.; Sellmyer, D. J. *Appl. Phys. Lett*.**1999**, 75, 3992.

16. Shipway, A. N.; Katz, E.; Willner, I. *Chem. Phys Chem*. **2000,** 1, 18.

17. Wang, X.; Neff, C.; Graugnard, E.; Ding, Y.; King, J. S.; Pranger, L. A.; Tannenbaum, R.; Wang Z. L.; Summers, C. J. *Adv. Mater*. **2005,** 17, 2103.

18. Revzin, A.; Russell, R. J.; Yadavalli, V. K.; Koh, W.G.; Deister, C.; Hile, D. D.; Mellott M. B.; Pishko, M. V. *Langmuir* **2001,** 17, 5440.

19. Ng, W. K.; Wu, L.; Moran, P. M. *Appl. Phys. Lett*. **2002,** 81, 3097.

20.(a) Li, J.; Stein, D.; McMullan, C.; Branton, D.; Aziz, M. J.; Golovchenko, J. A. *Nature* **2001** ,412, 166.

21. Hicks, E. M.; Zou, S.; Schatz, G. C.; Spears K. G.; Van Duyne, R. P. *Nano Lett*. **2005,** 5, 1065.

22. Ginger, D. S.; Zhang, H.; Mirkin, C. A. *Angew. Chem. Int. Ed*. **2004,** 43, 30**.**

23. Kim, K.; and Lee, I. *Langmuir* **2004**, 20, 7351.

24. Hawker, C.J.; Russell, T. P. *MRS Bulletin* **2005**, 30, 952.

25. Ahn, S. J.; Kaholek, M.; Lee, W.K.; LaMattina, B.; LaBean, T. H.; Zauscher, S. *Adv. Mater*.**2004**, 16, 2141.

26. Sarma, T. K.; Chowdhury, D.; Paul, A.; Chattopadhyay, A. *Chem.Commun*. **2002**, 1048.

27. Chowdhury, D.; Paul, A.; Chattopadhyay, A. *Langmuir* **2005**, 21, 4123.

28. Majumdar, G.; Gogoi, S. K.; Paul, A.; Chattopadhyay, A. *Langmuir* **2006**, 22, 3439.

29. Hohnholz, D.; Macdiarmid, A.G.; *Syn. Metal*. **2001,** 121, 1327.

30. de Barros,R.A.; Martins, C.R.; de Azevedo, W.M. *Syn Metal*. **2005,** 155, 35.

31. Guan, F.; Chen, M.; Yang, W.; Wang, J.; Zhang, R.; Yang, S.; Xue, Q. *Appl. Surf. Sci*. **2004**, 230, 131.

32. Huang, Z.; Wang, P-C.; Feng, J.; MacDiarmid, A. G. *Syn.Metal*, **1997,** 85, 1375..

33. Xia, Y. *Adv.Mater*. **2004**,16, 1245.

34. Chowdhury, D.; Paul, A.; Chattopadhyay, A. *Nano Lett.* **2001**, 1, 409.

35. Yang, X.; Lu Y.; *Polymer* **2005**, 46 ,5324.

36. Dutta, D.; Sarma, T. K.; Chowdhury, D.; Chattopadhyay, A. *J. Colloid. Interface. Sci.* **2005**, 283, 153.

List of Publications

1. Au Nanoparticles and Polyaniline Coated Resin Beads for Simultaneous Catalytic Oxidation of Glucose and Colorimetric Detection of the Product.

Gitanjali Majumdar, Mausumi Goswami, Tridib Kumar Sarma, Anumita Paul, Arun Chattopadhyay. ***Langmuir*** **2005**, 21(5), 1663-1667.

2. Solid-state Storage of Ag Nanoparticles in Anion Exchange Resin Beads and their Recovery.

S. Manikandan, **Gitanjali Majumdar,** Devasish Chowdhury,. Anumita Paul, Arun Chattopadhyay, .***Journal of Colloidal Interface Science*** **2006,** 295(1), 148-154.

3. Lithography for Imprinting Colored Patterns with Quantum Dots.

Gitanjali Majumdar, Sonit Kumar Gogoi,; Anumita Paul, Arun Chattopadhyay. ***Langmuir*** **2006**, 22(7), 3439-3444.

4. Sub-micron Scale Patterns of Au and Ag Composite Nanoparticles on Glass.

Gitanjali Majumdar, Sonit Kumar Gogoi, Anumita Paul and Arun Chattopadhay

(Communicated)